DAVID W. TAYLOR NAVAL SHIP RESEARCH AND DEVELOPMENT CENTER

Bethesda, Maryland 20084

STERN BOUNDARY-LAYER FLOW ON A THREE-DIMENSIONAL BODY OF 3:1 ELLIPTIC CROSS SECTION

by

Nancy C. Groves
Garnell S. Belt
Thomas T. Huang

APPROVED FOR PUBLIC RELEASE: DISTRIBUTION UNLIMITED

SHIP PERFORMANCE DEPARTMENT
RESEARCH AND DEVELOPMENT REPORT

May 1982 DTNSRDC-82/022

MAJOR DTNSRDC ORGANIZATIONAL COMPONENTS

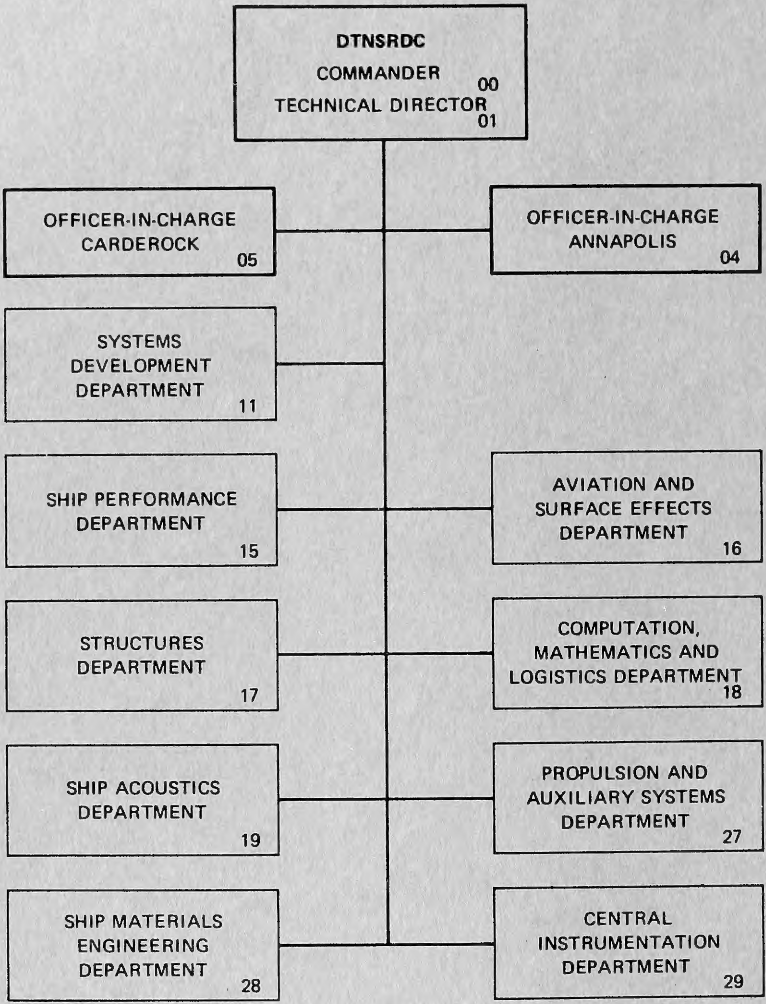

UNCLASSIFIED

SECURITY CLASSIFICATION OF THIS PAGE (When Data Entered)

REPORT DOCUMENTATION PAGE		READ INSTRUCTIONS BEFORE COMPLETING FORM
1. REPORT NUMBER DTNSRDC-82/022	2. GOVT ACCESSION NO.	3. RECIPIENT'S CATALOG NUMBER
4. TITLE (and Subtitle) STERN BOUNDARY-LAYER FLOW ON A THREE-DIMENSIONAL BODY OF 3:1 ELLIPTIC CROSS SECTION		5. TYPE OF REPORT & PERIOD COVERED Final 6. PERFORMING ORG. REPORT NUMBER
7. AUTHOR(s) Nancy C. Groves Garnell S. Belt Thomas T. Huang		8. CONTRACT OR GRANT NUMBER(s)
9. PERFORMING ORGANIZATION NAME AND ADDRESS David W. Taylor Naval Ship Research and Development Center Bethesda, Maryland 20084		10. PROGRAM ELEMENT, PROJECT, TASK AREA & WORK UNIT NUMBERS Program Element 61152N Project ZR 000 01 Work Unit 1542-103
11. CONTROLLING OFFICE NAME AND ADDRESS		12. REPORT DATE May 1982 13. NUMBER OF PAGES 116
14. MONITORING AGENCY NAME & ADDRESS(if different from Controlling Office)		15. SECURITY CLASS. (of this report) UNCLASSIFIED 15a. DECLASSIFICATION/DOWNGRADING SCHEDULE

16. DISTRIBUTION STATEMENT (of this Report)

APPROVED FOR PUBLIC RELEASE: DISTRIBUTION UNLIMITED

17. DISTRIBUTION STATEMENT (of the abstract entered in Block 20, if different from Report)

18. SUPPLEMENTARY NOTES

19. KEY WORDS (Continue on reverse side if necessary and identify by block number)

Three-Dimensional
Turbulent Boundary Layer
Thick Stern Boundary Layer
3:1 Elliptic Cross Section

20. ABSTRACT (Continue on reverse side if necessary and identify by block number)

A comprehensive set of experimental pressure, velocity, and turbulence data are presented across the stern of a three-dimensional model having 3:1 elliptic transverse cross sections. The axisymmetric displacement body concept is extended to three-dimensions and the pressure and velocity data are compared with the predictions of existing three-dimensional theoretical methods. The surface pressures for the displacement body are found to model,

(Continued on reverse side)

DD FORM 1473, 1 JAN 73 EDITION OF 1 NOV 65 IS OBSOLETE
S/N 0102-LF-014-6601

UNCLASSIFIED

SECURITY CLASSIFICATION OF THIS PAGE (When Data Entered)

(Block 20 continued)

satisfactorily, the measured pressure coefficients in all regions except over the aft 7 percent of body length. In this tail region, the boundary layer is much thicker than the cross section dimensions and the theory overpredicts the measured distributions of the mean velocity. Agreement is particularly poor in the inner region of the tail boundary layer, indicating a need to examine the eddy viscosity model currently used in computing the thick stern boundary layer of three-dimensional models. As was found in the axisymmetric case, the measured values of turbulence intensity, eddy viscosity, and mixing-length parameters in the stern region are much smaller than those of a thin boundary layer.

TABLE OF CONTENTS

LIST OF FIGURES

LIST OF TABLES

NOTATION

A	Van Driest's damping factor, $A = 26\nu \left(\frac{\tau_{tw}}{\rho}\right)^{-1/2}$
a	Length of major elliptical axis at given x/L
a_1	Turbulence structure parameter, $a_1 = \overline{-u'v'}/q^2$
a^*	Effective displacement thickness, see Equation (3)
b	Length of minor elliptical axis at given x/L
C_p	Pressure coefficient, $C_p = (p-p_o)/(1/2\rho U_o^2) = 1 - (U_e/U_o)^2$
h_1, h_2	Metric coefficients
K_1, K_2	Geodesic curvatures of the curves z = constant and x = constant, respectively
K_{12}, K_{21}	Functions of the geodesic curvatures and metric coefficients
L	Total body length
ℓ	Mixing length parameter: In the inner region

$$\ell = 0.4\, y\, [1-\exp(-y/A)]$$

In the outer region

$$\overline{uv} = \ell^2 \left[\left(\frac{\partial u}{\partial n_e}\right)^2 + \left(\frac{\partial w_\theta}{\partial n_e}\right)^2\right]^{1/2} \frac{\partial u}{\partial n_e}$$

n_e	Coordinate measured normal to the body profile in the y-z plane
p	Measured local static pressure
p_o	Measured ambient pressure
p_s	Measured static pressure
p_t	Measured dynamic total pressure

q^2	Turbulence parameter, $q^2 = \overline{u'^2} + \overline{v'^2} + \overline{w'^2}$
R_L	Reynolds number based on model length, $R_L = \frac{U_o L}{\nu}$
r_c	Radius of curvature at major or minor axis of elliptic cross section
U_e	Computed potential flow velocity on the displacement body
U_o	Free-stream velocity
U_δ	Potential flow velocity at the edge of the boundary layer
u, v, w	Mean velocity components in the x, y, and z directions, respectively
u_x, v_n, w_θ	Mean velocity components in the x, n_e, and θ directions, respectively
$\overline{u_x'^2}$, $\overline{v_n'^2}$, $\overline{w_\theta'^2}$	Turbulent fluctuations in the x, n_e, and θ directions, respectively
$\overline{u_x'v_n'}$, $\overline{u_x'w_\theta'}$	Reynolds stresses
x, n_e, θ	Coordinates used to present measured boundary layer data
x, y, z	Nonorthogonal boundary-layer coordinates, see Reference 6.
x_{TH}	Location of the thick stern boundary layer
α	Angle between the body surface and the body axis
δ_a, δ_b	Boundary-layer thickness at major and minor axis, respectively, of elliptical cross section
δ_r	Boundary-layer thickness measured in n_e-direction.
δ_p^*	Planar displacement thickness
ε	Eddy viscosity

ε_i, ε_o	Eddy viscosity in the inner and outer regions, respectively, see Equation (2)
θ	Angular coordinate measure in the y-z plane from the z-axis to the line joining the surface offset and elliptic center
$\bar{\theta}$	Angle between the x and z coordinates
Λ^*	Effective displacement area
ν	Kinematic viscosity of the fluid
ρ	Mass density of the fluid
τ_{tw}	Shear stress at the wall

ABSTRACT

A comprehensive set of experimental pressure, velocity, and turbulence data are presented across the stern of a three-dimensional model having 3:1 elliptic transverse cross sections. The axisymmetric displacement body concept is extended to three-dimensions and the pressure and velocity data are compared with the predictions of existing three-dimensional theoretical methods. The surface pressures for the displacement body are found to model, satisfactorily, the measured pressure coefficients in all regions except over the aft 7 percent of body length. In this tail region, the boundary layer is much thicker than the cross section dimensions and the theory overpredicts the measured distributions of the mean velocity. Agreement is particularly poor in the inner region of the tail boundary layer, indicating a need to examine the eddy viscosity model currently used in computing the thick stern boundary layer of three-dimensional models. As was found in the axisymmetric case, the measured values of turbulence intensity, eddy viscosity, and mixing-length parameters in the stern region are much smaller than those of a thin boundary layer.

ADMINISTRATIVE INFORMATION

The work described in this report was funded under the David W. Taylor Naval Ship Research and Development Center's Independent Research Program, Program Element 61152N, Project Number ZR 000 01, and Work Unit 1542-103.

INTRODUCTION

Many single-screw ship propellers operate inside of thick stern boundary layers. Satisfactory predictions of turbulent boundary-layer characteristics can be made for the forward portions of a body by solving the boundary-layer equations in either integral or differential forms. However, at the ship stern, the thickness of the boundary layer increases rapidly, mainly due to the diminishing cross-sectional area. The thickness of the stern boundary layer usually exceeds the thickness of the body. Detailed measurements of the turbulent boundary-layer characteristics in the thick stern boundary layers of axisymmetric bodies have been made by Huang et al.[*1,2] in order to gain insight into the physics of thick stern boundary layers. These measurements have been used to validate the displacement body concept as suggested by Preston[3] and Lighthill[4] for solving viscid-inviscid flow interaction and an improved turbulence model has been obtained for computing thick axisymmetric boundary

*A complete listing of references is given on page 105.

layers on two convex sterns and one concave stern.[1,2] The present work is an initial investigation into extending to three-dimensions the previous studies on axisymmetric bodies by Huang et al.[1,2]

Experiments have been made to measure the flow across the thick stern boundary layer of a three-dimensional body having a 3:1 elliptical transverse cross section. A 10.06 ft (3.07 m) fiberglass model was tested in the Center's Anechoic Flow Facility at a speed of 100 ft/sec (30.48 m/s), resulting in an overall Reynolds number based on length of 6.5×10^6. Pressure taps, embedded in the model, were used to measure the pressure distribution on the surface. Velocity and turbulence characteristics were measured using a two-element hot-film sensor and were analyzed with an on-line computer. Measurements include mean velocity profiles, turbulence intensities, Reynolds stresses, eddy viscosity, and mixing length.

Several experimental quantities are compared with data from existing theoretical methods using an iterative scheme. The potential flow distribution on the body surface is computed using the XYZ Potential Flow (XYZPF) computer code of Dawson and Dean.[5] An initial boundary-layer computation, using the McDonnell Douglas Corporation,[6] Cebeci, Chang, Kaups (C^2K) computer code, is made using the potential-flow pressure distribution on the body. Flow separation is predicted for this model by the C^2K code at axial locations greater than 4 percent of the body length and angular locations greater than 75 degrees. Excessive boundary-layer growth in the separated region caused the boundary-layer calculation to abort prematurely at 81 percent of the body length. Predictions of the effective displacement thickness for the remaining 19 percent of the body length are obtained by extrapolation. The potential and boundary-layer flow calculations are repeated once for a modified body and wake geometry, formed by adding the computed effective displacement thickness. Comparison of predicted and measured results shows that this procedure predicts accurate values of pressure over the forward 93 percent of the body and accurate mean velocity profiles in locations where the boundary layer is thin compared with cross-sectional area. The measured eddy viscosity distribution is compared with the thin boundary-layer model of Cebeci[6,7] and is found to be smaller than predictions.

In the following sections, the experimental techniques and model geometry are given in detail. The experimental data are presented and compared with theoretical predictions. The raw data and derived results are given in tabular form for independent use by other investigators.

WIND TUNNEL AND MODEL

The experimental investigation was conducted in the DTNSRDC Anechoic Wind Tunnel Facility. The wind tunnel has a closed jet test section that is 8 ft (2.4 m) square and 13.75 ft (4.19 m) long. The corners have fillets which are carried through the contraction. The test section is followed by an acoustically-lined large chamber 23.5 ft (7.16 m) long. It was found previously, by Huang et al.,[1] that the ambient free-stream turbulence levels, $\left(\sqrt{\overline{u'^2}}/U_o\right) \times 100$, are 0.075, 0.090, 0.100 and from 0.12 to 0.15 for free-stream velocities, U_o, of 24.4, 30.5, 38.1, and 45.7 m/s, respectively. Integration of the measured noise spectrum levels in the test section from 10 to 10,000 Hz indicated that the typical background acoustic noise levels at 30.5 m/s were about 93 dB re 0.0002 dyne/cm^2 (0.0002 Pa). These levels of ambient turbulence and acoustic noise were considered low enough so as not to unfavorably affect the measurement of boundary-layer characteristics. The maximum air speed that can be achieved is 200 ft/sec (61 m/s); in the present experiments the wind tunnel velocity was held constant at 100 ft/sec (30.48 m/s).

A simple three-dimensional body, having a 3:1 elliptic transverse cross section with a bow entrance length of 6.23 ft (1.897 m), was used for the present experimental investigation. The total model length is 10.06 ft (3.07 m) with a maximum major axis of 1.588 ft (0.48 m) and a maximum minor axis of 6.35 in. (16.12 cm). A schematic of the three-dimensional afterbody with the 3:1 elliptic cross section is shown in Figure 1. The major and minor elliptic axes are shown in Figure 1 as a and b, respectively. The model is shown in the anechoic wind tunnel facility in Figure 2. The support struts shown in the figure are not the struts used for this experiment. Model offsets are presented in Table 1.

The model was supported by two streamlined struts separated by one-third of the model length. The struts are 0.5-in. (1.27-cm) thick with a 1.5-in. (3.81-cm) chord upstream and 2.25-in. (5.72-cm) thick with a 6.0-in. (15.24-cm) chord downstream. The model is designed to rotate 90 degrees radially about a center axis to permit vertical traversing normal to the surface pressure taps (see section on Instrumentation). The disturbances generated by the supporting struts were within the region below the horizontal centerplane. Therefore, all of the experimental data were taken above the model on the vertical centerplane along the upper meridian

where there was no effect from the supporting struts. One-half of the model length protruded beyond the closed jet working section into the open-jet section. The ambient static pressure coefficients across and along the entire open-jet chamber (7.2 m × 7.2 m × 6.4 m) were found to vary less than 0.3 percent of the dynamic pressure. Tunnel blockage and longitudinal pressure gradient effects along the tunnel length were almost completely removed by testing the afterbody in the open-jet section.

The location of the boundary-layer transition from laminar to turbulent flow was artificially induced by a 0.024-in. (0.61-mm) diameter trip wire located at x/L = 0.05. Huang et al.[1] found that the trip wire effectively moved the location of the virtual origin to x/L = 0.015 for axisymmetric models at a length Reynolds number of 5.9×10^6. The virtual origin[8] for the turbulent flow is defined such that the sum of the laminar frictional drag from the nose to the trip wire, the parasitic drag of the trip wire, and the turbulent frictional drag aft of the trip wire is equal to the sum of the laminar frictional drag from the nose to the virtual origin and the turbulent frictional drag from the virtual origin to the after end of the model. The virtual origin locations for the three-dimensional body are expected to be different for different streamlines. Due to the limited number of grid locations used in the present calculation, the location of the transition for the C^2K boundary-layer calculation is set at a constant value of x/L = 0.030. The computed differences in velocities using x/L = 0.01 and x/L = 0.03, for axisymmetric body 1,[1,2] are found to be less than 0.1 percent of the free-stream velocities in the tail region. Thus, the error of using the constant transition location of x/L = 0.03 for the present C^2K computation is expected to be negligible.

INSTRUMENTATION

A series of 0.031-in. (0.8-mm) diameter pressure taps were embedded normal to the surface of the stern at nine x/L locations. When the model was rotated about its axis, the pressure taps were at the upper meridian location. Additional taps were added for model alinement; see Figures 3 and 4. The model was alined by balancing the surface static pressure about a line of symmetry. From Figure 3, the model is alined when symmetrically located pressure taps at c and d, and at e and f, give equal pressures, i.e., p (c) = p (d), p (e) = p (f). The model was rotated to

eight test positions and the alinement was checked by the pressure balance technique. A Preston tube using a 0.072-in. (1.83-mm) inside diameter was attached and alined with the flow at the pressure taps to measure the shear stress. The Preston tube was calibrated in a 1-in. (2.54-cm) diameter water-pipe flow facility described by Huang and von Kerczek.[9] These pressure taps were connected to a multiple pressure scanivalve system that takes one integral pressure transducer with its zeroing circuit and measures a single pressure in sequence along the stern upper meridian. The pressure transducer was designed for measuring low pressures of up to 1 psi (6.895×10^{-3} Pa). The zero-drift linearity, scanivalve hysteresis, and pressure transducer zeroing circuit were carefully checked and the overall accuracy was found to be within 0.5 percent of the dynamic pressure.

The mean axial and radial velocities and the turbulence intensities for the Reynolds stress calculations were measured by a TSI, Inc. Model 1241-20 "X" type hot-film probe. The probe elements are 0.002 in. (0.05 mm) in diameter with a sensing length of 0.04 in. (1.0 mm). The spacing between the two cross elements is 0.04 in. (1.0 mm). A typical schematic of the hot-film probe used is shown in Figure 5. A two-channel hot-wire and hot-film anemometer with linearizers was used to monitor the response of the hot-film probe. A temperature compensating sensor (probe) was used with each hot-film element to regulate the operating temperature of the sensor with changes in air temperature. The "X" hot film and its temperature-compensated sensor were calibrated together through the expected air temperature-range and supplied with their individual linearization polynomial coefficients at the factory.

The frequency response of the anemometer system, for reliable measurements claimed by the manufacturer, is 0 to 100 kHz. Calibration of the "X" hot film was made before and after each set of measurements. It was found that the hot-film anemometer system had a ± 0.5 percent accuracy, ± 0.75 ft/sec (± 0.23 m/s) accuracy at the free-stream velocity of 150 ft/sec (45.72 m/s), during the entire experiment. An estimate was made of the crossflow velocity by yawing the "X" hot-film probe in the free stream. It was found that the crossflow velocities were about one percent of the free-stream velocity.

The linearized signals were fed into a Time/Data Model 1923-C real-time analyzer. Both channels of the analog signal were digitized at a rate of 128 points

per second for 8 sec. These data were immediately analyzed by a computer to obtain the individual components of mean velocity, turbulence fluctuation, and Reynolds stress on a real time basis.

A traversing system with a streamlined strut was mounted on a guide plate that permitted the traverse to be locked in various stationary positions parallel to the longitudinal model axis.

DISPLACEMENT BODY METHOD

The theoretical method evaluated in this report is an initial attempt at extending to three-dimensions the displacement body concept described by Wang and Huang[10] and by Huang et al.,[1,2] for axisymmetric bodies. The pressure distribution is calculated using the XYZ Potential Flow (XYZPF) computer code of Dawson and Dean.[5] The input offsets to the XYZPF code are given in Table 1. The boundary-layer flow over the body is calculated by using the differential method of Cebeci, Chang, and Kaups (denoted C^2K).[6] The flow in the wake is modeled only in the near wake region of $0.93 \leq x/L \leq 1.05$.

The C^2K method consists of using Keller's two-point finite difference method[11] and Cebeci and Stewartson's procedure[6] for computing flows in which the transverse velocity component contains regions of reverse flow to solve three-dimensional boundary-layer equations. The governing equations for three-dimensional incompressible laminar and turbulent flows are given by

Continuity Equation

$$\frac{\partial}{\partial x}(uh_2 \sin \overline{\theta}) + \frac{\partial}{\partial z}(wh_1 \sin \overline{\theta}) + \frac{\partial}{\partial y}(vh_1h_2 \sin \overline{\theta}) = 0 \quad (1a)$$

x-Momentum Equation

$$\frac{u}{h_1}\frac{\partial u}{\partial x} + \frac{w}{h_2}\frac{\partial u}{\partial z} + v\frac{\partial u}{\partial y} - K_1u^2 \cot \overline{\theta} + K_2w^2 \csc \overline{\theta} + K_{12}uw$$

$$= -\frac{\csc^2 \overline{\theta}}{h_1}\frac{\partial(p/\rho)}{\partial x} + \frac{\cot \overline{\theta} \csc \overline{\theta}}{h_2}\frac{\partial(p/\rho)}{\partial z} + \frac{\partial}{\partial y}\left(\nu\frac{\partial u}{\partial y} - \overline{u'v'}\right) \quad (1b)$$

z-Momentum Equation

$$\frac{u}{h_1}\frac{\partial w}{\partial x} + \frac{w}{h_2}\frac{\partial w}{\partial z} + v\frac{\partial w}{\partial y} - K_2 w^2 \cot\overline{\theta} + K_1 u^2 \csc\overline{\theta} + K_{21}uw$$

$$= \frac{\cot\overline{\theta}\csc\overline{\theta}}{h_1}\frac{\partial(p/\rho)}{\partial x} - \frac{\csc^2\overline{\theta}}{h_2}\frac{\partial(p/\rho)}{\partial z} + \frac{\partial}{\partial y}\left(\nu\frac{\partial w}{\partial y} - \overline{v'w'}\right) \tag{1c}$$

where u, v, and w = velocity components in the x, y, and z directions, respectively

x, y, and z = nonorthogonal boundary-layer coordinates, as given in Reference 6

ρ = fluid density

p = pressure on the body

h_1, h_2 = metric coefficients

K_1, K_2 = geodesic curvatures of the curves z = constant and x = constant, respectively

K_{12}, K_{21} = functions of the geodesic curvatures and metric coefficients

$\overline{\theta}$ = angle between the coordinates x and z

ν = kinematic viscosity of the fluid

$\overline{u'v'}$, $\overline{v'w'}$ = Reynolds stresses

The eddy-viscosity concept is used to relate the Reynolds stresses to the mean velocity profiles by

$$\overline{u'v'} = \begin{cases} \varepsilon_i \dfrac{\partial u}{\partial y}, & \text{inner region } 0 \leq y \leq y_c \\ \\ \varepsilon_o' \dfrac{\partial u}{\partial y}, & \text{outer region } y_c < y \end{cases} \tag{2}$$

where $\varepsilon_i = \ell^2 \left[\left(\frac{\partial u}{\partial y}\right)^2 + \left(\frac{\partial w}{\partial y}\right)^2 + 2\cos\overline{\theta}\left(\frac{\partial u}{\partial y}\right)\left(\frac{\partial w}{\partial y}\right)\right]^{1/2}$

which is the eddy viscosity in the inner region

with $\ell = 0.4y \left[1-\exp\left(-\frac{y}{A}\right)\right]$

$$A = 26 \frac{\nu}{u_\tau}$$

$$u_\tau = \left(\frac{\tau_{tw}}{\rho}\right)^{1/2}$$

$$\tau_{tw} = \mu \left[\left(\frac{\partial u}{\partial y}\right)_w^2 + \left(\frac{\partial w}{\partial y}\right)_w^2 + 2 \cos \overline{\theta} \left(\frac{\partial u}{\partial y}\right)_w \left(\frac{\partial w}{\partial y}\right)_w\right]^{1/2}$$

$$\varepsilon_o = 0.0168 \left| \int_0^\infty (u_{te}-u_t)dy \right|$$

$$u_{te} = (u_e^2+w_e^2+2u_e w_e \cos \overline{\theta})^{1/2}$$

$$u_t = (u^2+w^2+2uw \cos \overline{\theta})^{1/2}$$

y_c is the value of y at which $\varepsilon_i = \varepsilon_o$

The displacement model presently used for this body adds the theoretical effective displacement thickness (defined below) to the body surface along the major (y)- and minor (z)-axes of the elliptic cross section. The surface profile along each of these axes is extended by hand-fairing from the location of separation, or 93 percent of body length (whichever occurs first), to 5-percent aft of the body, resulting in an open body. An elliptical cross section is defined between the offsets of the major and minor axes.

The C^2K computer program has been modified to compute the effective displacement thickness a* at the major and minor axes along the axial length of the body. The definition for a*, which is similar to the axisymmetric expression, is

$$a^* = \frac{-r_c + \sqrt{r_c^2+2\Lambda^* \cos \alpha}}{\cos^2 \alpha} \tag{3}$$

where r_c = radius of curvature at the particular axis of interest in the y-z plane, i.e.,

$$r_{c_{y\text{-axis}}} = \frac{\left[1 + \left(\frac{dy}{dz}\right)^2\right]^{3/2}}{\frac{d^2y}{dz^2}}$$

and

$$r_{c_{z\text{-axis}}} = \frac{\left[1 + \left(\frac{dz}{dy}\right)^2\right]^{3/2}}{\frac{d^2z}{dy^2}}$$

Λ^* = effective displacement area, $\Lambda^* = \int_0^{\delta} \left(1 - \frac{u_t}{u_{te}}\right) r dy$

α = angle between the body surface and the body axis,

$$\alpha = \tan^{-1}\left(\frac{\Delta y}{\Delta x}\right) \text{ or } \alpha = \tan^{-1}\left(\frac{\Delta z}{\Delta x}\right)$$

r = $r_c + y \cos \alpha$

y = normal distance from the wall

Unlike the procedure for an axisymmetric body, which uses an iterative procedure consisting of the calculation of pressure and boundary-layer flow over successive displacement bodies, the present scheme for three-dimensional bodies uses only one iteration. The uncertainties in defining the displacement body in the region between the major and minor axes and in the near-wake region lead one to question the usefulness of an iterative procedure at present. It is anticipated, however, that once improvements are made in defining the displacement model over the entire body length and in the wake region, an iterative procedure will be adopted again.

One further obstacle arose in defining the displacement body for the 3:1 transverse cross-sectional model. Excessive boundary-layer growth in the C^2K boundary-layer computation caused the computer program to abort prematurely. No values for

the effective displacement thickness were computed along the major elliptic axis meridian for locations greater than 81 percent of the body length. A careful hand-fairing was used to define the effective displacement thickness along the major axis meridian.

COMPARISON OF EXPERIMENTAL AND THEORETICAL RESULTS

All data are presented in the coordinate system used to experimentally measure the boundary-layer flow. The coordinate system, denoted $x - n_e - \theta$, is given in Figures 1 and 4. The axial coordinate x is measured from the nose of the body and passes through the center of the elliptic profile. The coordinates n_e and θ are defined along an axial cut normal to the x-axis, i.e., in the y-z plane. The normal component n_e is measured from the model surface and is normal to the elliptic surface. The angular coordinate θ is defined as the angle, in degrees, measured from the z-axis to the line joining the surface offset and elliptic center.

PRESSURE DISTRIBUTION

The steady pressure was measured along the stern surface using pressure taps. These taps are located at nine axial and five radial positions, for a total of 45 measurements. The pressure coefficient C_p is computed from the measured pressures by the relationship

$$C_p = \frac{p - p_o}{p_t - p_s} = \frac{p - p_o}{\frac{1}{2}\rho U_o^2} \tag{4}$$

where p = measured local static pressure

p_o = measured ambient pressure

p_t = measured dynamic total pressure

p_s = measured static pressure

ρ = mass density of the fluid

U_o = free-stream velocity

The measured values of the pressure coefficients are given in Table 2 and compared in Figure 6 with two analytically-predicted distributions of pressure

coefficient. The dashed curve, denoted by potential flow theory, represents the predictions of the XYZ potential flow method of Dawson and Dean[5] before using the displacement body concept. The solid curve shows C_p on the displacement body after one iteration of the displacement body procedure. The computed pressure coefficient is

$$C_p = 1 - \left(\frac{U_e}{U_o}\right)^2 \tag{5}$$

where U_e is the computed potential flow velocity on the displacement body and U_o is the free-stream velocity, 100 ft/sec (30.48 m/s).

Two results are immediately apparent from the comparisons given in Figure 6. First, the theory was not able to predict accurately the values of the pressure coefficient for $x/L > 0.93$. At these locations, the boundary layer is much thicker than the body cross section and theoretical displacement thicknesses were not available due to premature abortion of the computer code calculation in the separation region. Second, the predictions using the displacement body concept agree more closely with the measured values than do the data denoted as potential flow. After one iteration of the displacement procedure, overall agreement between theoretical and measured values of the pressure coefficient is considered good even though the predicted values are slightly lower than the measured values. No further iterations of the displacement method have been implemented at present. Further refinement of the three-dimensional wake and near wake region by the displacement body conception should improve the accuracy of the theoretical prediction.

MEAN VELOCITY PROFILES

Mean velocity measurements were taken with an "X" hot-film sensor which was stepped away from the body in the n_e direction. Measurements of velocity in the axial x and normal n_e directions, u_x and v_n, respectively, were taken with the probe elements alined vertically. The sensor elements were rotated 90 degrees to the horizontal position to measure the mean velocity w_θ in the θ direction. An on-line computer was used to collect data at a sample rate of 1024 data values in 8 sec.

The measured values of the mean velocity components are listed in Tables 3 through 9 along with other measured quantities. Tables 3 through 9 give the measured data along the 0, 67, 80, 83, 86, 87, and 90-degree planes, respectively, for various axial locations along the model. The velocity components are nondimensionalized by the free-stream velocity U_o. As shown in the tables, the mean axial velocity is the largest of the three measured components. Measured mean velocity profiles in the x and n_e directions are shown in Figures 7a through 7c. Each figure presents the profiles at various angular positions for a particular axial location. Figure 7a shows that the mean axial velocity profiles vary only slightly with angular position on the model at $x/L = 0.719$. Also, the boundary layer is thin, with an overall thickness of less than 1 in. Little variation in the normal velocity component is noted. Examining the profiles further aft on the model, the boundary layer thickens with increased angular position. Little variation in profile occurs for angles less than or equal to 80 degrees. However, profiles between 80 and 90 degrees become increasingly fuller with increased angular location. From repeated measurements, the accuracies of the experimental measurements of u_x/U_o and v_n/U_o are estimated to be about 0.5 percent and 1.0 percent, respectively.

Comparisons of the measured and predicted mean axial velocity profiles are shown in Figure 8 at selected positions along the model. The circular symbols represent the "X" hot-film measurements and the solid curves represent the theoretical results of the C^2K method[6] using the displacement body concept. Calculations using the C^2K computer code were made using the initial velocity profiles generated within the computer code. Calculations were begun at 1.5 percent of the body length with the transition located at 3 percent of the body length. Use of a limited, discrete set of offsets to define the model for computational purposes forced the use of this transition location. As shown in Figure 8a, the C^2K method, used with and without the displacement body, predicted the same profile at $x/L = 0.719$ and 0 degrees. For the basic body geometry, prior to using the displacement body concept, the C^2K method experienced excessive boundary-layer growth and aborted prematurely, giving no predictions for axial locations $x/L \geq 0.81$ and angles greater than 80 degrees. The agreement between the computed and measured mean axial velocity profiles is good at $x/L = 0.719$ and 0 degrees where the boundary layer is thin.

Agreement is also fairly good at x/L = 0.954 and 0 degrees. However, at x/L = 0.954 and angular positions 83, 86, and 90 degrees, the measured axial velocity components are smaller than the predicted components, with flow reversal predicted at 83 and 86 degrees. Agreement inside the boundary layer is particularly poor. Since the eddy viscosity model plays an important role in this region, it is essential to examine the eddy viscosity model used for computing the thick three-dimensional stern boundary layer.

MEASURED TURBULENCE CHARACTERISTICS

The turbulence characteristics of the thick three-dimensional boundary layer were measured using an "X" hot-film probe. An on-line computer was used to collect data at a sample rate of 1024 data values in 8 sec. The root-mean-square values of turbulence velocity were recorded at each probe position and the eddy viscosity and mixing length values were computed from the measured Reynolds stresses and the measured mean velocity profiles.

MEASURED REYNOLDS STRESSES

The distribution of the Reynolds stresses $\overline{-u'_x v'_n}$, $\overline{-u'_x w'_\theta}$, $\overline{u'^2_x}$, $\overline{v'^2_n}$, and $\overline{w'^2_\theta}$ represent the turbulence characteristics in the thick boundary layer. The mean-square turbulent velocity fluctuations $\overline{u'^2_x}$ in the axial direction and $\overline{v'^2_n}$ in the n_e direction, and the Reynolds stress $\overline{-u'_x v'_n}$ were measured with the "X" hot-film probe elements alined vertically. The probe elements were rotated 90 degrees to the horizontal position to measure both the turbulent fluctuation $\overline{w'^2_\theta}$ in the θ direction and the Reynolds stress $\overline{-u'_x w'_\theta}$. Linear interpolation was used to approximate $\overline{w'^2_\theta}$ and $\overline{-u'_x w'_\theta}$ at the same off-body positions as the data measured in the vertical direction. All measured values of the turbulent fluctuations and the measured Reynolds stresses are given in Tables 3 through 9.

The nondimensionalized distributions of the measured turbulent fluctuations $\sqrt{\overline{u'^2_x}}/U_o$, $\sqrt{\overline{v'^2_n}}/U_o$, and $\sqrt{\overline{w'^2_\theta}}/U_o$ and Reynolds stress $-100\ \overline{u'_x v'_n}/U_o$ at selected locations along the model, are shown in Figures 9 through 13. As can be seen

in Tables 4 through 8, the Reynolds stress $-\overline{u_x' w_\theta'}$ is typically one order of magnitude less than the Reynolds stress $-\overline{u_x' v_n'}$. An exception to this trend occurs for the angular location of 80 degrees, where measured values of $-\overline{u_x' w_\theta'}$ exceed the values of $-\overline{u_x' v_n'}$. This is the region of predicted separation by the C^2K computer code. The measured distributions of $-\overline{u_x' w_\theta'}$ are not depicted graphically.

The results given in Figures 9 through 13 and in Tables 4 through 8 indicate that $\overline{u_x'^2}/U_o$ is the largest component of turbulent velocity fluctuation and that the normal component $\overline{v_n'^2}/U_o$ is the smallest component. In addition, the fluctuations are larger near the body's surface and reduce to values near zero as the edge of the boundary layer is approached. At the body's surface, the no-slip boundary condition requires the velocity and turbulent fluctuations to be zero, indicating that a sharp gradient exists in the turbulent fluctuations at the wall. This gradient, which becomes apparent in the measured data as the boundary layer thickens, is evident at all angular locations where $x/L \geq 0.914$. Similar trends have been noted by Huang et al.[1,2] for axisymmetric bodies.

The measured distributions of the Reynolds stress $- 100\ \overline{u_x' v_n'}/U_o$ are also shown in Figures 9 through 13. The maximum value of this component of Reynolds stress generally occurs near the body wall showing little variation with location along the model. When the boundary layer is thin, the spatial resolution of the "X" hot-film probe may not be fine enough to measure precisely the Reynolds stress distributions near the wall. The maximum value of the $-\overline{u_x' v_n'}$ Reynolds stress occurs near the wall for all locations measured except $x/L = 0.914$ and $\theta = 86$ degrees.

A turbulence structure parameter a_1, where $a_1 = \overline{u_x' v_n'}/q^2$ and $q^2 = \overline{u_x'^2} + \overline{v_n'^2} + \overline{w_\theta'^2}$, was investigated by Huang et al.[1,2] for axisymmetric bodies. Huang's results for axisymmetric bodies showed that this parameter has a value of 0.16 for $0 \leq n_e \leq 0.6\ \delta_r$ and that the value of a_1 decreases toward the edge of the boundary layer. The parameter δ_r, used to normalize the distance from the model n_e, is defined as the distance from the wall surface in the n_e direction at which the measured turbulent fluctuation $\overline{u_x'^2}/U_o$ reaches the value 0.01. Figures 14a through 14d show the

range of values of the parameter a_1 for the three-dimensional body. At most axial positions for the 0- and 67-degree locations, the value of a_1 is, approximately, 0.16 for $n_e/\delta_r \leq 0.8$. The value of a_1 reduces to 0.07 at the 80-degree plane, the region of separation predicted by the C^2K computer code. For the remaining angular positions, the value a_1 fluctuates between 0.04 and 0.16. A reduction in the value of the parameter a_1 was also found by Shiloh et al.[12] near separation for an airfoil type flow.

The free-stream turbulent velocity fluctuations were not removed from the measured values of q^2. The reduction in the values of a_1 near the edge of the boundary layer may be caused, in part, more by the larger contribution of the free-stream turbulence to q^2 than to $\overline{-u'_x v'_n}$.

EDDY VISCOSITY AND MIXING LENGTH

The values of eddy viscosity and mixing length are not measured directly, but are obtained, as in the axisymmetric case,[1,2] from the measured values of the Reynolds stress $\overline{-u'_x v'_n}$ and the mean velocity gradient $\partial u_x/\partial n_e$. The definitions used to compute these quantities are

$$\overline{-u'_x v'_n} = \varepsilon \frac{\partial u_x}{\partial n_e}$$

$$= \ell^2 \left[\left(\frac{\partial u_x}{\partial n_e} \right)^2 + \left(\frac{\partial w_\theta}{\partial n_e} \right)^2 + 2 \left(\frac{\partial u_x}{\partial n_e} \right) \left(\frac{\partial w_\theta}{\partial n_e} \right) \cos \bar{\theta} \right]^{1/2} \frac{\partial u_x}{\partial n_e} \tag{6}$$

When the values of w_θ/u_x are less than 0.1 and the value of $\bar{\theta}$ is 90 degrees for the present measurements, Equation (6) may be approximated by

$$\overline{u'_x v'_n} = \ell^2 \left| \frac{\partial u_x}{\partial n_e} \right| \frac{\partial u_x}{\partial n_e} \tag{7}$$

A spline curve is used to fair the experimental data before the velocity gradient is obtained numerically.

The nondimensional distributions of the eddy viscosity $\varepsilon/(U_\delta \delta_p^*)$ determined from the data are shown in Figures 15a through 15d. The parameters U_δ and δ_p^* are defined as the potential flow velocity at the edge of the boundary layer and the planar displacement thickness, respectively, for the displacement body. The solid curve shown in these figures is the Cebeci and Smith[7] thin boundary layer formula, given by

$$\frac{\varepsilon}{U_\delta \delta_p^*} = \frac{0.0168}{1 + 5.5\left(\frac{n_e}{\delta_r}\right)} \tag{8}$$

All values of eddy viscosity for the 3:1 elliptic model are smaller than the experimentally-derived values recommended by Cebeci and Smith for thin boundary layers.

The experimentally-determined distributions of the nondimensional mixing length, ℓ_p/δ_r, are shown in Figures 16a through 16d. The solid curve in these figures represents the thin boundary-layer model of Bradshaw et al.[13] Agreement between theory and measurements is, at best, fair for angular locations of 0 and 67 degrees; for angular locations greater than 67 degrees, the measured values of mixing length are much smaller than the predictions.

For an axisymmetric turbulent boundary layer, Huang et al.[1,2] proposed a turbulence model relating the mixing length to the square root of the entire turbulence annulus area between the body surface and the edge of the boundary layer. As seen in Figures 14 through 16, the values of measured turbulence intensity, eddy viscosity, and intermittency across a turbulent boundary layer decrease from a maximum value at 60 percent of the boundary-layer thickness to zero at the outside edge of the boundary layer. The effective gross turbulence area relevant to the mixing length parameter is $[(a+0.6\delta_a)(b+0.6\delta_b)-(a+\varepsilon_a)(b+\varepsilon_b)]$; where ε_a and ε_b are the effective thicknesses of the separation bubble (low turbulence mixing) in the direction of the major and minor axes, a and b, respectively, of the elliptical cross-section, and δ_a and δ_b are the boundary-layer thicknesses along the a and b

axes. A new mixing length model is assumed to apply to a thick three-dimensional stern boundary layer. The schematic representation of effective turbulence areas, as determined by the areas between the body surfaces and the contours of $0.6\delta_r$ at $x/L = 0.81$ and 0.95, are shown in Figure 17. The outside edges of the effective turbulence areas are very close to the contours of $\sqrt{\overline{u_x'^2}}/U_o = 0.04$. Further outside of these edges, turbulence intensities reduce to 0.01 at the edge of the boundary layer. The mixing length parameter is assumed to be proportional to the square-root of these effective turbulence areas, e.g.,

$$\ell \sim \sqrt{(a+0.6\delta_a)(b+0.6\delta_b)-ab} \equiv A(x)$$

where the value of ε_a is assumed to be small and will be neglected and the value of ε_b is zero since no separation occurs there. The values of ε_a and ε_b may not be negligible if the separation region is so large that the effective turbulence area is reduced significantly. However, in the inner region, the conventional mixing length in the wall region, Equation (2), is assumed to apply. The mixing length ℓ is assumed to be the same at the intersection of the inner and the outer region, $y = y_c$ in Equation (2). Figures 18a through 18c show the normalized mixing length distributions for three axisymmetric bodies studied by Huang et al.[1,2] These figures show that the measured values for the three axisymmetric models agree reasonably well; each peaking at a value of approximately 0.05. The values of ℓ/A at various locations for the present three-dimensional model are shown in Figures 18d through 18j. With the exception of the 80-degree angular location, values of the non-dimensional mixing length remain fairly constant over the stern with respect to both angular and axial positions.

The data in Figure 18 support the use of a revised mixing length formulation. The existing thin turbulent boundary-layer method can be applied to the axisymmetric or three-dimensional elliptical body at locations forward of where the boundary layer thickness reaches 20 percent of the major or minor axis value. Downstream of this location, the apparent mixing length ℓ may be approximated by the thin flat boundary layer of Bradshaw et al.[13] as

$$\frac{\ell}{\ell_o} = 1 \qquad \text{for } \delta_a \leq 0.2a \quad \text{and} \quad \delta_b \leq 0.2b$$

$$\frac{\ell}{\ell_o} = \frac{\sqrt{[a(x)+0.6\delta_a(x)][b(x)+0.6\delta_b(x)]-a(x)b(x)}}{\sqrt{[a(x_{TH})+0.6\delta_a(x_{TH})][b(x_{TH})+0.6\delta_b(x_{TH})]-a(x_{TH})b(x_{TH})}} \qquad \begin{array}{l}\text{for } \delta_a > 0.2a \\ \text{or } \delta_b > 0.2b\end{array} \tag{9}$$

where x is the axial location downstream of the initial location of the thick stern boundary layer x_{TH}. The beginning of the thick stern boundary layer is selected as the axial location where the local value of δ_a or δ_b grows to the value of 0.2a or 0.2b, respectively (whichever occurs first). The new formulation can be incorporated into existing axisymmetric and three-dimensional turbulent boundary-layer differential methods and must be evaluated for a variety of stern boundary layers before its validity can be fully established.

CONCLUSIONS

The results of recent experimental investigations of the thick stern boundary layer on a three-dimensional body having 3:1 elliptic transverse cross sections are presented. Comprehensive boundary layer measurements, including mean and turbulence velocity profiles and static pressure distributions are given in detail.

An initial attempt has been made at extending to three dimensions the Lighthill and Preston displacement body concept used to treat the viscid-inviscid stern flow interaction on axisymmetric bodies. The results of this initial investigation indicate that the use of the displacement model method significantly improves theoretical predictions of the measured pressure coefficients on the body surface. However, agreement between measured and predicted pressure coefficients remains poor in the thick stern boundary-layer region over the last 7 percent of the body. Theoretical predictions of the measured mean axial velocity profiles are satisfactory in the thin boundary-layer region, but are generally larger than the measured values when the boundary layer thickens. Refinements in the present displacement body modeling scheme to determine the effective displacement thickness accurately over the entire model surface and wake may improve the pressure distribution predictions in the thick stern boundary layer.

Measured values of eddy viscosity and mixing length in the thick stern boundary layer were found to be smaller than values which have been proposed for thin boundary layers. Because eddy viscosity and mixing length models play an important role in boundary-layer calculations, a modification of the theoretical mixing length model is proposed which may improve the prediction of the boundary layer.

Further work in this area is needed. A larger data base of experimental results on a variety of three-dimensional geometries will aid in the development of improved theoretical models to predict the viscid-inviscid stern flow interaction. The proposed new mixing length formulation must be evaluated further.

ACKNOWLEDGMENTS

The authors would like to thank the staff at the DTNSRDC Anechoic Flow Facility for their cooperation during the testing and to express their gratitude to Dr. K.C. Chang for his many consultation sessions on the use of the C^2K computer program.

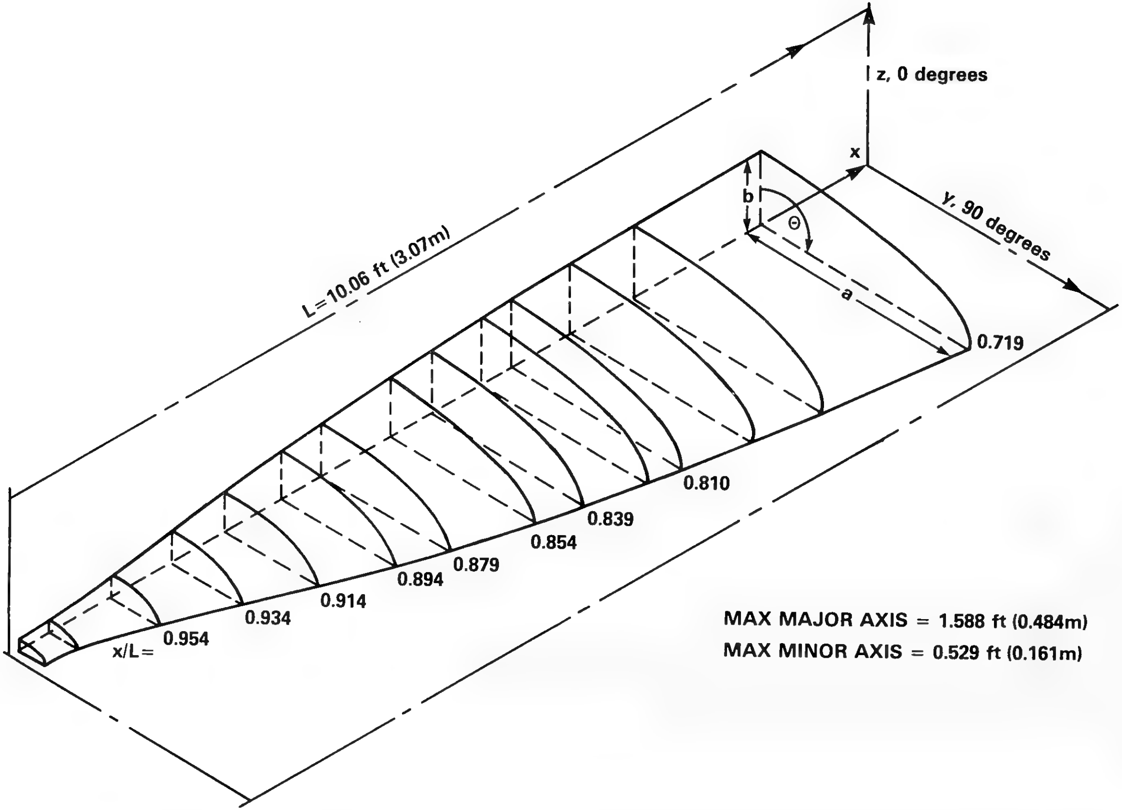

Figure 1 - Schematic of the Three-Dimensional Afterbody Having a 3:1 Elliptic Transverse Cross Section

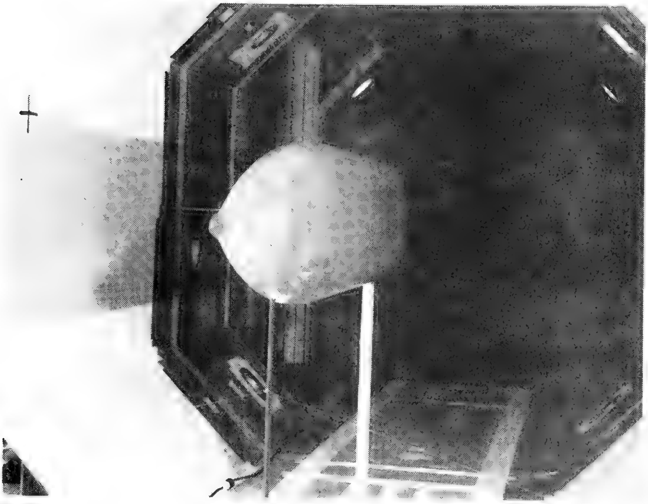

Figure 2a - Stern View

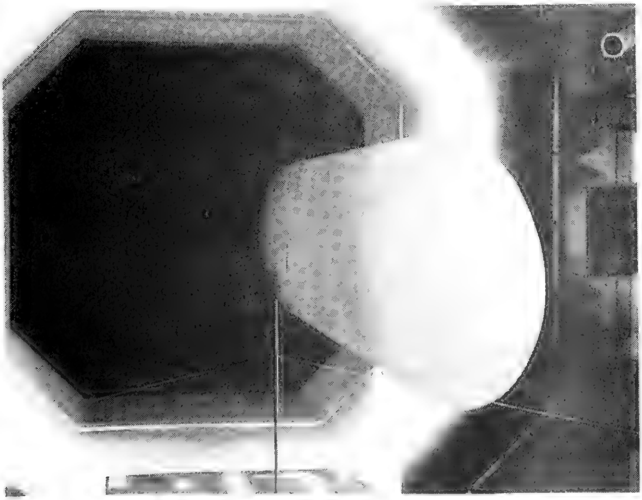

Figure 2b - Frontal View

Figure 2 - Model Mounted in Anechoic Wind Tunnel

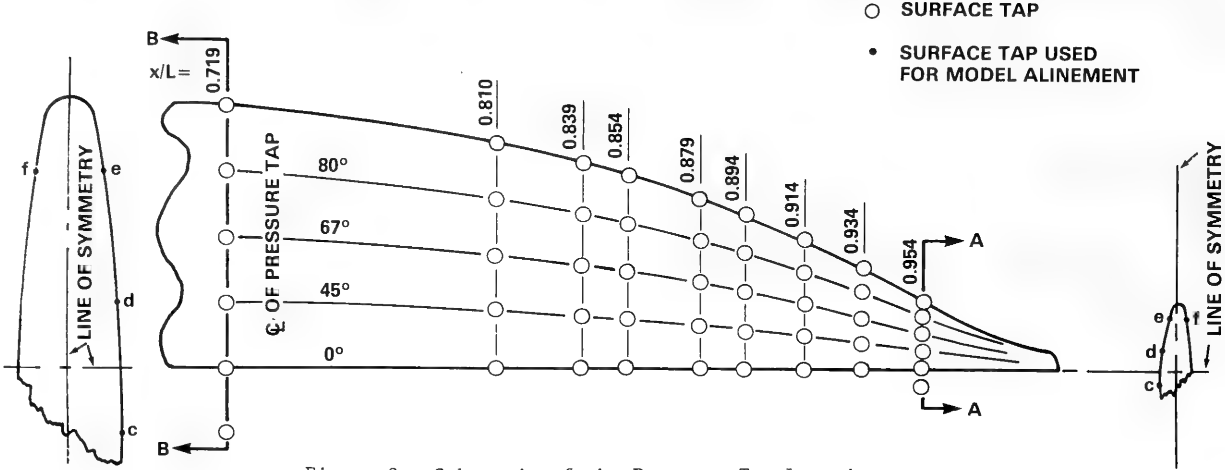

Figure 3 - Schematic of the Pressure Tap Locations

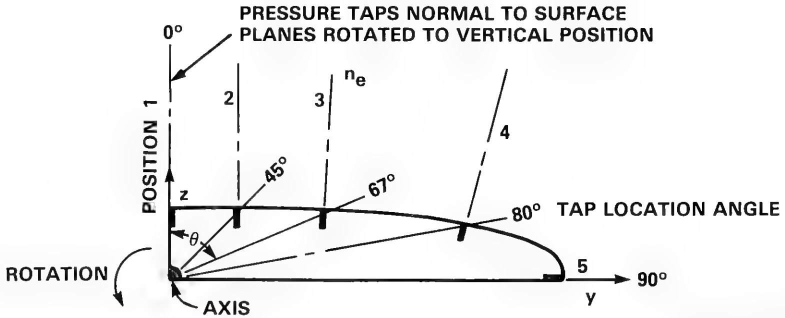

Figure 4 - Schematic of a Typical Section at x/L

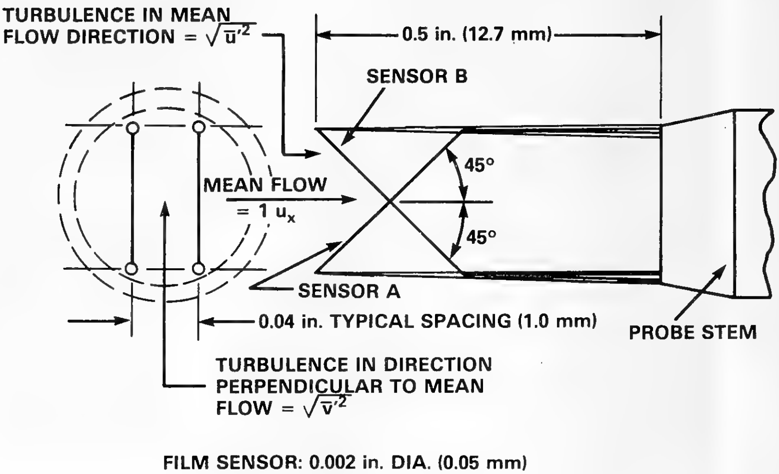

Figure 5 - Schematic of a Two-Element Sensor Alined 90 Degrees to Each Other and 45 Degrees to the Probe Axis

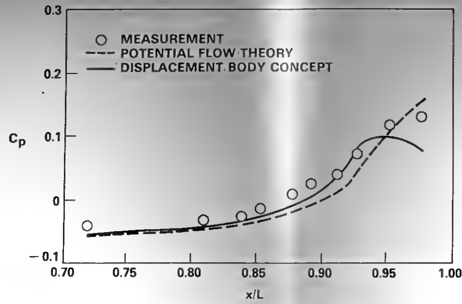

Figure 6a - θ = 0 Degrees

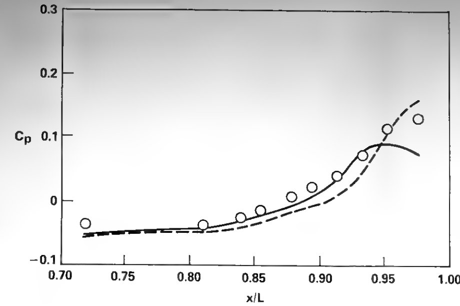

Figure 6b - θ = 45 Degrees

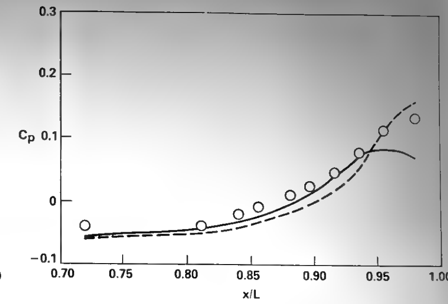

Figure 6c - θ = 67 Degrees

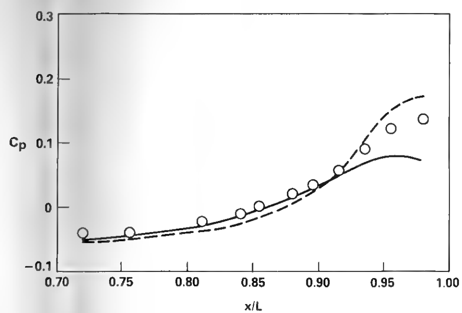

Figure 6d - θ = 80 Degrees

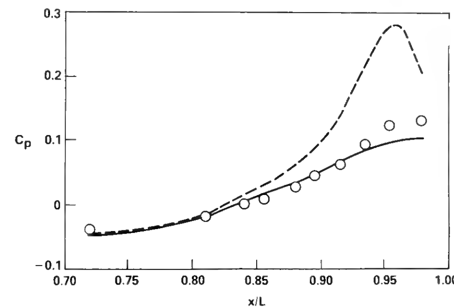

Figure 6e - θ = 90 Degrees

Figure 6 - Computed and Measured Stern Pressure Distribution for Angular Location

Figure 7 - Measured Mean Axial and Radial Velocity Distributions

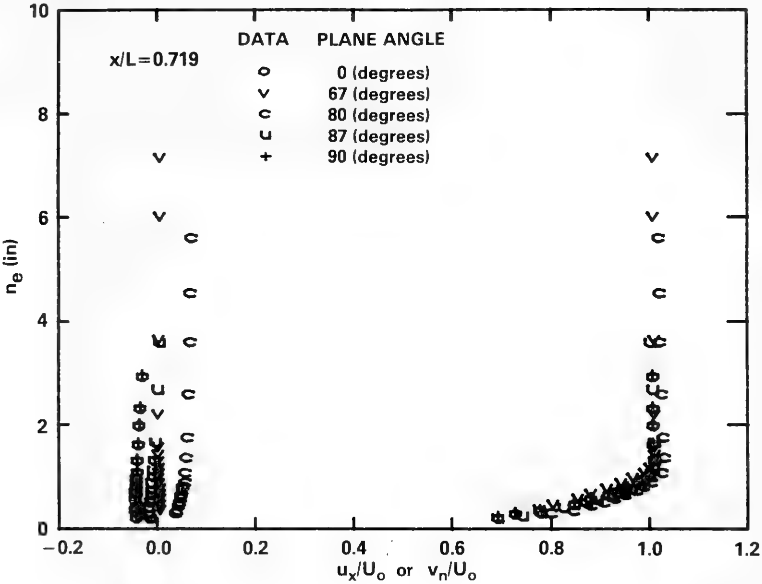

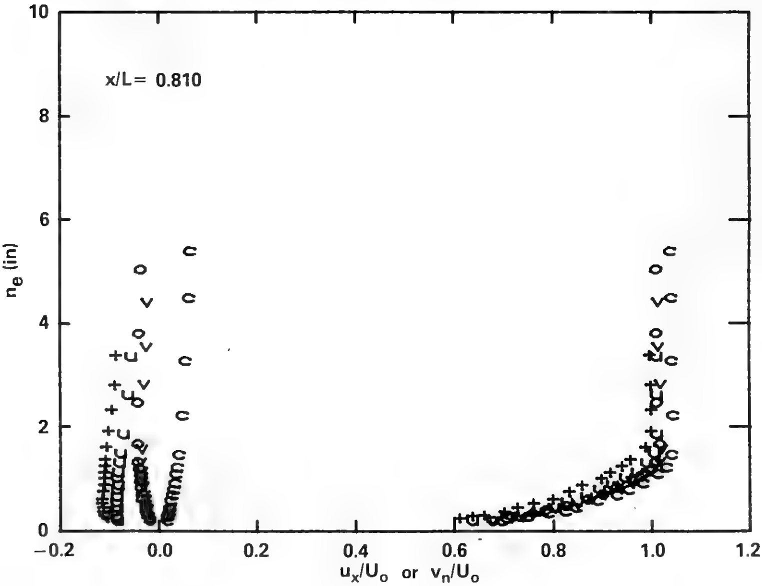

Figure 7a - Nondimensional Axial Lengths, x/L = 0.719 and 0.810

Figure 7 (Continued)

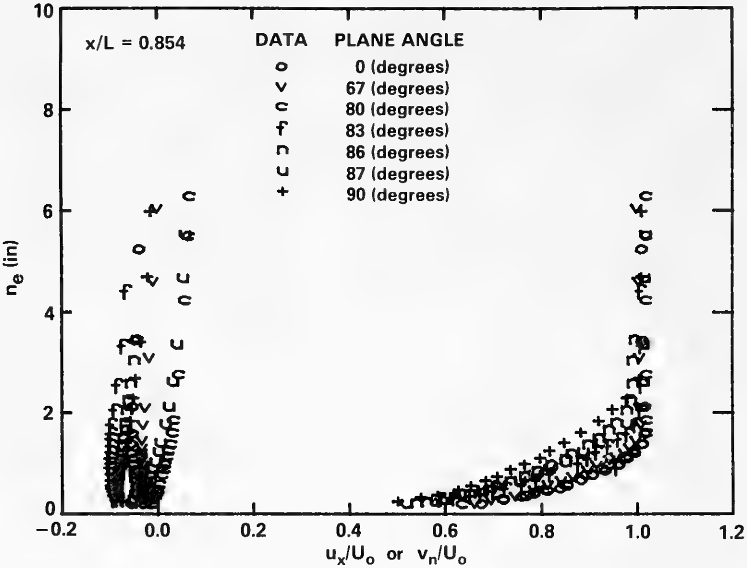

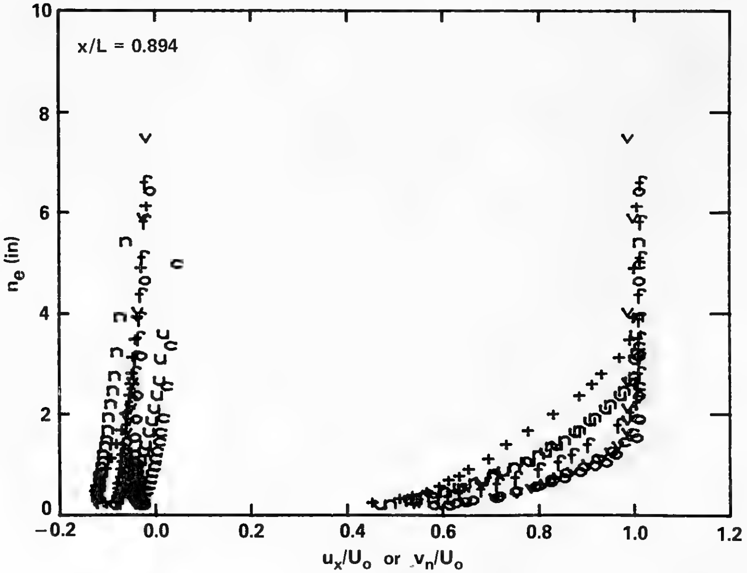

Figure 7b - Nondimensional Axial Lengths, x/L = 0.854 and 0.894

Figure 7 (Continued)

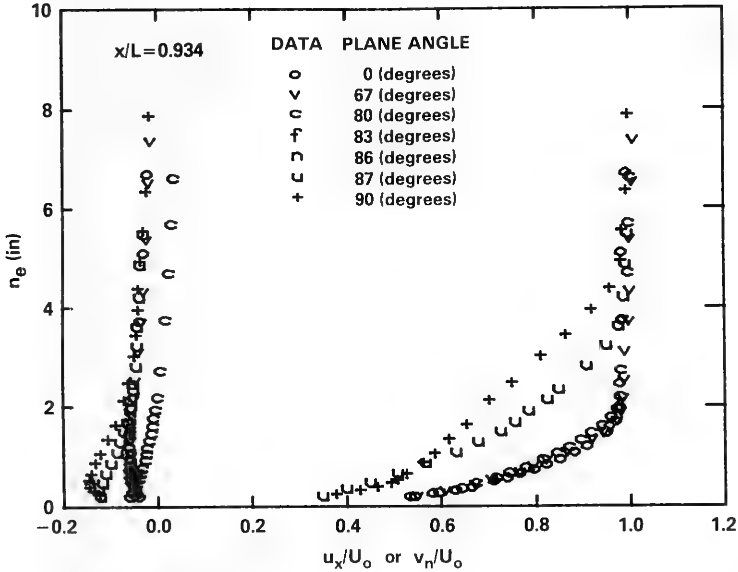

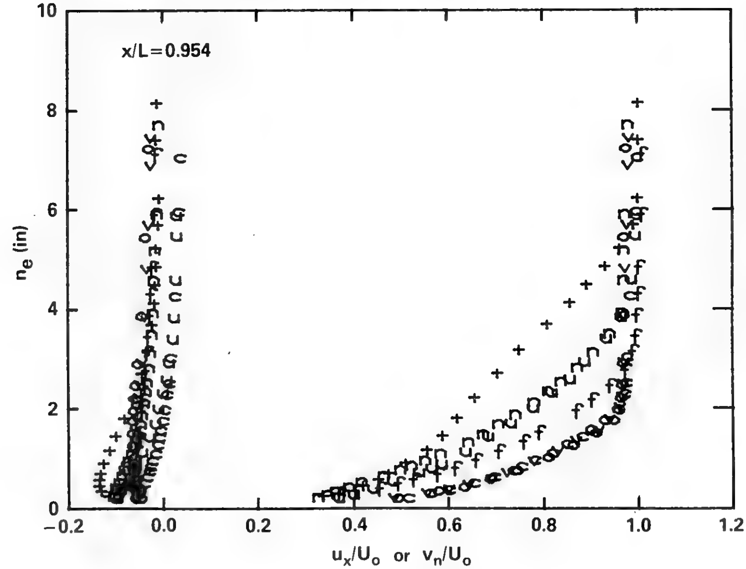

Figure 7c - Nondimensional Axial Lengths, x/L = 0.934 and 0.954

Figure 8 - Computed and Measured Mean Axial Velocity Distributions

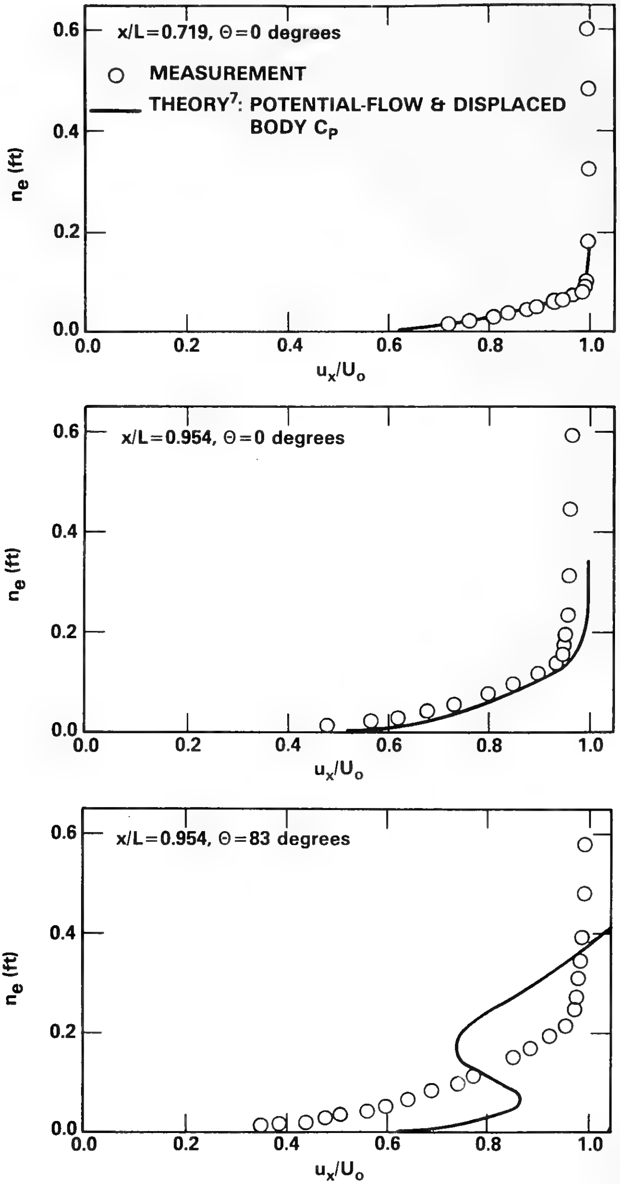

Figure 8 (Continued)

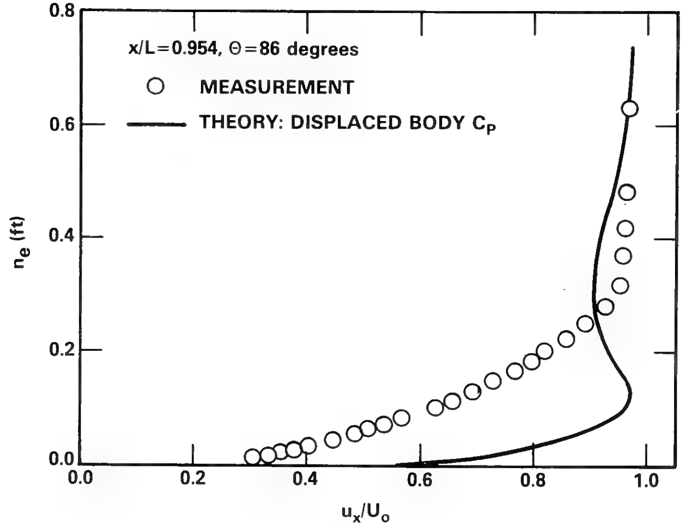

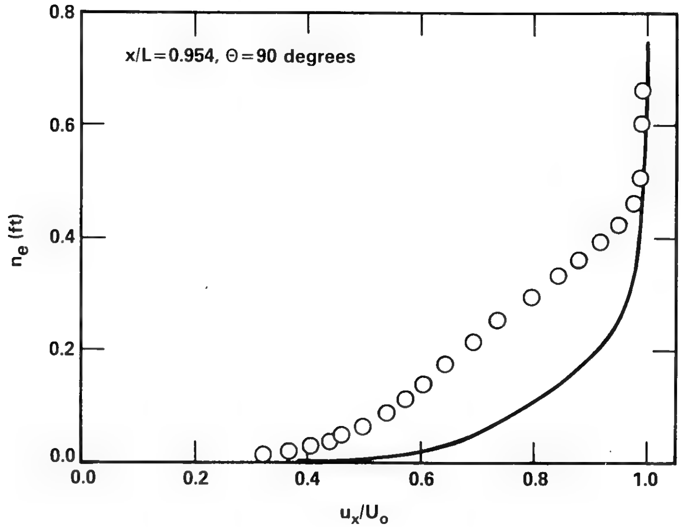

Figure 9 - Measured Distributions of Reynolds Stresses at Angular Location θ = 67 Degrees

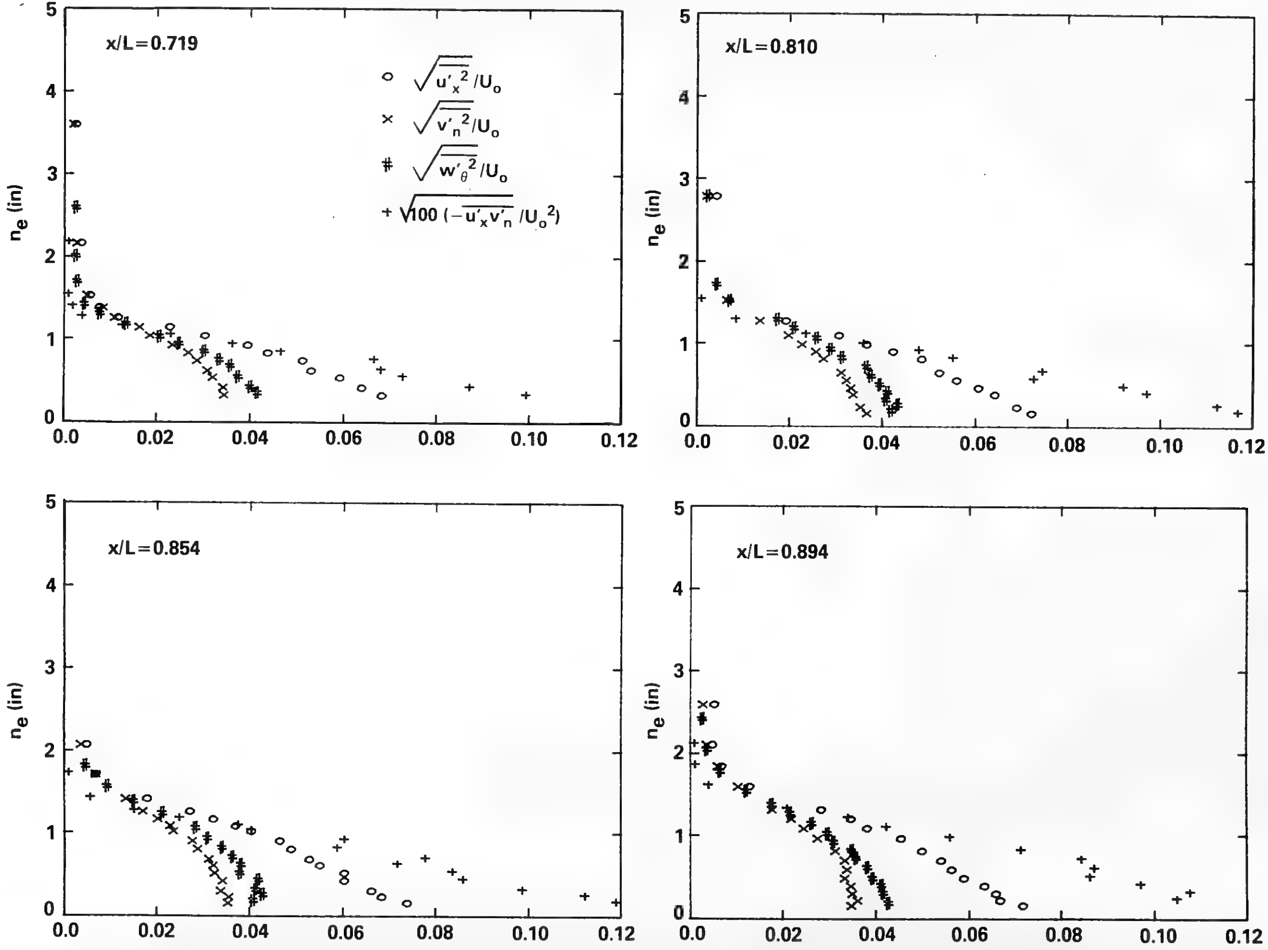

Figure 9a - Nondimensional Axial Lengths, x/L = 0.719, 0.810, 0.854, and 0.894

Figure 9 (Continued)

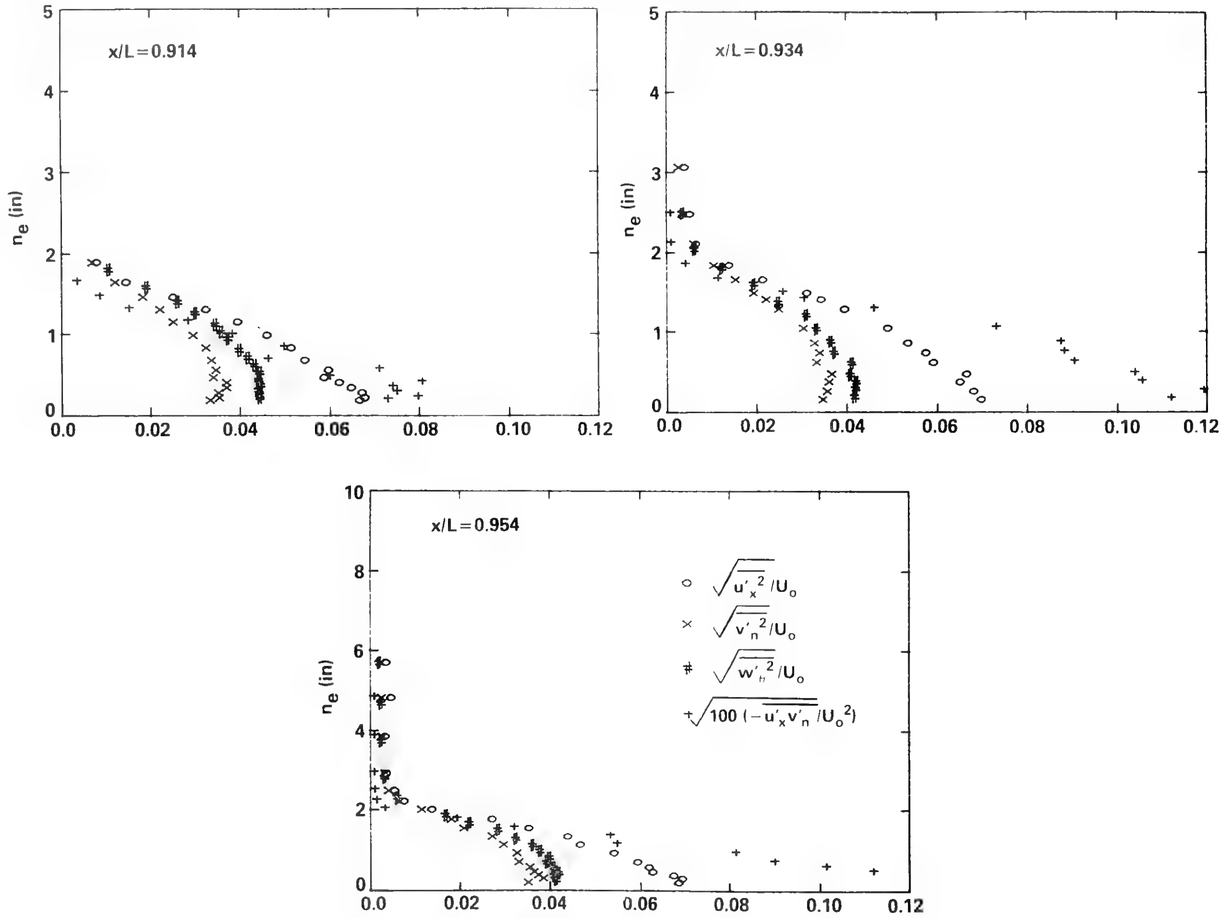

Figure 9b - Nondimensional Axial Lengths, x/L = 0.914, 0.934, and 0.954

Figure 10 - Measured Distributions of Reynolds Stresses at Angular Location θ = 80 Degrees

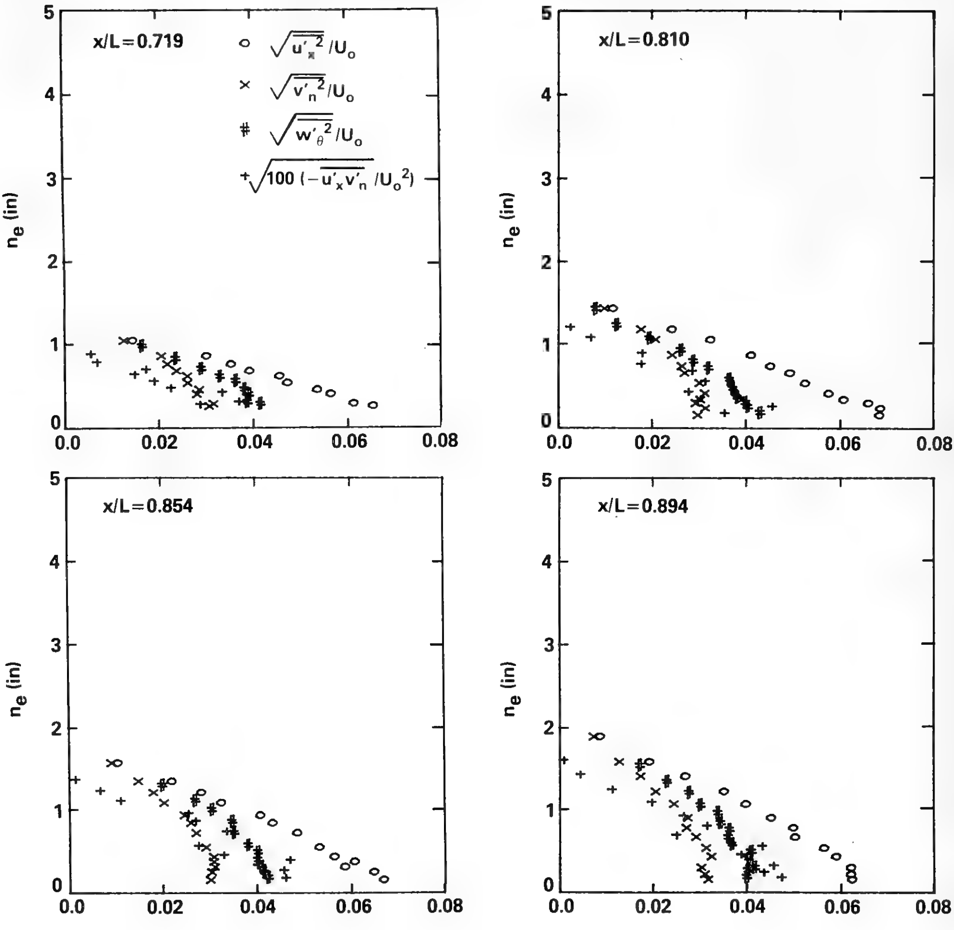

Figure 10a - Nondimensional Axial Lengths, x/L = 0.719, 0.810, 0.854, and 0.894

Figure 10 (Continued)

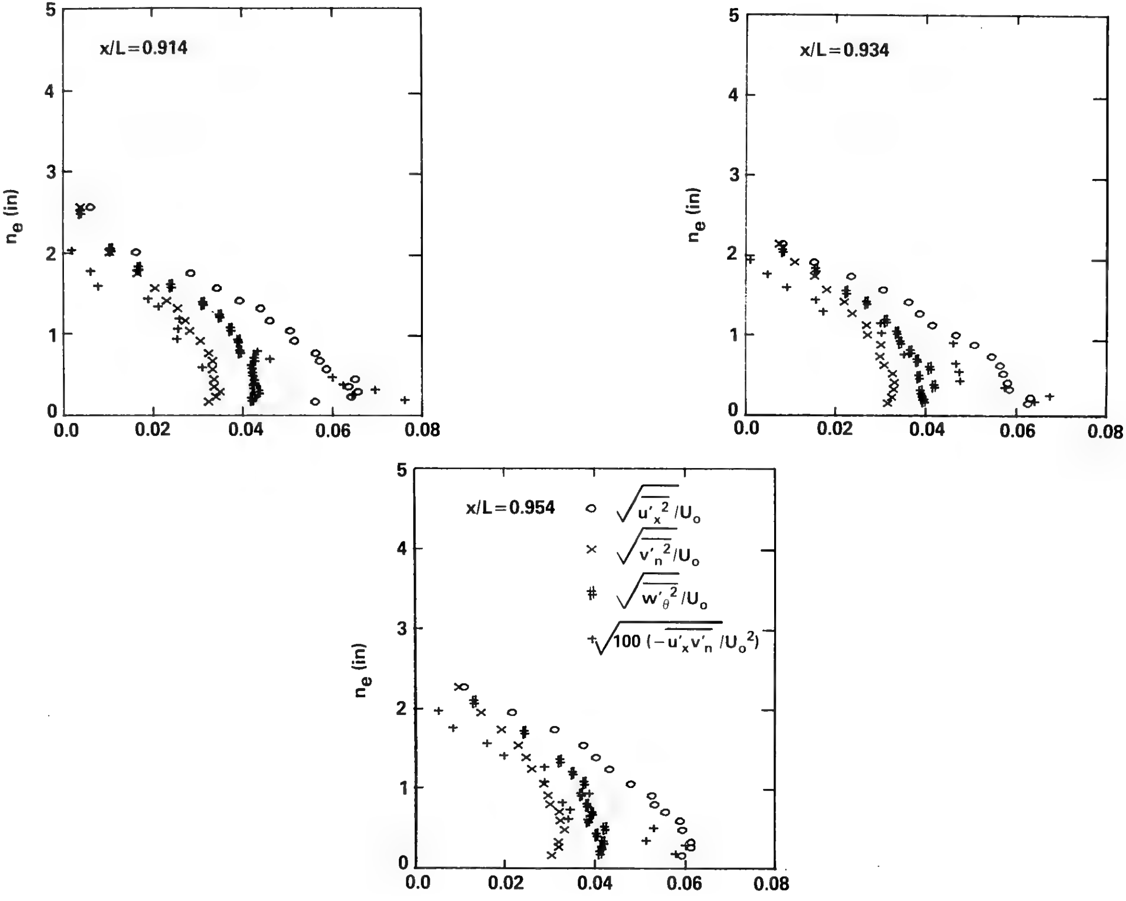

Figure 10b - Nondimensional Axial Lengths, x/L = 0.914, 0.934, and 0.954

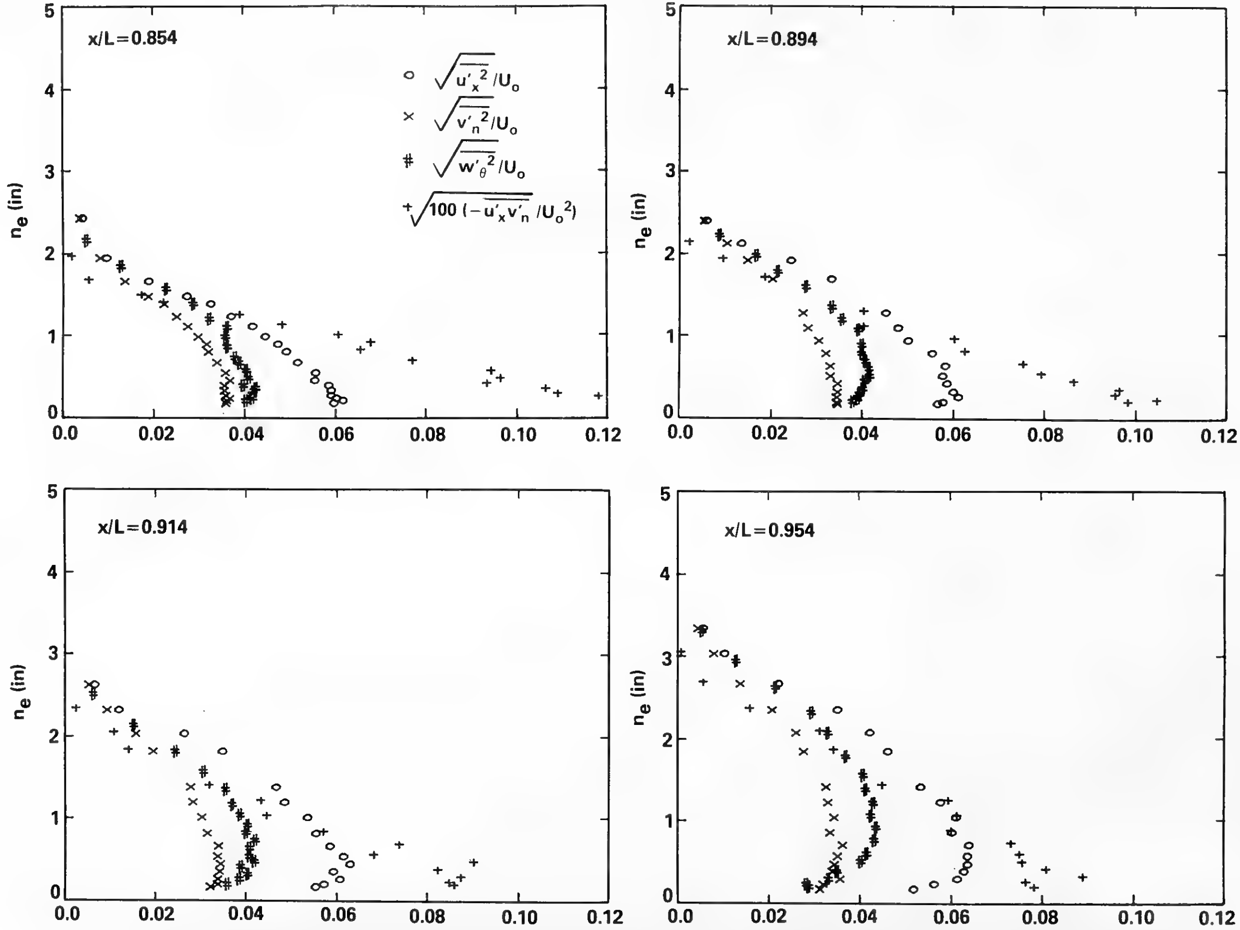

Figure 11 - Measured Distributions of Reynolds Stresses at Angular Location θ = 83 Degrees

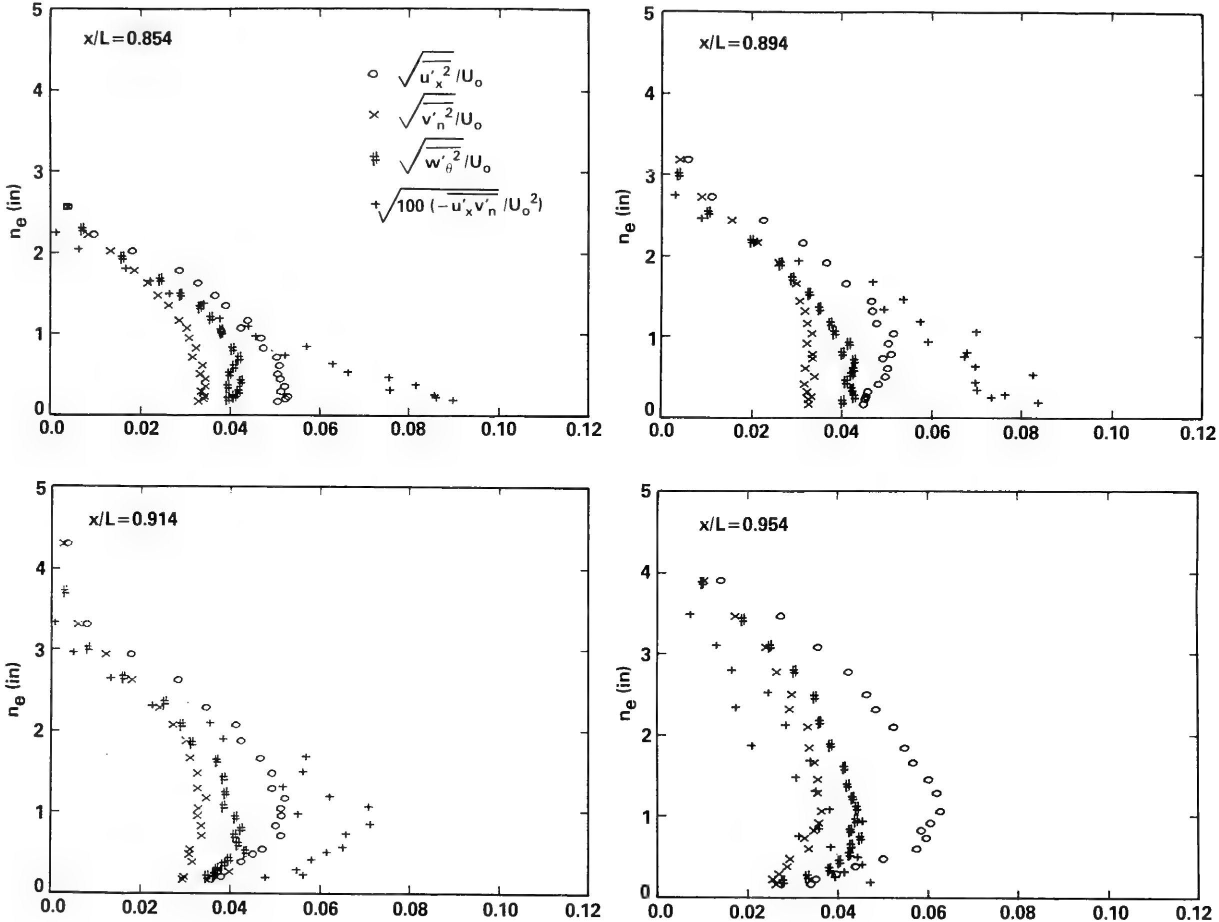

Figure 12 - Measured Distributions of Reynolds Stresses at Angular Location θ = 86 Degrees

Figure 13 - Measured Distributions of Reynolds Stresses at Angular Location θ = 87 Degrees

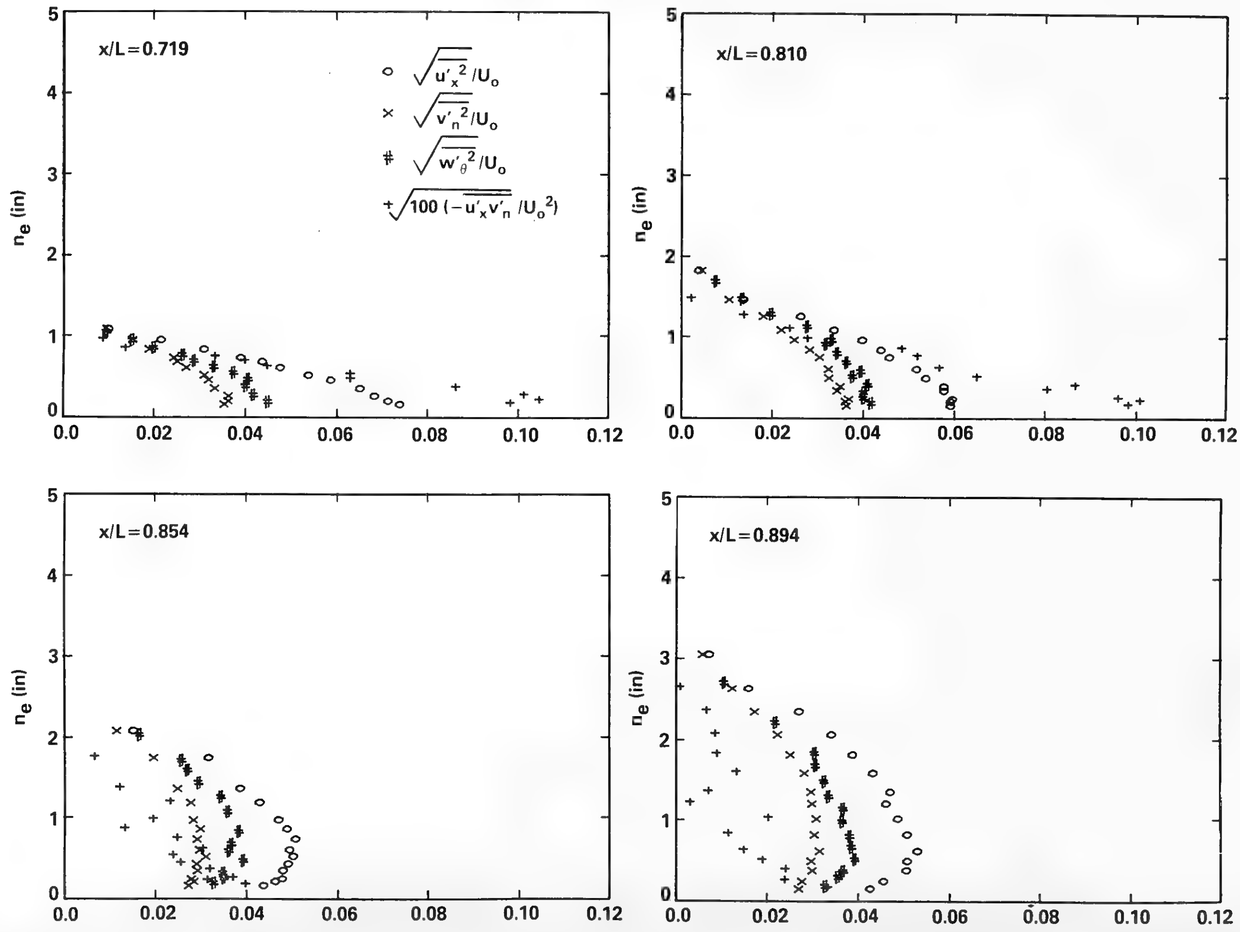

Figure 13a - Nondimensional Axial Lengths, x/L = 0.719, 0.810, 0.854, and 0.894

Figure 13 (Continued)

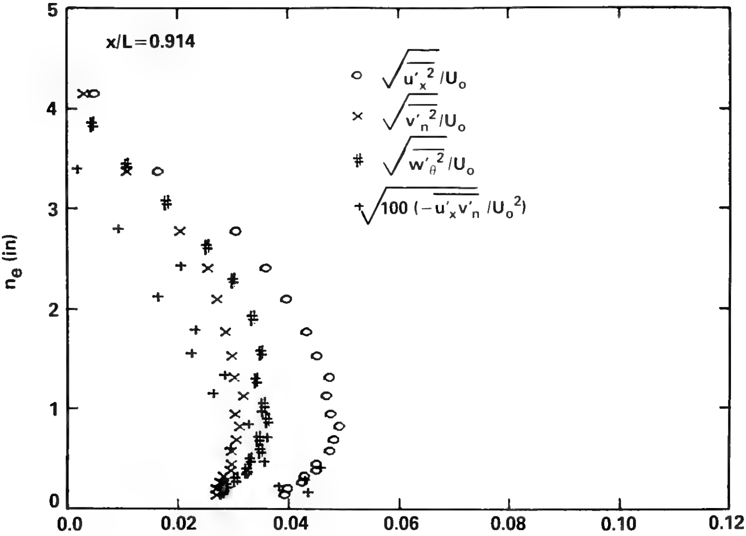

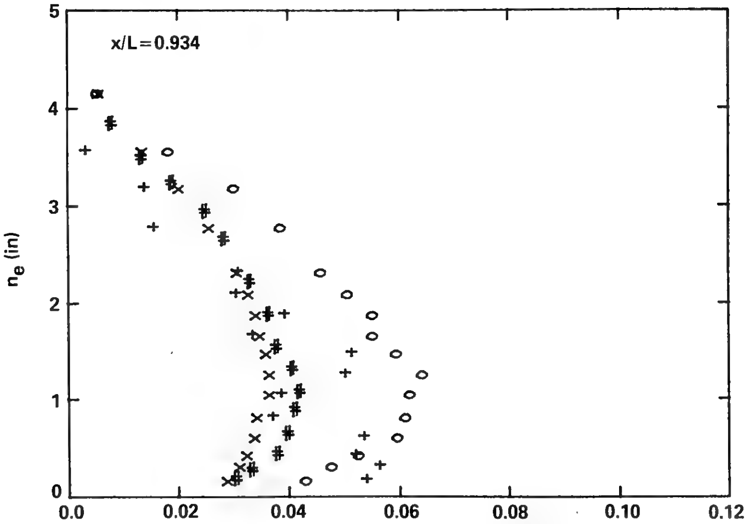

Figure 13b - Nondimensional Axial Lengths, x/L = 0.914 and 0.934

Figure 14 - Measured Distributions of Turbulent Structure Parameter

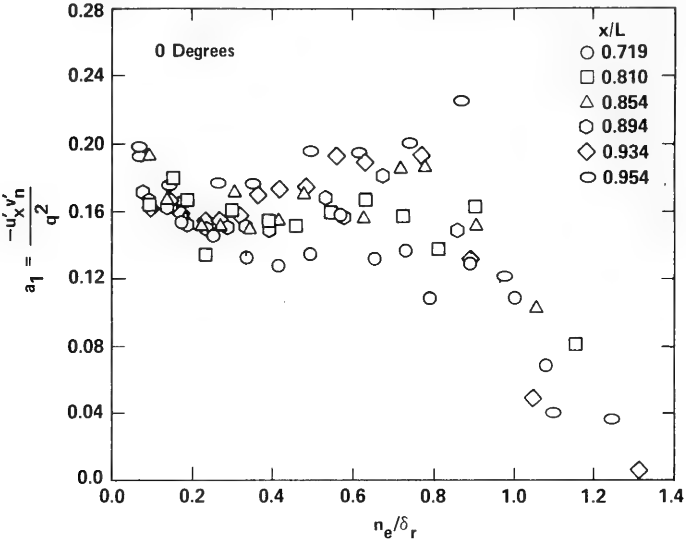

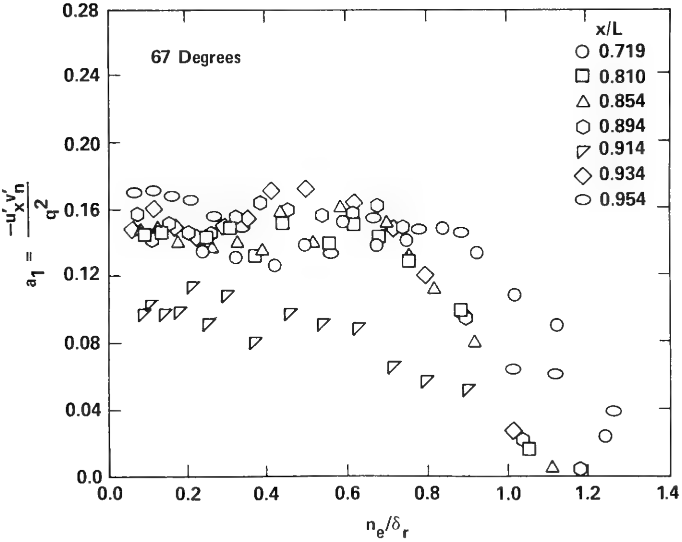

Figure 14a - Angular Locations, θ = 0 and 67 Degrees

Figure 14 (Continued)

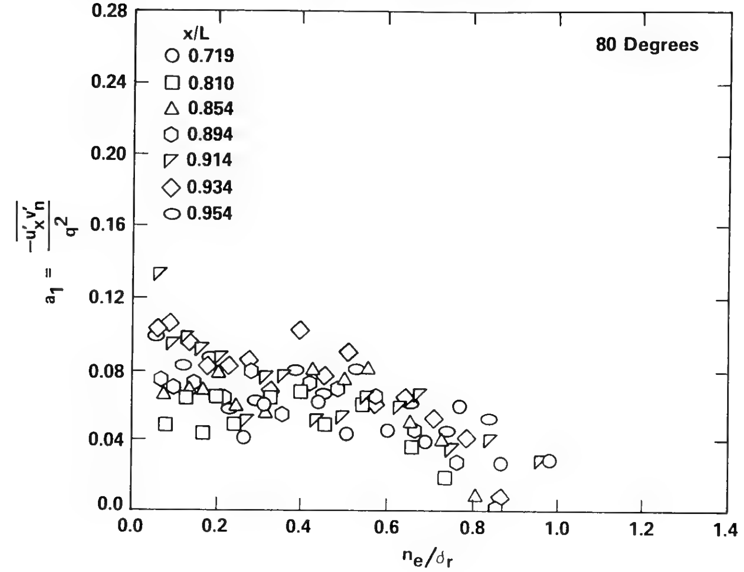

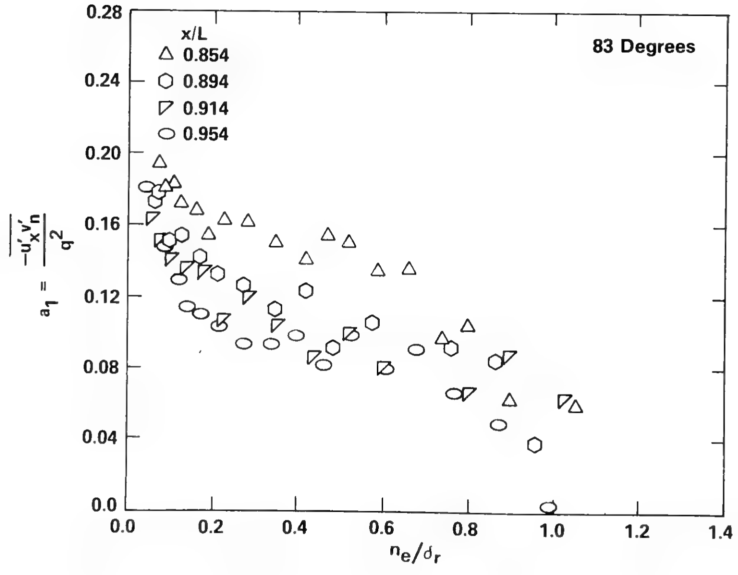

Figure 14b - Angular Locations θ = 80 and 83 Degrees

Figure 14 (Continued)

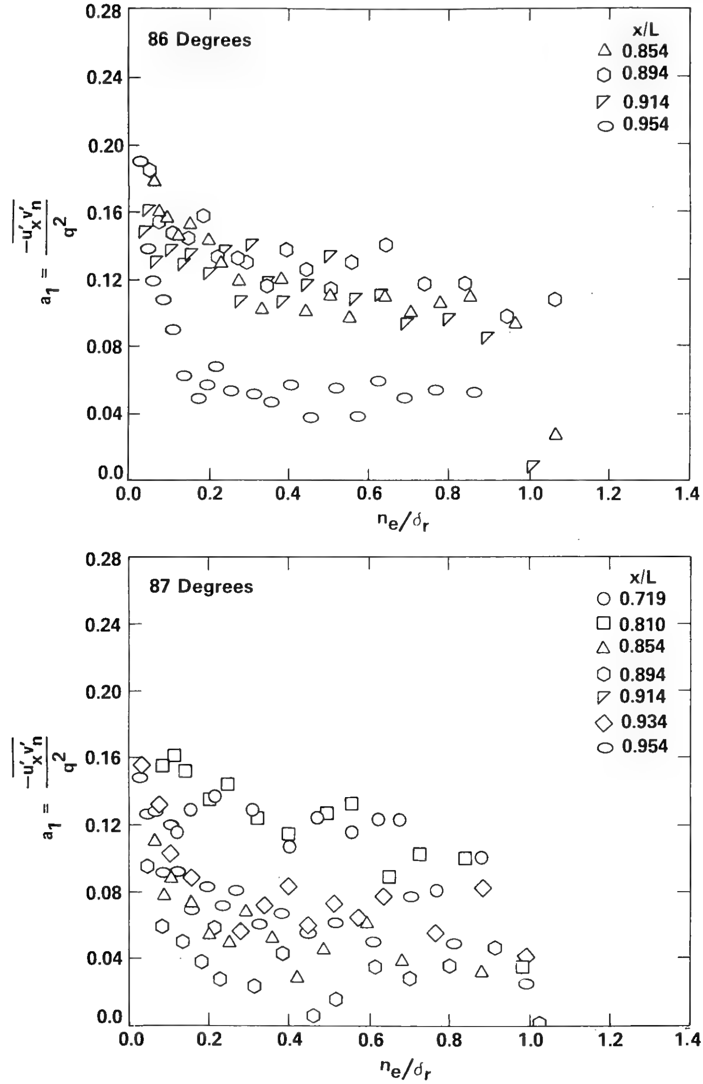

Figure 14c - Angular Locations, θ = 86 and 87 Degrees

Figure 14 (Continued)

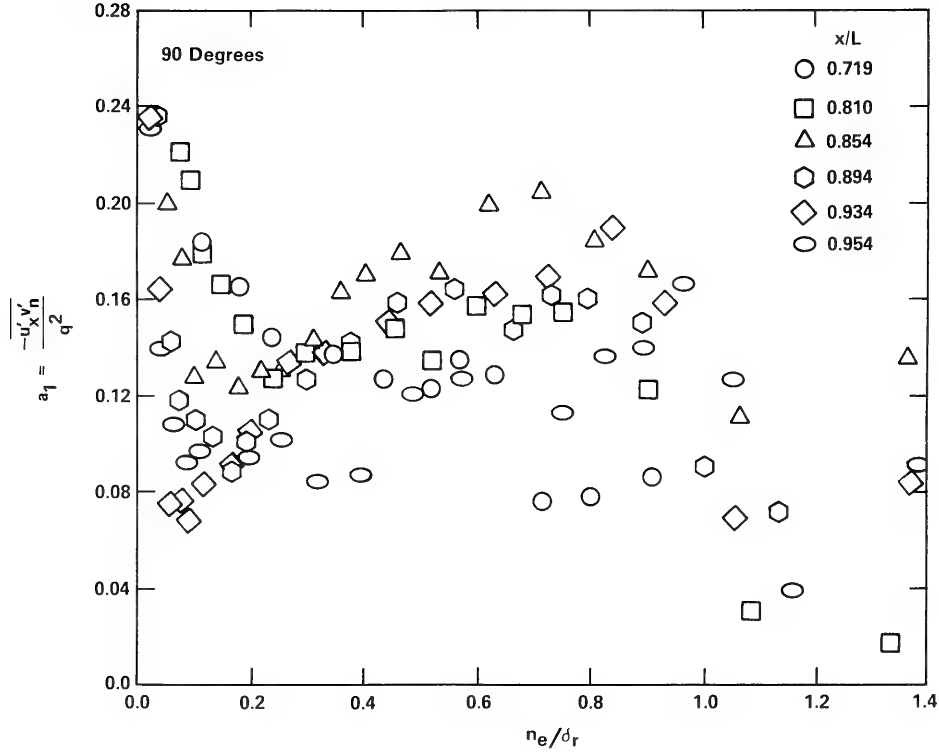

Figure 14d - Angular Location, θ = 90 Degrees

Figure 15 - Measured Distributions of Eddy Viscosity

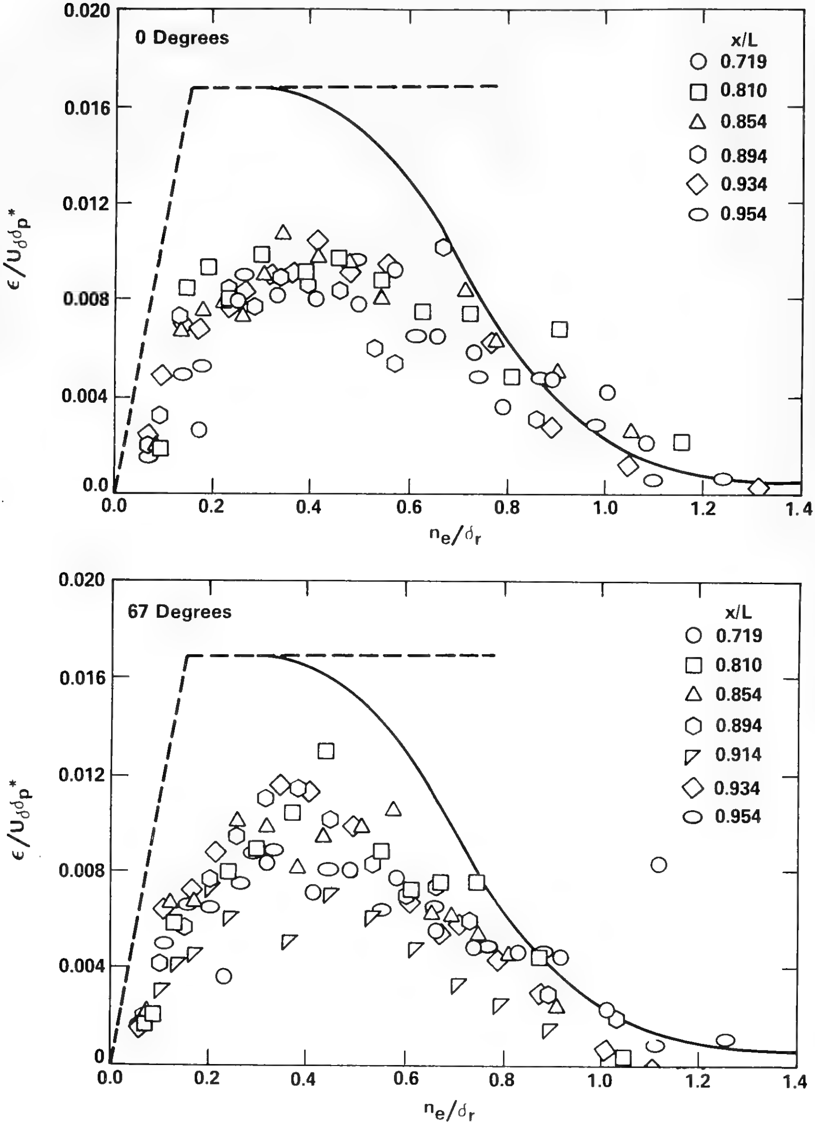

Figure 15a - Angular Locations, θ = 0 and 67 Degrees

Figure 15 (Continued)

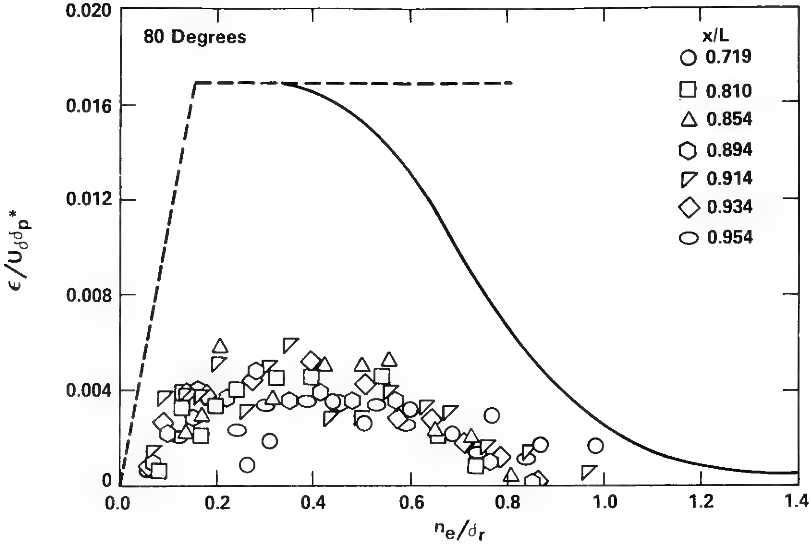

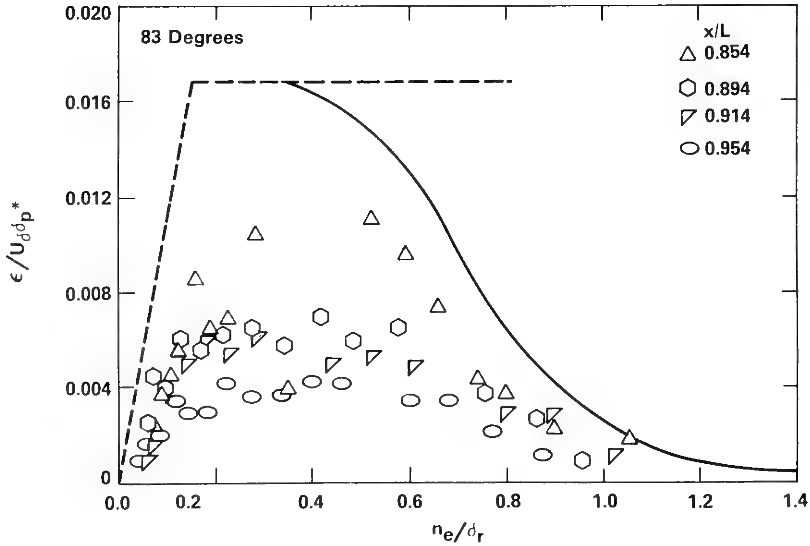

Figure 15b - Angular Locations, θ = 80 and 83 Degrees

Figure 15 (Continued)

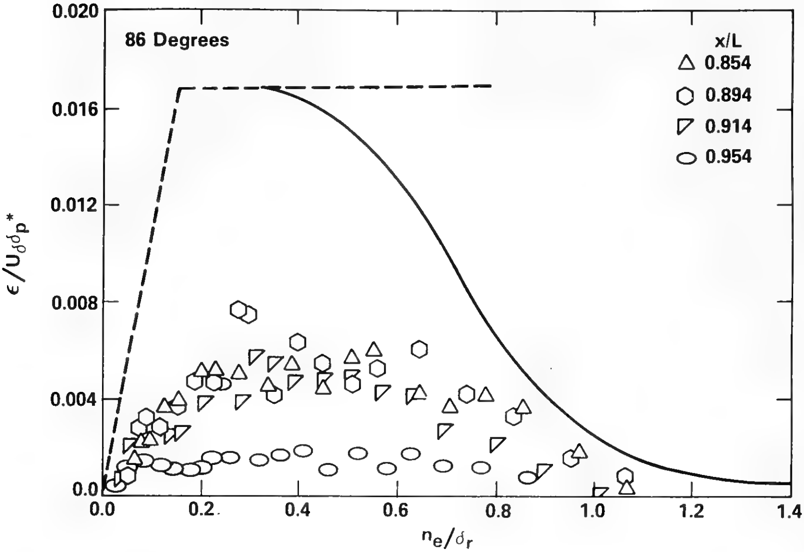

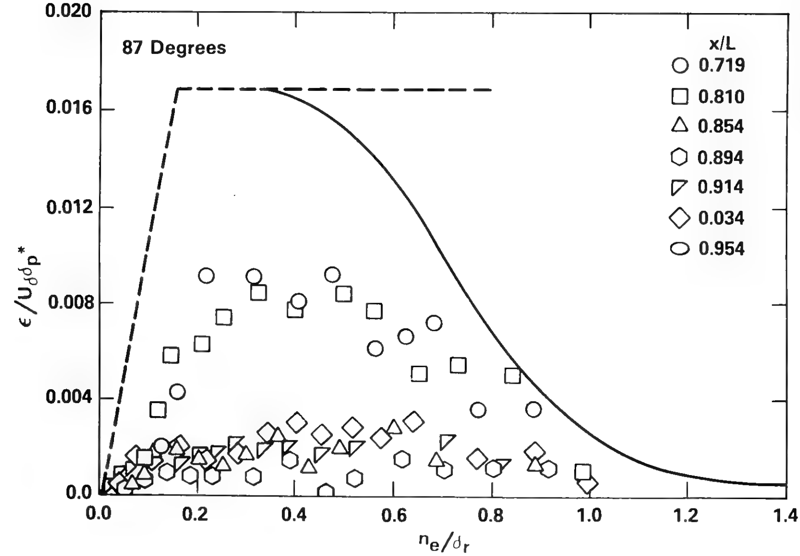

Figure 15c - Angular Locations, θ = 86 and 87 Degrees

Figure 15 (Continued)

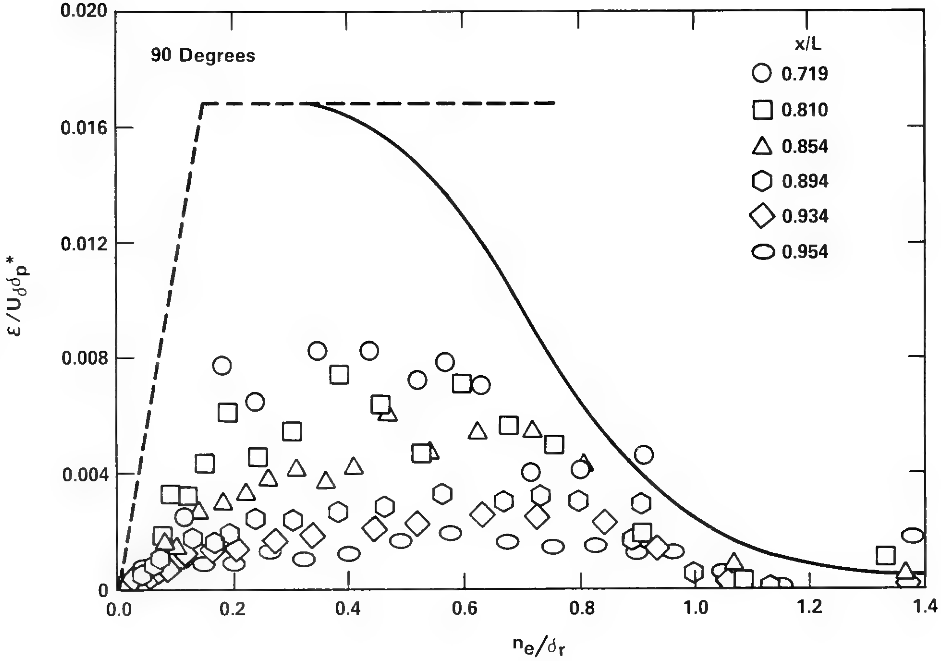

Figure 15d - Angular Location, θ = 90 Degrees

Figure 16 - Measured Distributions of Mixing Length

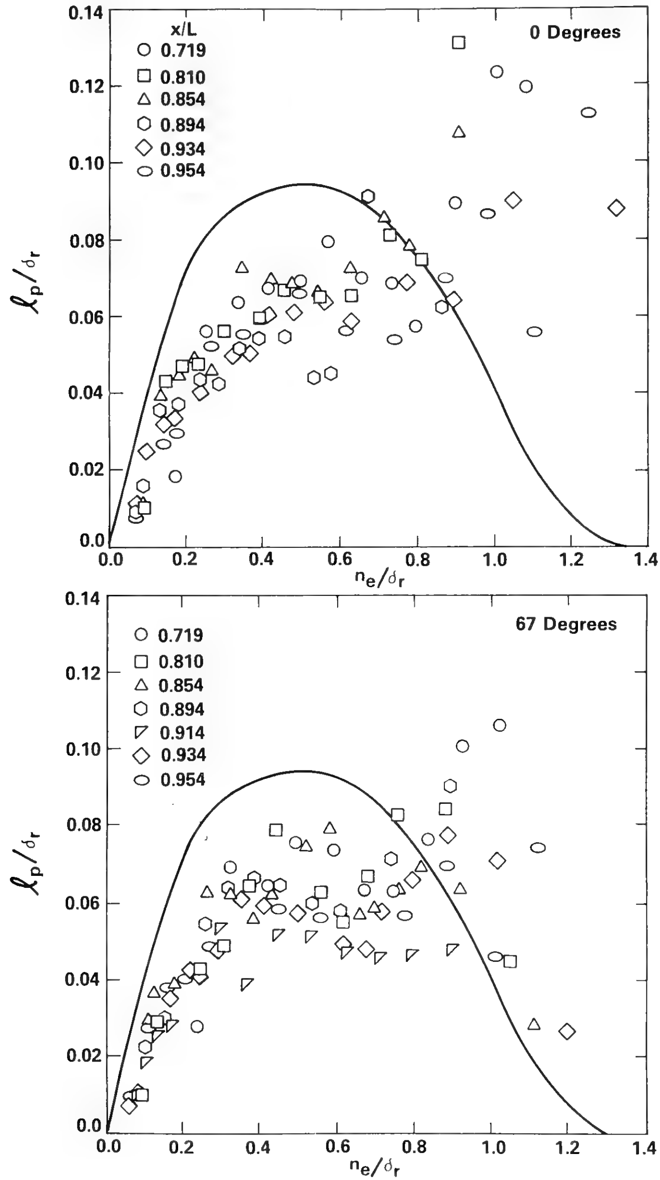

Figure 16a - Angular Locations, θ = 0 and 67 Degrees

Figure 16 (Continued)

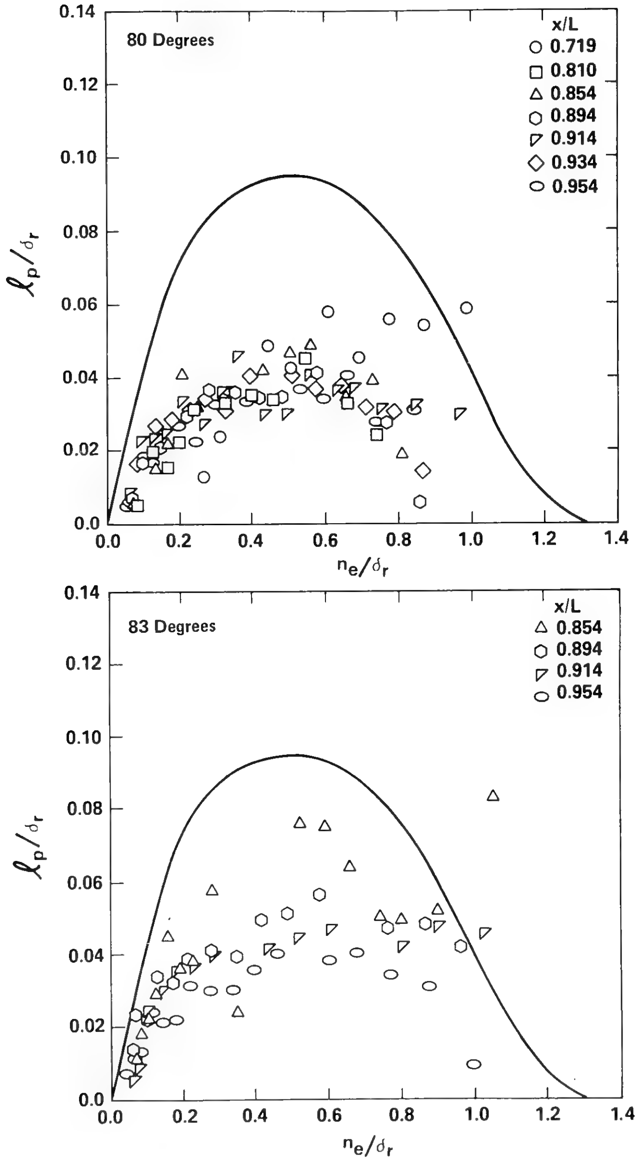

Figure 16b - Angular Locations, θ = 80 and 83 Degrees

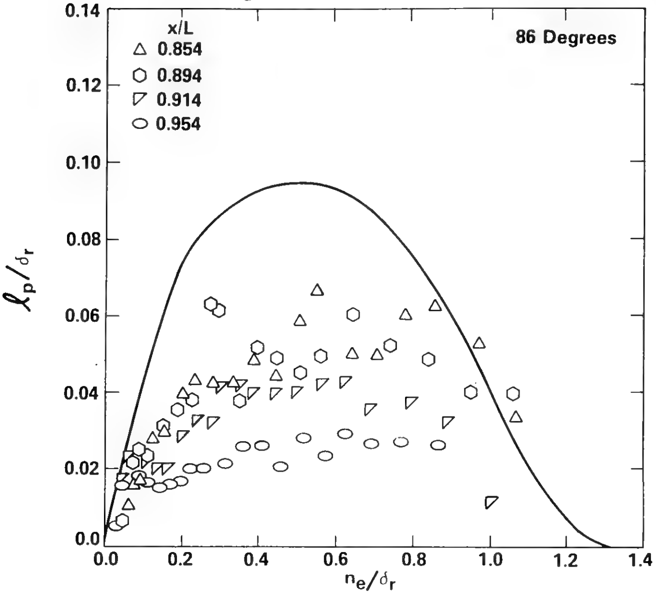

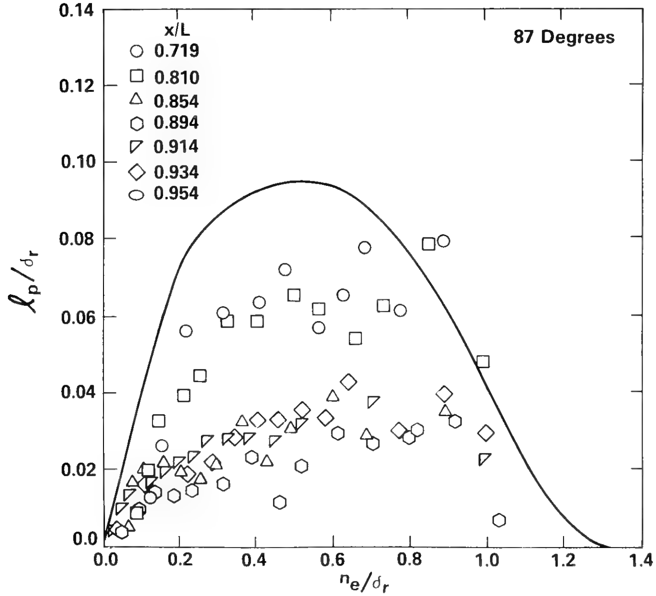

Figure 16c - Angular Locations, θ = 86 and 87 Degrees

Figure 16 (Continued)

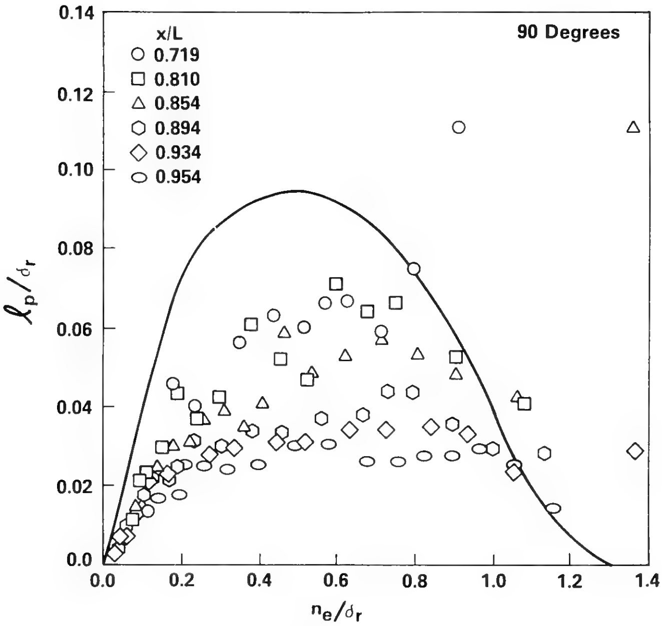

Figure 16d - Angular Location, θ = 90 Degrees

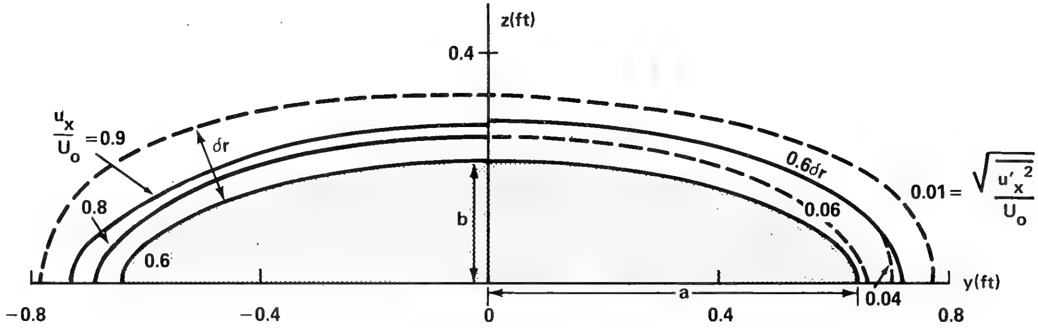

Figure 17a - Axial Location, x/L = 0.810

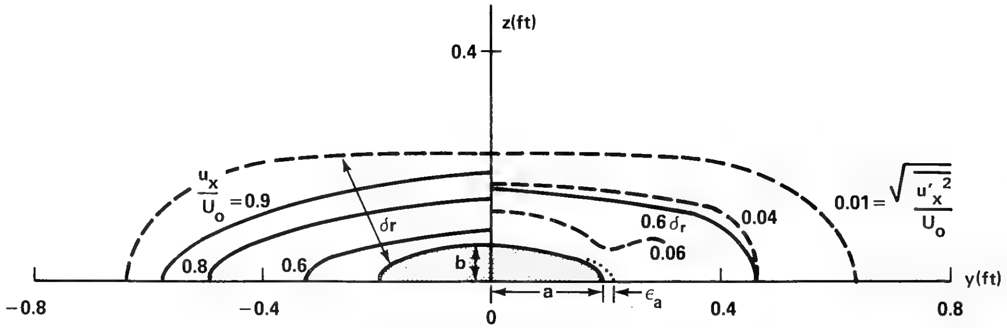

Figure 17b - Axial Location, x/L = 0.95

Figure 17 - Turbulence Area Representing the Square-Root of the Mixing Length

Figure 18 - Proposed Similarity Concept for Mixing Length of Turbulent Boundary Layer

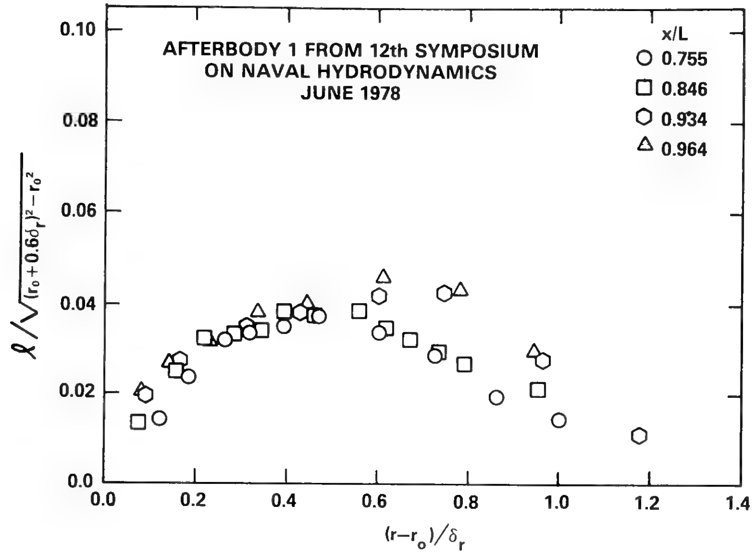

Figure 18a - Afterbody 1

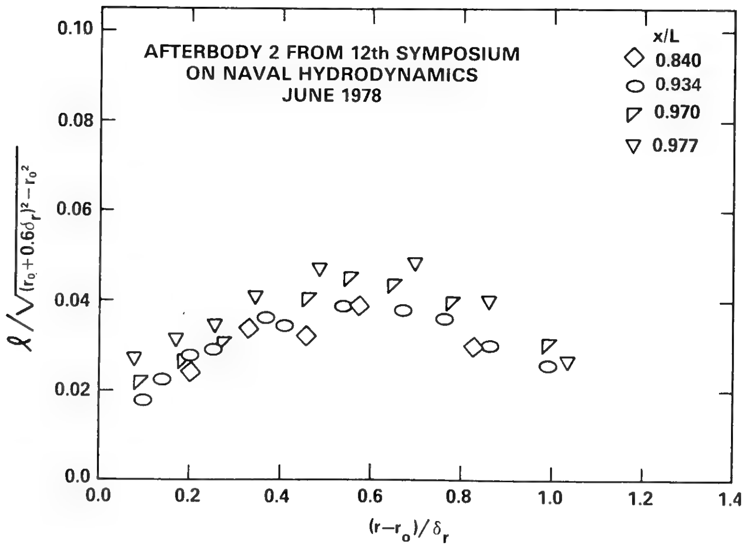

Figure 18b - Afterbody 2

Figure 18 (Continued)

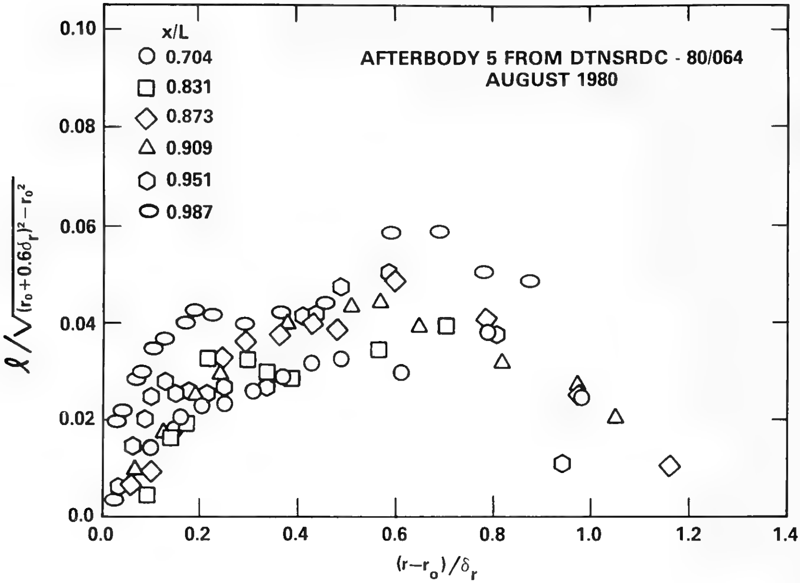

Figure 18c - Afterbody 5

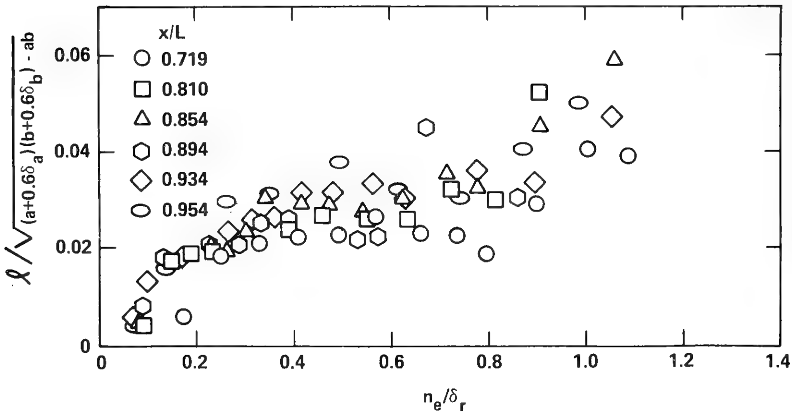

Figure 18d - Present Model, 0 Degree Plane

Figure 18 (Continued)

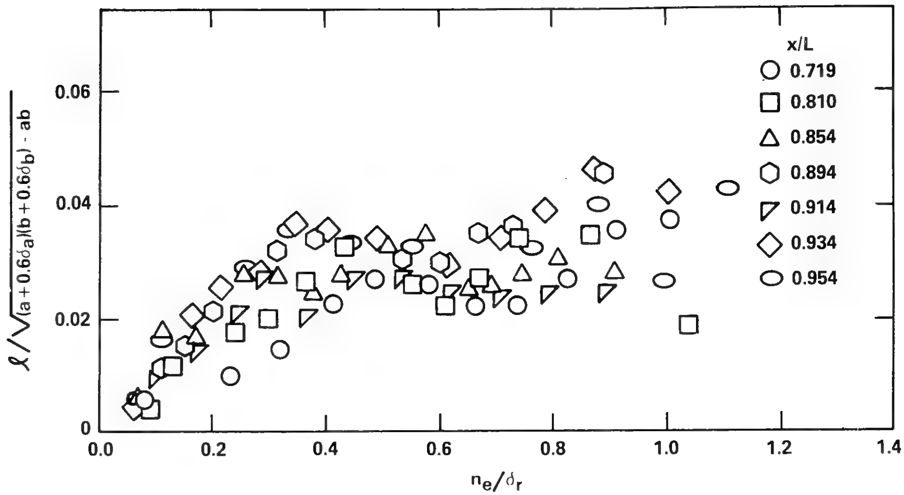

Figure 18e - Present Model, 67 Degree Plane

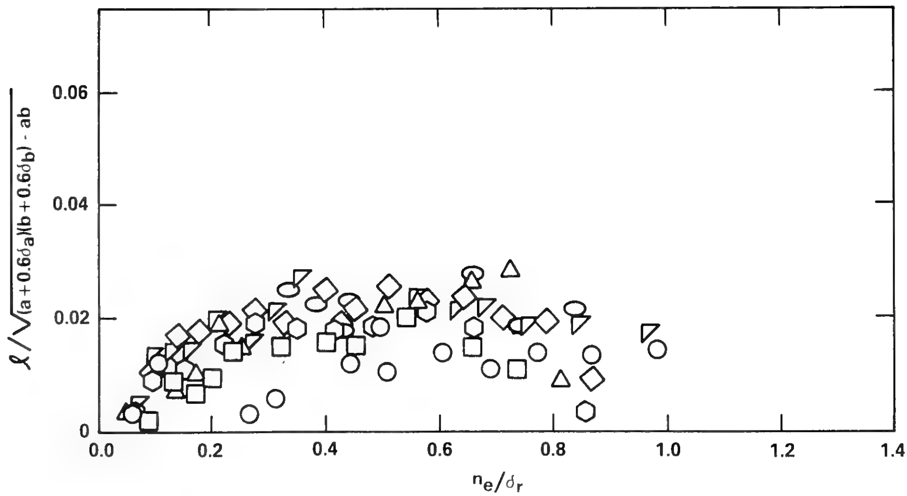

Figure 18f - Present Model, 80 Degree Plane

Figure 18 (Continued)

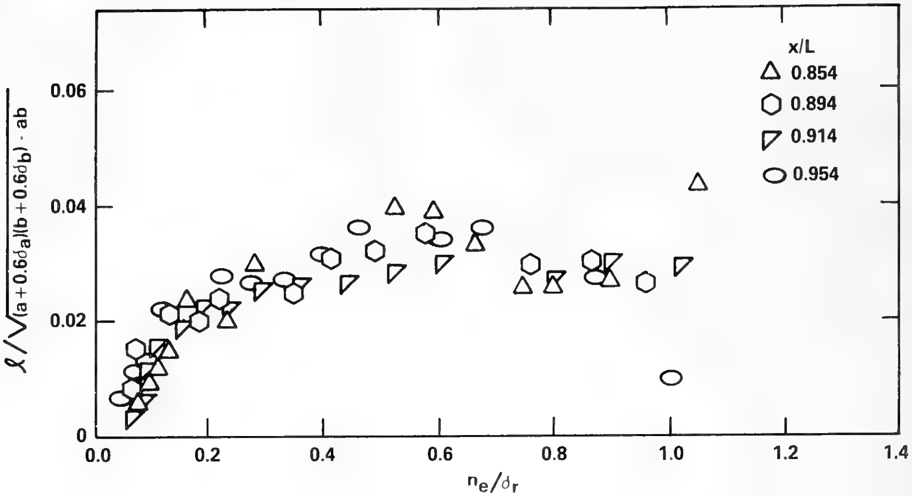

Figure 18g - Present Model, 83 Degree Plane

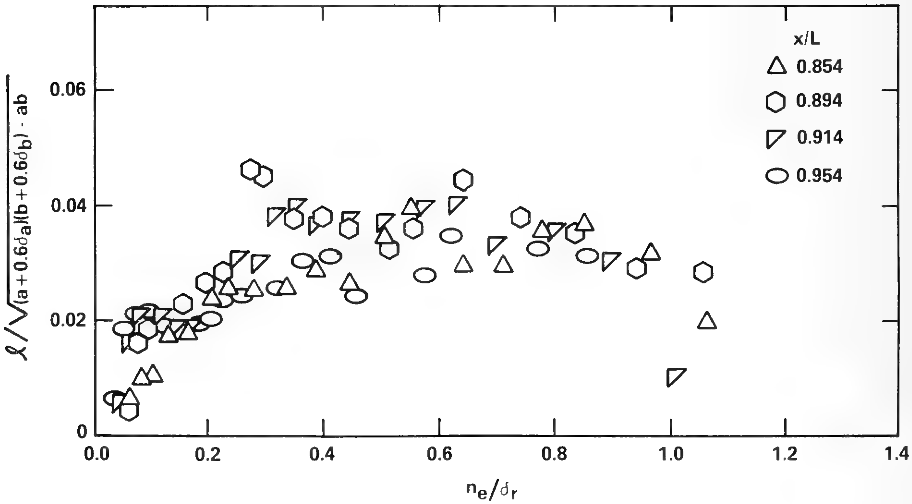

Figure 18h - Present Model, 86 Degree Plane

Figure 18 (Continued)

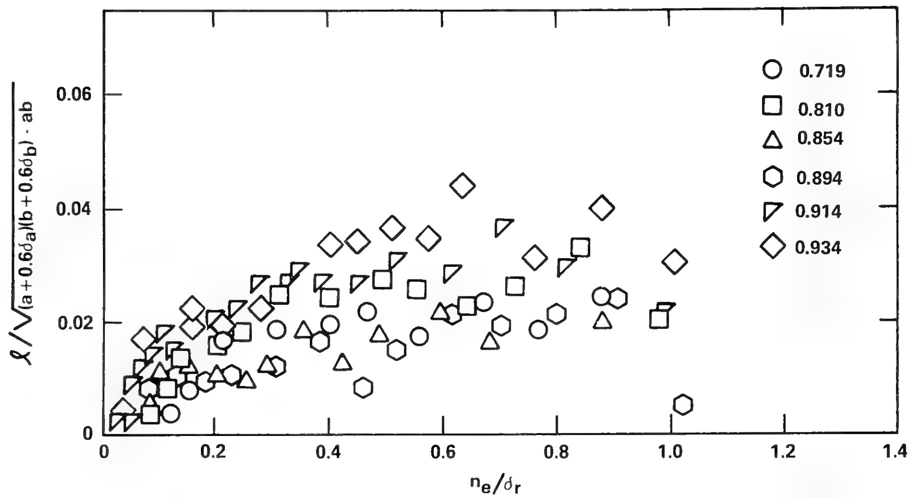

Figue 18i - Present Model, 87 Degree Plane

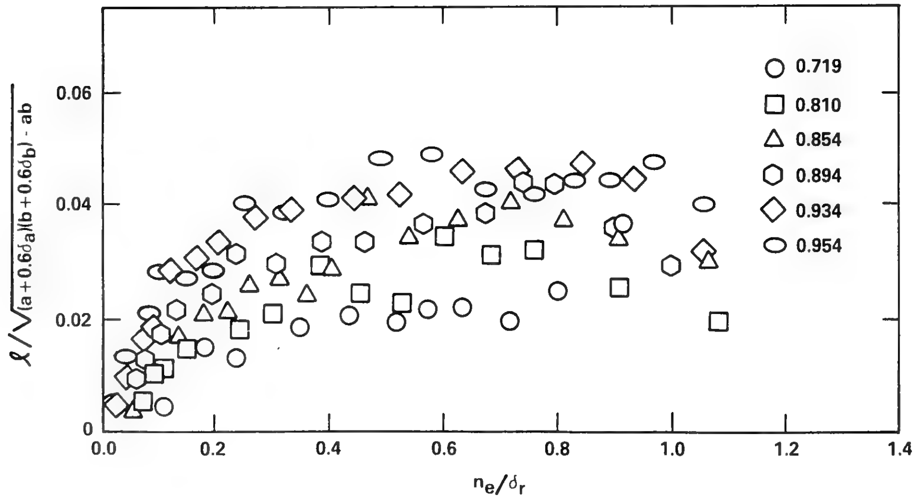

Figure 18j - Present Model, 90 Degree Plane

TABLE 1 - MODEL OFFSETS (INCHES)

x	y	z
0.00000	0.00000	0.00000
0.00000	0.00000	0.00000
0.00000	0.00000	0.00000
0.00000	0.00000	0.00000
0.00000	0.00000	0.00000
0.00000	0.00000	0.00000
0.00000	0.00000	0.00000
0.00000	0.00000	0.00000
0.00000	0.00000	0.00000
0.00000	0.00000	0.00000
0.00000	0.00000	0.00000
-0.60000	0.00000	-0.69647
-0.60000	0.18805	-0.69365
-0.60000	0.37610	-0.68510
-0.60000	0.62683	-0.66439
-0.60000	0.87756	-0.63207
-0.60000	1.14918	-0.58167
-0.60000	1.42081	-0.51066
-0.60000	1.67154	-0.41788
-0.60000	1.88048	-0.30359
-0.60000	2.01838	-0.18007
-0.60000	2.08942	0.00000
-1.20000	0.00000	-0.99022
-1.20000	0.26736	-0.98621
-1.20000	0.53472	-0.97405
-1.20000	0.89120	-0.94461
-1.20000	1.24768	-0.89865
-1.20000	1.63387	-0.82700
-1.20000	2.02006	-0.72604
-1.20000	2.37654	-0.59413
-1.20000	2.67361	-0.43163
-1.20000	2.86967	-0.25601
-1.20000	2.97067	0.00000
-1.80000	0.00000	-1.21776
-1.80000	0.32880	-1.21282
-1.80000	0.65759	-1.19787
-1.80000	1.09599	-1.16167
-1.80000	1.53438	-1.10515
-1.80000	2.00931	-1.01703
-1.80000	2.48424	-0.89288
-1.80000	2.92263	-0.73066
-1.80000	3.28796	-0.53081
-1.80000	3.52908	-0.31484
-1.80000	3.65329	0.00000
-2.40000	0.00000	-1.41032
-2.40000	0.38079	-1.40459
-2.40000	0.76157	-1.38728
-2.40000	1.26928	-1.34536
-2.40000	1.77700	-1.27990
-2.40000	2.32702	-1.17785
-2.40000	2.87705	-1.03406
-2.40000	3.38476	-0.84619
-2.40000	3.80785	-0.61474
-2.40000	4.08710	-0.36463
-2.40000	4.23095	0.00000
-3.00000	0.00000	-1.57974
-3.00000	0.42653	-1.57333
-3.00000	0.85306	-1.55394
-3.00000	1.42177	-1.50698
-3.00000	1.99047	-1.43365
-3.00000	2.60657	-1.31934
-3.00000	3.22267	-1.15828
-3.00000	3.79138	-0.94784
-3.00000	4.26530	-0.68859
-3.00000	4.57809	-0.40843
-3.00000	4.73922	0.00000
-4.20000	0.00000	-1.87052
-4.20000	0.50504	-1.86293
-4.20000	1.01008	-1.83996
-4.20000	1.68347	-1.78436
-4.20000	2.35685	-1.69754
-4.20000	3.08635	-1.56219
-4.20000	3.81585	-1.37149
-4.20000	4.48924	-1.12231
-4.20000	5.05040	-0.81534
-4.20000	5.42076	-0.48361
-4.20000	5.61155	0.00000
-5.40000	0.00000	-2.11461
-5.40000	0.57095	-2.10603
-5.40000	1.14189	-2.08008
-5.40000	1.90315	-2.01721
-5.40000	2.66441	-1.91906
-5.40000	3.48911	-1.76605
-5.40000	4.31381	-1.55046
-5.40000	5.07508	-1.26877
-5.40000	5.70946	-0.92174
-5.40000	6.12815	-0.54672
-5.40000	6.34384	0.00000
-6.60000	0.00000	-2.32285
-6.60000	0.62717	-2.31343
-6.60000	1.25434	-2.28491
-6.60000	2.09057	-2.21586
-6.60000	2.92680	-2.10805
-6.60000	3.83271	-1.93997
-6.60000	4.73862	-1.70314
-6.60000	5.57485	-1.39371
-6.60000	6.27170	-1.01251
-6.60000	6.73163	-0.60056
-6.60000	6.96856	0.00000
-7.80000	0.00000	-2.50114
-7.80000	0.67531	-2.49099
-7.80000	1.35062	-2.46029

TABLE 1 (Continued)

x	y	z	x	y	z
-7.80000	2.25103	-2.38594	-14.40000	9.21719	0.00000
-7.80000	3.15144	-2.26985	-16.20000	0.00000	-3.13374
-7.80000	4.12689	-2.08887	-16.20000	0.84611	-3.12102
-7.80000	5.10234	-1.83387	-16.20000	1.69222	-3.08255
-7.80000	6.00275	-1.50069	-16.20000	2.82036	-2.98939
-7.80000	6.75309	-1.09022	-16.20000	3.94851	-2.84394
-7.80000	7.24832	-0.64665	-16.20000	5.17066	-2.61719
-7.80000	7.50343	0.00000	-16.20000	6.39282	-2.29769
-9.00000	0.00000	-2.65320	-16.20000	7.52097	-1.88024
-9.00000	0.71636	-2.64243	-16.20000	8.46109	-1.36596
-9.00000	1.43273	-2.60987	-16.20000	9.08157	-0.81020
-9.00000	2.38788	-2.53099	-16.20000	9.40121	0.00000
-9.00000	3.34303	-2.40784	-18.00000	0.00000	-3.16563
-9.00000	4.37778	-2.21586	-18.00000	0.85472	-3.15279
-9.00000	5.41253	-1.94536	-18.00000	1.70944	-3.11393
-9.00000	6.36768	-1.59192	-18.00000	2.84907	-3.01982
-9.00000	7.16364	-1.15650	-18.00000	3.98870	-2.87289
-9.00000	7.68898	-0.68596	-18.00000	5.22330	-2.64383
-9.00000	7.95960	0.00000	-18.00000	6.45789	-2.32108
-10.80000	0.00000	-2.83767	-18.00000	7.59752	-1.89938
-10.80000	0.76617	-2.82615	-18.00000	8.54721	-1.37987
-10.80000	1.53234	-2.79132	-18.00000	9.17401	-0.81845
-10.80000	2.55390	-2.70696	-18.00000	9.49690	0.00000
-10.80000	3.57546	-2.57525	-20.40000	0.00000	-3.17543
-10.80000	4.68215	-2.36992	-20.40000	0.85737	-3.16254
-10.80000	5.78884	-2.08061	-20.40000	1.71473	-3.12356
-10.80000	6.81040	-1.70260	-20.40000	2.85788	-3.02916
-10.80000	7.66170	-1.23691	-20.40000	4.00104	-2.88178
-10.80000	8.22355	-0.73366	-20.40000	5.23945	-2.65200
-10.80000	8.51300	0.00000	-20.40000	6.47787	-2.32826
-13.20000	0.00000	-3.01212	-20.40000	7.62102	-1.90526
-13.20000	0.81327	-2.99989	-20.40000	8.57365	-1.38414
-13.20000	1.62654	-2.96292	-20.40000	9.20239	-0.82098
-13.20000	2.71091	-2.87338	-20.40000	9.52628	0.00000
-13.20000	3.79527	-2.73357	-22.80000	0.00000	-3.17543
-13.20000	4.96999	-2.51561	-22.80000	0.85737	-3.16254
-13.20000	6.14472	-2.20852	-22.80000	1.71473	-3.12356
-13.20000	7.22908	-1.80727	-22.80000	2.85788	-3.02916
-13.20000	8.13272	-1.31295	-22.80000	4.00104	-2.88178
-13.20000	8.72912	-0.77876	-22.80000	5.23945	-2.65200
-13.20000	9.03635	0.00000	-22.80000	6.47787	-2.32826
-14.40000	0.00000	-3.07240	-22.80000	7.62102	-1.90526
-14.40000	0.82955	-3.05993	-22.80000	8.57365	-1.38414
-14.40000	1.65910	-3.02222	-22.80000	9.20239	-0.82098
-14.40000	2.76516	-2.93088	-22.80000	9.52628	0.00000
-14.40000	3.87122	-2.78828	-27.60000	0.00000	-3.17543
-14.40000	5.06946	-2.56596	-27.60000	0.85737	-3.16254
-14.40000	6.26769	-2.25272	-27.60000	1.71473	-3.12356
-14.40000	7.37376	-1.84344	-27.60000	2.85788	-3.02916
-14.40000	8.29548	-1.33923	-27.60000	4.00104	-2.88178
-14.40000	8.90381	-0.79434	-27.60000	5.23945	-2.65200

TABLE 1 (Continued)

x	y	z
-27.60000	6.47787	-2.32826
-27.60000	7.62102	-1.90526
-27.60000	8.57365	-1.38414
-27.60000	9.20239	-0.82098
-27.60000	9.52628	0.00000
-31.20000	0.00000	-3.17543
-31.20000	0.85737	-3.16254
-31.20000	1.71473	-3.12356
-31.20000	2.85788	-3.02916
-31.20000	4.00104	-2.88178
-31.20000	5.23945	-2.65200
-31.20000	6.47787	-2.32826
-31.20000	7.62102	-1.90526
-31.20000	8.57365	-1.38414
-31.20000	9.20239	-0.82098
-31.20000	9.52628	0.00000
-36.00000	0.00000	-3.17543
-36.00000	0.85737	-3.16254
-36.00000	1.71473	-3.12356
-36.00000	2.85788	-3.02916
-36.00000	4.00104	-2.88178
-36.00000	5.23945	-2.65200
-36.00000	6.47787	-2.32826
-36.00000	7.62102	-1.90526
-36.00000	8.57365	-1.38414
-36.00000	9.20239	-0.82098
-36.00000	9.52628	0.00000
-39.60000	0.00000	-3.17543
-39.60000	0.85737	-3.16254
-39.60000	1.71473	-3.12356
-39.60000	2.85788	-3.02916
-39.60000	4.00104	-2.88178
-39.60000	5.23945	-2.65200
-39.60000	6.47787	-2.32826
-39.60000	7.62102	-1.90526
-39.60000	8.57365	-1.38414
-39.60000	9.20239	-0.82098
-39.60000	9.52628	0.00000
-44.40000	0.00000	-3.17543
-44.40000	0.85737	-3.16254
-44.40000	1.71473	-3.12356
-44.40000	2.85788	-3.02916
-44.40000	4.00104	-2.88178
-44.40000	5.23945	-2.65200
-44.40000	6.47787	-2.32826
-44.40000	7.62102	-1.90526
-44.40000	8.57365	-1.38414
-44.40000	9.20239	-0.82098
-44.40000	9.52628	0.00000
-50.40000	0.00000	-3.17543
-50.40000	0.85737	-3.16254
-50.40000	1.71473	-3.12356
-50.40000	2.85788	-3.02916
-50.40000	4.00104	-2.88178
-50.40000	5.23945	-2.65200
-50.40000	6.47787	-2.32826
-50.40000	7.62102	-1.90526
-50.40000	8.57365	-1.38414
-50.40000	9.20239	-0.82098
-50.40000	9.52628	0.00000
-56.40000	0.00000	-3.17543
-56.40000	0.85737	-3.16254
-56.40000	1.71473	-3.12356
-56.40000	2.85788	-3.02916
-56.40000	4.00104	-2.88178
-56.40000	5.23945	-2.65200
-56.40000	6.47787	-2.32826
-56.40000	7.62102	-1.90526
-56.40000	8.57365	-1.38414
-56.40000	9.20239	-0.82098
-56.40000	9.52628	0.00000
-60.00000	0.00000	-3.17543
-60.00000	0.85737	-3.16254
-60.00000	1.71473	-3.12356
-60.00000	2.85788	-3.02916
-60.00000	4.00104	-2.88178
-60.00000	5.23945	-2.65200
-60.00000	6.47787	-2.32826
-60.00000	7.62102	-1.90526
-60.00000	8.57365	-1.38414
-60.00000	9.20239	-0.82098
-60.00000	9.52628	0.00000
-63.60000	0.00000	-3.17543
-63.60000	0.85737	-3.16254
-63.60000	1.71473	-3.12356
-63.60000	2.85788	-3.02916
-63.60000	4.00104	-2.88178
-63.60000	5.23945	-2.65200
-63.60000	6.47787	-2.32826
-63.60000	7.62102	-1.90526
-63.60000	8.57365	-1.38414
-63.60000	9.20239	-0.82098
-63.60000	9.52628	0.00000
-68.40000	0.00000	-3.17543
-68.40000	0.85737	-3.16254
-68.40000	1.71473	-3.12356
-68.40000	2.85788	-3.02916
-68.40000	4.00104	-2.88178
-68.40000	5.23945	-2.65200
-68.40000	6.47787	-2.32826
-68.40000	7.62102	-1.90526
-68.40000	8.57365	-1.38414

TABLE 1 (Continued)

x	y	z	x	y	z
-68.40000	9.20239	-0.82098	-88.88892	4.91543	-2.48799
-68.40000	9.52628	0.00000	-88.88892	6.07725	-2.18427
-73.20000	0.00000	-3.17543	-88.88892	7.14971	-1.78743
-73.20000	0.85737	-3.16254	-88.88892	8.04343	-1.29854
-73.20000	1.71473	-3.12356	-88.88892	8.63328	-0.77021
-73.20000	2.85788	-3.02916	-88.88892	8.93714	0.00000
-73.20000	4.00104	-2.88178	-91.17648	0.00000	-2.89825
-73.20000	5.23945	-2.65200	-91.17648	0.78253	-2.88648
-73.20000	6.47787	-2.32826	-91.17648	1.56505	-2.85091
-73.20000	7.62102	-1.90526	-91.17648	2.60842	-2.76475
-73.20000	8.57365	-1.38414	-91.17648	3.65179	-2.63023
-73.20000	9.20239	-0.82098	-91.17648	4.78211	-2.42051
-73.20000	9.52628	0.00000	-91.17648	5.91242	-2.12503
-76.99344	0.00000	-3.17158	-91.17648	6.95579	-1.73895
-76.99344	0.85633	-3.15871	-91.17648	7.82527	-1.26332
-76.99344	1.71265	-3.11978	-91.17648	8.39912	-0.74932
-76.99344	2.85442	-3.02550	-91.17648	8.69474	0.00000
-76.99344	3.99619	-2.87829	-94.83660	0.00000	-2.73555
-76.99344	5.23311	-2.64879	-94.83660	0.73860	-2.72445
-76.99344	6.47003	-2.32544	-94.83660	1.47720	-2.69087
-76.99344	7.61180	-1.90295	-94.83660	2.46199	-2.60955
-76.99344	8.56327	-1.38246	-94.83660	3.44679	-2.48258
-76.99344	9.19124	-0.81999	-94.83660	4.51366	-2.28463
-76.99344	9.51474	0.00000	-94.83660	5.58052	-2.00574
-81.56868	0.00000	-3.13836	-94.83660	6.56532	-1.64133
-81.56868	0.84736	-3.12562	-94.83660	7.38598	-1.19240
-81.56868	1.69471	-3.08710	-94.83660	7.92762	-0.70725
-81.56868	2.82452	-2.99381	-94.83660	8.20665	0.00000
-81.56868	3.95433	-2.84814	-97.12416	0.00000	-2.61164
-81.56868	5.17829	-2.62105	-97.12416	0.70514	-2.60105
-81.56868	6.40226	-2.30108	-97.12416	1.41029	-2.56899
-81.56868	7.53207	-1.88302	-97.12416	2.35048	-2.49135
-81.56868	8.47357	-1.36798	-97.12416	3.29067	-2.37013
-81.56868	9.09497	-0.81140	-97.12416	4.30921	-2.18115
-81.56868	9.41508	0.00000	-97.12416	5.32775	-1.91489
-85.22880	0.00000	-3.07684	-97.12416	6.26795	-1.56699
-85.22880	0.83075	-3.06435	-97.12416	7.05144	-1.13839
-85.22880	1.66149	-3.02658	-97.12416	7.56854	-0.67522
-85.22880	2.76915	-2.93512	-97.12416	7.83493	0.00000
-85.22880	3.87682	-2.79230	-100.78428	0.00000	-2.37435
-85.22880	5.07678	-2.56967	-100.78428	0.64108	-2.36472
-85.22880	6.27675	-2.25597	-100.78428	1.28215	-2.33557
-85.22880	7.38441	-1.84610	-100.78428	2.13692	-2.26499
-85.22880	8.30746	-1.34116	-100.78428	2.99168	-2.15478
-85.22880	8.91668	-0.79549	-100.78428	3.91768	-1.98298
-85.22880	9.23051	0.00000	-100.78428	4.84368	-1.74090
-88.88892	0.00000	-2.97905	-100.78428	5.69845	-1.42461
-88.88892	0.80434	-2.96696	-100.78428	6.41075	-1.03496
-88.88892	1.60869	-2.93039	-100.78428	6.88087	-0.61387
-88.88892	2.68114	-2.84183	-100.78428	7.12306	0.00000
-88.88892	3.75360	-2.70356	-103.52940	0.00000	-2.16142

TABLE 1 (Continued)

x	y	z	x	y	z
-103.52940	0.58358	-2.15265	-111.60000	3.55573	-0.57404
-103.52940	1.16717	-2.12612	-111.60000	3.81648	-0.34048
-103.52940	1.94528	-2.06186	-111.60000	3.95081	0.00000
-103.52940	2.72339	-1.96154	-114.00000	0.00000	-0.97745
-103.52940	3.56634	-1.80514	-114.00000	0.26391	-0.97349
-103.52940	4.40930	-1.58478	-114.00000	0.52783	-0.96149
-103.52940	5.18741	-1.29685	-114.00000	0.87971	-0.93243
-103.52940	5.83584	-0.94214	-114.00000	1.23159	-0.88706
-103.52940	6.26380	-0.55882	-114.00000	1.61280	-0.81634
-103.52940	6.48426	0.00000	-114.00000	1.99401	-0.71668
-105.81696	0.00000	-1.95826	-114.00000	2.34589	-0.58647
-105.81696	0.52873	-1.95032	-114.00000	2.63913	-0.42606
-105.81696	1.05746	-1.92628	-114.00000	2.83266	-0.25271
-105.81696	1.76244	-1.86806	-114.00000	2.93236	0.00000
-105.81696	2.46741	-1.77717	-114.84000	0.00000	-0.84870
-105.81696	3.23113	-1.63547	-114.84000	0.22915	-0.84526
-105.81696	3.99486	-1.43582	-114.84000	0.45830	-0.83484
-105.81696	4.69983	-1.17496	-114.84000	0.76383	-0.80961
-105.81696	5.28731	-0.85359	-114.84000	1.06937	-0.77022
-105.81696	5.67504	-0.50629	-114.84000	1.40036	-0.70881
-105.81696	5.87479	0.00000	-114.84000	1.73136	-0.62228
-108.10452	0.00000	-1.72912	-114.84000	2.03689	-0.50922
-108.10452	0.46686	-1.72211	-114.84000	2.29150	-0.36994
-108.10452	0.93373	-1.70088	-114.84000	2.45955	-0.21943
-108.10452	1.55621	-1.64948	-114.84000	2.54611	0.00000
-108.10452	2.17870	-1.56922	-116.04000	0.00000	-0.66049
-108.10452	2.85305	-1.44410	-116.04000	0.17833	-0.65781
-108.10452	3.52741	-1.26781	-116.04000	0.35666	-0.64970
-108.10452	4.14990	-1.03747	-116.04000	0.59444	-0.63007
-108.10452	4.66863	-0.75371	-116.04000	0.83222	-0.59941
-108.10452	5.01100	-0.44705	-116.04000	1.08981	-0.55162
-108.10452	5.18737	0.00000	-116.04000	1.34740	-0.48428
-110.39220	0.00000	-1.47123	-116.04000	1.58517	-0.39629
-110.39220	0.39723	-1.46526	-116.04000	1.78332	-0.28790
-110.39220	0.79447	-1.44720	-116.04000	1.91410	-0.17076
-110.39220	1.32411	-1.40347	-116.04000	1.98147	0.00000
-110.39220	1.85375	-1.33518	-116.88000	0.00000	-0.53001
-110.39220	2.42753	-1.22872	-116.88000	0.14310	-0.52786
-110.39220	3.00131	-1.07873	-116.88000	0.28620	-0.52135
-110.39220	3.53096	-0.88274	-116.88000	0.47701	-0.50559
-110.39220	3.97233	-0.64130	-116.88000	0.66781	-0.48099
-110.39220	4.26363	-0.38038	-116.88000	0.87451	-0.44264
-110.39220	4.41370	0.00000	-116.88000	1.08122	-0.38861
-111.60000	0.00000	-1.31694	-116.88000	1.27202	-0.31800
-111.60000	0.35557	-1.31159	-116.88000	1.43102	-0.23102
-111.60000	0.71115	-1.29543	-116.88000	1.53596	-0.13703
-111.60000	1.18524	-1.25628	-116.88000	1.59002	0.00000
-111.60000	1.65934	-1.19515	-117.36000	0.00000	-0.47285
-111.60000	2.17294	-1.09986	-117.36000	0.12767	-0.47093
-111.60000	2.68655	-0.96559	-117.36000	0.25534	-0.46513
-111.60000	3.16065	-0.79016	-117.36000	0.42556	-0.45107

TABLE 1 (Continued)

x	y	z	x	y	z
-117.36000	0.59579	-0.42912	-119.76000	0.00000	-0.27944
-117.36000	0.78020	-0.39491	-119.76000	0.07545	-0.27830
-117.36000	0.96461	-0.34670	-119.76000	0.15090	-0.27487
-117.36000	1.13484	-0.28371	-119.76000	0.25149	-0.26657
-117.36000	1.27669	-0.20611	-119.76000	0.35209	-0.25360
-117.36000	1.37032	-0.12225	-119.76000	0.46107	-0.23338
-117.36000	1.41855	0.00000	-119.76000	0.57005	-0.20489
-117.72000	0.00000	-0.44225	-119.76000	0.67065	-0.16766
-117.72000	0.11941	-0.44046	-119.76000	0.75448	-0.12180
-117.72000	0.23882	-0.43503	-119.76000	0.80981	-0.07225
-117.72000	0.39803	-0.42188	-119.76000	0.83831	0.00000
-117.72000	0.55724	-0.40135	-120.24000	0.00000	-0.19861
-117.72000	0.72971	-0.36935	-120.24000	0.05362	-0.19780
-117.72000	0.90219	-0.32426	-120.24000	0.10725	-0.19536
-117.72000	1.06140	-0.26535	-120.24000	0.17875	-0.18946
-117.72000	1.19408	-0.19277	-120.24000	0.25025	-0.18024
-117.72000	1.28164	-0.11434	-120.24000	0.32770	-0.16587
-117.72000	1.32675	0.00000	-120.24000	0.40516	-0.14562
-118.44000	0.00000	-0.38798	-120.24000	0.47666	-0.11917
-118.44000	0.10475	-0.38640	-120.24000	0.53624	-0.08657
-118.44000	0.20951	-0.38164	-120.24000	0.57557	-0.05135
-118.44000	0.34918	-0.37011	-120.24000	0.59583	0.00000
-118.44000	0.48885	-0.35210	-120.48000	0.00000	-0.13106
-118.44000	0.64017	-0.32403	-120.48000	0.03539	-0.13053
-118.44000	0.79148	-0.28447	-120.48000	0.07077	-0.12892
-118.44000	0.93115	-0.23279	-120.48000	0.11795	-0.12502
-118.44000	1.04754	-0.16912	-120.48000	0.16513	-0.11894
-118.44000	1.12436	-0.10031	-120.48000	0.21625	-0.10946
-118.44000	1.16394	0.00000	-120.48000	0.26736	-0.09609
-118.92000	0.00000	-0.35161	-120.48000	0.31454	-0.07864
-118.92000	0.09493	-0.35018	-120.48000	0.35386	-0.05713
-118.92000	0.18987	-0.34586	-120.48000	0.37981	-0.03388
-118.92000	0.31645	-0.33541	-120.48000	0.39318	0.00000
-118.92000	0.44302	-0.31909	-120.72000	0.00000	0.00000
-118.92000	0.58015	-0.29365	-120.72000	0.00000	0.00000
-118.92000	0.71728	-0.25780	-120.72000	0.00000	0.00000
-118.92000	0.84386	-0.21096	-120.72000	0.00000	0.00000
-118.92000	0.94934	-0.15326	-120.72000	0.00000	0.00000
-118.92000	1.01896	-0.09091	-120.72000	0.00000	0.00000
-118.92000	1.05482	0.00000	-120.72000	0.00000	0.00000
-119.52000	0.00000	-0.30195	-120.72000	0.00000	0.00000
-119.52000	0.08153	-0.30073	-120.72000	0.00000	0.00000
-119.52000	0.16306	-0.29702	-120.72000	0.00000	0.00000
-119.52000	0.27176	-0.28805	-120.72000	0.00000	0.00000
-119.52000	0.38046	-0.27403			
-119.52000	0.49822	-0.25218			
-119.52000	0.61599	-0.22140			
-119.52000	0.72469	-0.18117			
-119.52000	0.81528	-0.13162			
-119.52000	0.87506	-0.07807			
-119.52000	0.90586	0.00000			

TABLE 2 - MEASURED PRESSURE COEFFICIENTS

x/L	θ, Angular Position (deg)				
	0	45	67	80	90
0.719	-0.0442	-0.0397	-0.0385	-0.0421	-0.0397
0.810	-0.0349	-0.0385	-0.0385	-0.0241	-0.0193
0.839	-0.0277	-0.0277	-0.0205	-0.0144	-0.0012
0.854	-0.0169	-0.0157	-0.0085	-0.0012	+0.0073
0.879	+0.0073	+0.0061	+0.0097	+0.0182	+0.0278
0.894	+0.0230	+0.0218	+0.0230	+0.0339	+0.0448
0.914	+0.0375	+0.0387	+0.0448	+0.0557	+0.0617
0.934	+0.0714	+0.0714	+0.0787	+0.0896	+0.0932
0.954	+0.1150	+0.1126	+0.1138	+0.1211	+0.1235

TABLE 3 - MEASURED MEAN AND TURBULENT VELOCITY CHARACTERISTICS FOR VARYING AXIAL LOCATIONS ALONG 0-DEGREE PLANE

TABLE 3A - $\dot{x}/L = 0.719$

n_e(ft)	$\frac{u_x}{U_o}$	$\frac{v_n}{U_o}$	$\frac{\sqrt{\overline{u_x'^2}}}{U_o}$	$\frac{\sqrt{\overline{v_n'^2}}}{U_o}$	$100\,\frac{\overline{-u_x'v_n'}}{U_o^2}$	$\frac{\overline{-u_x'v_n'}}{q^2}$	$\frac{n_e}{\delta_r}$	$\frac{\varepsilon}{U_\delta \delta_p^*}$	$\frac{\ell_p}{\delta_r}$	$\frac{\ell}{\sqrt{(a+0.6\delta_a)(b+0.6\delta_b)-ab}}$
0.0156	0.720	-0.010	0.070	0.035	0.1058	0.154	0.1689	0.0027	0.0184	0.0061
0.0229	0.767	-0.014	0.066	0.033	0.1030	0.146	0.2477	0.0080	0.0559	0.0184
0.0306	0.813	-0.017	0.061	0.033	0.0835	0.133	0.3306	0.0082	0.0636	0.0209
0.0378	0.841	-0.016	0.057	0.031	0.0721	0.129	0.4090	0.0081	0.0677	0.0223
0.0455	0.877	-0.016	0.052	0.029	0.0648	0.135	0.4919	0.0079	0.0692	0.0228
0.0524	0.900	-0.017	0.048	0.029	0.0684	0.159	0.5667	0.0093	0.0795	0.0262
0.0605	0.931	-0.021	0.042	0.024	0.0441	0.133	0.6541	0.0066	0.0700	0.0230
0.0677	0.951	-0.020	0.038	0.023	0.0373	0.138	0.7324	0.0059	0.0685	0.0225
0.0734	0.969	-0.022	0.032	0.019	0.0208	0.109	0.7937	0.0037	0.0570	0.0188
0.0828	0.987	-0.022	0.023	0.016	0.0146	0.129	0.8946	0.0048	0.0897	0.0295
0.0928	0.997	-0.022	0.015	0.013	0.0059	0.109	1.0036	0.0042	0.1234	0.0406
0.1001	1.000	-0.023	0.009	0.009	0.0017	0.070	1.0820	0.0022	0.1198	0.0394
0.1837	1.000	-0.024	0.002	0.002						
0.3288	1.000	-0.024	0.002	0.001						
0.4888	1.000	-0.023	0.004	0.002						
0.6069	0.997	-0.024	0.005	0.001						

$\delta_p^* = 0.0202$ ft $\delta_r = 0.093$ ft $\frac{U_\delta}{U_o} = 1.0275$

$a = 0.7598$ ft $\delta_a = 0.1188$ ft $b = 0.2533$ ft $\delta_b = 0.1241$ ft

TABLE 3 (Continued)

TABLE 3B - x/L = 0.810

n_e(ft)	$\frac{u_x}{U_o}$	$\frac{v_n}{U_o}$	$\frac{\sqrt{\overline{u_x'^2}}}{U_o}$	$\frac{\sqrt{\overline{v_n'^2}}}{U_o}$	$100\frac{\overline{-u_x'v_n'}}{U_o^2}$	$\frac{\overline{-u_x'v_n'}}{q^2}$	$\frac{n_e}{\delta_r}$	$\frac{\varepsilon}{U_\delta \delta_p^*}$	$\frac{\ell_p}{\delta_r}$	$\frac{\ell}{\sqrt{(a+0.6\delta_a)(b+0.6\delta_b)-ab}}$
0.0104	0.668	-0.029	0.072	0.035	0.1105	0.165	0.0906	0.0019	0.0104	0.0041
0.0165	0.708	-0.032	0.070	0.035	0.1246	0.181	0.1435	0.0085	0.0430	0.0172
0.0218	0.748	-0.035	0.070	0.036	0.1262	0.167	0.1891	0.0094	0.0471	0.0188
0.0266	0.775	-0.037	0.065	0.032	0.0917	0.135	0.2312	0.0081	0.0476	0.0190
0.0343	0.816	-0.038	0.060	0.035	0.1002	0.160	0.2978	0.0099	0.0560	0.0224
0.0448	0.861	-0.044	0.052	0.031	0.0755	0.154	0.3891	0.0092	0.0596	0.0239
0.0524	0.890	-0.044	0.050	0.029	0.0681	0.151	0.4558	0.0098	0.0669	0.0267
0.0626	0.918	-0.046	0.045	0.028	0.0587	0.160	0.5442	0.0088	0.0651	0.0260
0.0723	0.954	-0.050	0.037	0.023	0.0421	0.167	0.6283	0.0076	0.0656	0.0262
0.0832	0.972	-0.049	0.031	0.021	0.0268	0.158	0.7232	0.0075	0.0813	0.0325
0.0932	0.991	-0.051	0.023	0.016	0.0133	0.138	0.8109	0.0049	0.0751	0.0300
0.1042	0.999	-0.052	0.017	0.014	0.0087	0.164	0.9058	0.0069	0.1312	0.0524
0.1328	1.006	-0.053	0.007	0.006	0.0007	0.082	1.1551	0.0022	0.1506	0.0602
0.2003	1.001	-0.052	0.004	0.002						
0.3111	1.000	-0.050	0.003	0.001						
0.4125	1.000	-0.046	0.001	0.001						

$\delta_p^* = 0.0200$ ft $\delta_r = 0.115$ ft $\frac{U_\delta}{U_o} = 1.0230$

$a = 0.6429$ ft $\delta_a = 0.1549$ ft $b = 0.2143$ ft $\delta_b = 0.1423$ ft

TABLE 3 (Continued)

TABLE 3C - $x/L = 0.854$

n_e(ft)	$\frac{u_x}{U_o}$	$\frac{v_n}{U_o}$	$\frac{\sqrt{\overline{u_x'^2}}}{U_o}$	$\frac{\sqrt{\overline{v_n'^2}}}{U_o}$	$100\,\frac{\overline{-u_x'v_n'}}{U_o^2}$	$\frac{\overline{-u_x'v_n'}}{q^2}$	$\frac{n_e}{\delta_r}$	$\frac{\varepsilon}{U_\delta \delta_p^*}$	$\frac{\ell_p}{\delta_r}$	$\frac{\ell}{\sqrt{(a+0.6\delta_a)(b+0.6\delta_b)-ab}}$
0.0104	0.666	-0.042	0.071	0.034	0.1262	0.194	0.0868	0.0019	0.0107	0.0045
0.0161	0.711	-0.045	0.070	0.035	0.1152	0.167	0.1340	0.0068	0.0392	0.0164
0.0218	0.748	-0.049	0.065	0.034	0.1074	0.157	0.1813	0.0075	0.0448	0.0188
0.0266	0.776	-0.050	0.062	0.034	0.0996	0.152	0.2215	0.0078	0.0485	0.0203
0.0318	0.803	-0.053	0.062	0.034	0.0976	0.152	0.2653	0.0073	0.0458	0.0192
0.0362	0.830	-0.054	0.058	0.034	0.1017	0.172	0.3021	0.0091	0.0557	0.0234
0.0408	0.845	-0.055	0.057	0.032	0.0833	0.150	0.3396	0.0108	0.0730	0.0306
0.0496	0.873	-0.057	0.051	0.031	0.0752	0.155	0.4132	0.0098	0.0698	0.0292
0.0569	0.898	-0.059	0.048	0.031	0.0739	0.170	0.4743	0.0096	0.0688	0.0289
0.0650	0.924	-0.060	0.045	0.027	0.0582	0.161	0.5417	0.0081	0.0656	0.0276
0.0751	0.952	-0.062	0.038	0.024	0.0395	0.157	0.6257	0.0074	0.0726	0.0305
0.0856	0.970	-0.062	0.035	0.022	0.0369	0.186	0.7132	0.0084	0.0857	0.0359
0.0932	0.986	-0.065	0.028	0.020	0.0248	0.187	0.7771	0.0063	0.0782	0.0328
0.1086	1.002	-0.065	0.019	0.014	0.0084	0.152	0.9049	0.0051	0.1079	0.0453
0.1268	1.007	-0.065	0.008	0.007	0.0012	0.103	1.0569	0.0026	0.1480	0.0586
0.1704	1.007	-0.063	0.004	0.002						
0.2804	1.003	-0.056	0.006	0.001						
0.4295	1.001	-0.047	0.004	0.002						

$\delta_p^* = 0.0224$ ft $\delta_r = 0.120$ ft $\frac{U_\delta}{U_o} = 1.0444$

$a = 0.5491$ ft $\delta_a = 0.1902$ ft $b = 0.1830$ ft $\delta_b = 0.1531$ ft

TABLE 3 (Continued)

TABLE 3D - x/L = 0.894

n_e(ft)	$\frac{u_x}{U_o}$	$\frac{v_n}{U_o}$	$\frac{\sqrt{\overline{u_x'^2}}}{U_o}$	$\frac{\sqrt{\overline{v_n'^2}}}{U_o}$	$100\frac{\overline{-u_x'v_n'}}{U_o^2}$	$\frac{\overline{-u_x'v_n'}}{q^2}$	$\frac{n_e}{\delta_r}$	$\frac{\epsilon}{U_\delta \delta_p^*}$	$\frac{\ell_p}{\delta_r}$	$\frac{\ell}{\sqrt{(a+0.6\delta_a)(b+0.6\delta_b)-ab}}$
0.0104	0.572	-0.033	0.072	0.035	0.1161	0.172	0.0744	0.0019	0.0094	0.0047
0.0128	0.618	-0.036	0.073	0.035	0.1169	0.166	0.0917	0.0033	0.0161	0.0079
0.0185	0.652	-0.039	0.072	0.035	0.1214	0.164	0.1321	0.0074	0.0353	0.0173
0.0253	0.709	-0.043	0.069	0.035	0.1161	0.153	0.1810	0.0076	0.0371	0.0182
0.0327	0.743	-0.044	0.064	0.035	0.1025	0.151	0.2333	0.0084	0.0440	0.0217
0.0399	0.784	-0.044	0.060	0.034	0.0924	0.152	0.2851	0.0078	0.0427	0.0210
0.0472	0.817	-0.047	0.057	0.033	0.0839	0.150	0.3369	0.0089	0.0515	0.0253
0.0548	0.844	-0.049	0.052	0.031	0.0716	0.150	0.3917	0.0087	0.0541	0.0266
0.0642	0.877	-0.049	0.050	0.030	0.0657	0.153	0.4583	0.0084	0.0547	0.0269
0.0742	0.908	-0.049	0.043	0.027	0.0526	0.169	0.5304	0.0060	0.0441	0.0217
0.0803	0.933	-0.051	0.041	0.025	0.0415	0.157	0.5738	0.0055	0.0449	0.0221
0.0941	0.952	-0.052	0.036	0.022	0.0351	0.183	0.6720	0.0102	0.0914	0.0449
0.1208	0.995	-0.053	0.017	0.013	0.0073	0.149	0.8625	0.0032	0.0626	0.0307
0.1523	1.002	-0.050	0.005	0.005						
0.1902	1.001	-0.047	0.005	0.003						
0.2565	1.001	-0.040	0.004	0.002						
0.3814	1.001	-0.030	0.004	0.002						
0.5302	1.000	-0.020	0.004	0.002						

$\delta_p^* = 0.0234$ ft $\delta_r = 0.140$ ft $\frac{U_\delta}{U_o} = 0.9990$

a = 0.4369 ft $\delta_a = 0.2458$ ft b = 0.1457 ft $\delta_b = 0.1702$ ft

TABLE 3 (Continued)

TABLE 3E - x/L = 0.934

n_e(ft)	$\frac{u_x}{U_o}$	$\frac{v_n}{U_o}$	$\frac{\sqrt{\overline{u_x'^2}}}{U_o}$	$\frac{\sqrt{\overline{v_n'^2}}}{U_o}$	$100\,\frac{-\overline{u_x'v_n'}}{U_o^2}$	$\frac{-\overline{u_x'v_n'}}{q^2}$	$\frac{n_e}{\delta_r}$	$\frac{\varepsilon}{U_\delta \delta_p^*}$	$\frac{\ell_p}{\delta_r}$	$\frac{\ell}{\sqrt{(a+0.6\delta_a)(b+0.6\delta_b)-ab}}$
0.0104	0.533	-0.051	0.071	0.035	0.1289	0.193	0.0694	0.0024	0.0112	0.0059
0.0144	0.572	-0.054	0.070	0.034	0.1095	0.163	0.0961	0.0050	0.0251	0.0132
0.0209	0.618	-0.058	0.070	0.037	0.1264	0.167	0.1394	0.0069	0.0324	0.0170
0.0257	0.654	-0.060	0.065	0.035	0.1128	0.159	0.1717	0.0068	0.0338	0.0177
0.0351	0.701	-0.065	0.064	0.034	0.1040	0.154	0.2339	0.0078	0.0400	0.0209
0.0399	0.728	-0.065	0.063	0.033	0.1000	0.155	0.2661	0.0084	0.0441	0.0231
0.0476	0.755	-0.066	0.058	0.034	0.0920	0.158	0.3172	0.0091	0.0498	0.0261
0.0545	0.787	-0.068	0.056	0.033	0.0909	0.170	0.3633	0.0091	0.0504	0.0264
0.0622	0.813	-0.067	0.054	0.031	0.0825	0.174	0.4144	0.0104	0.0604	0.0316
0.0718	0.841	-0.068	0.047	0.029	0.0632	0.174	0.4789	0.0092	0.0610	0.0319
0.0840	0.872	-0.069	0.047	0.027	0.0619	0.194	0.5600	0.0096	0.0639	0.0335
0.0941	0.898	-0.070	0.040	0.024	0.0438	0.190	0.6272	0.0074	0.0586	0.0307
0.1159	0.939	-0.070	0.029	0.019	0.0232	0.193	0.7728	0.0063	0.0690	0.0361
0.1341	0.960	-0.069	0.016	0.012	0.0053	0.131	0.8939	0.0028	0.0646	0.0339
0.1579	0.966	-0.066	0.007	0.006	0.0005	0.049	1.0528	0.0012	0.0901	0.0472
0.1975	0.967	-0.061	0.005	0.003						
0.3043	0.971	-0.048	0.003	0.002						
0.4178	0.973	-0.039	0.004	0.001						
0.5512	0.982	-0.032	0.003	0.001						

$\delta_p^* = 0.0260$ ft $\delta_r = 0.150$ ft $\frac{U_\delta}{U_o} = 0.9583$

$a = 0.2903$ ft $\delta_a = 0.3625$ ft $b = 0.0968$ ft $\delta_b = 0.2001$ ft

TABLE 3 (Continued)

TABLE 3F - x/L = 0.954

n_e(ft)	$\frac{u_x}{U_o}$	$\frac{v_n}{U_o}$	$\frac{\sqrt{\overline{u_x'^2}}}{U_o}$	$\frac{\sqrt{\overline{v_n'^2}}}{U_o}$	$100\frac{\overline{-u_x'v_n'}}{U_o^2}$	$\frac{\overline{-u_x'v_n'}}{q^2}$	$\frac{n_e}{\delta_r}$	$\frac{\varepsilon}{U_\delta \delta_p^*}$	$\frac{\ell_p}{\delta_r}$	$\frac{\ell}{\sqrt{(a+0.6\delta_a)(b+0.6\delta_b)-ab}}$
0.0104	0.483	-0.057	0.070	0.035	0.1277	0.199	0.0651	0.0015	0.0080	0.0045
0.0218	0.568	-0.061	0.068	0.035	0.1284	0.177	0.1359	0.0050	0.0269	0.0155
0.0280	0.623	-0.065	0.067	0.035	0.1208	0.166	0.1750	0.0053	0.0297	0.0171
0.0415	0.679	-0.070	0.062	0.036	0.1144	0.177	0.2594	0.0091	0.0519	0.0300
0.0557	0.736	-0.071	0.058	0.035	0.0990	0.176	0.3479	0.0090	0.0552	0.0319
0.0787	0.801	-0.074	0.053	0.031	0.0814	0.197	0.4922	0.0097	0.0657	0.0380
0.0985	0.853	-0.075	0.043	0.025	0.0504	0.196	0.6156	0.0065	0.0561	0.0324
0.1187	0.901	-0.076	0.035	0.020	0.0324	0.202	0.7422	0.0049	0.0532	0.0307
0.1389	0.938	-0.074	0.022	0.016	0.0176	0.226	0.8682	0.0048	0.0700	0.0404
0.1568	0.949	-0.073	0.015	0.011	0.0042	0.122	0.9797	0.0029	0.0865	0.0499
0.1765	0.955	-0.071	0.007	0.006	0.0003	0.041	1.1031	0.0005	0.0550	0.0313
0.1992	0.957	-0.067	0.005	0.003	0.0002	0.036	1.2448	0.0007	0.1123	0.0649
0.2359	0.959	-0.064	0.005	0.002						
0.3159	0.960	-0.055	0.002	0.002						
0.4473	0.962	-0.046	0.003	0.001						
0.5956	0.964	-0.039	0.004	0.001						

$\delta_p^* = 0.0326$ ft $\delta_r = 0.160$ ft $\frac{U_\delta}{U_o} = 0.9520$

$a = 0.1995$ ft $\delta_a = 0.4378$ ft $b = 0.0665$ ft $\delta_b = 0.2139$ ft

TABLE 4 - MEASURED MEAN AND TURBULENT VELOCITY CHARACTERISTICS FOR VARYING AXIAL LOCATIONS ALONG 67-DEGREE PLANE

TABLE 4A - x/L = 0.719

n_e(ft)	$\frac{u_x}{U_o}$	$\frac{v_n}{U_o}$	$\frac{w_\theta}{U_o}$	$\frac{\sqrt{\overline{u_x'^2}}}{U_o}$	$\frac{\sqrt{\overline{v_n'^2}}}{U_o}$	$\frac{\sqrt{\overline{w_\theta'^2}}}{U_o}$	$100\frac{\overline{-u_x'v_n'}}{U_o^2}$	$100\frac{\overline{-u_x'w_\theta'}}{U_o^2}$	$\frac{\overline{-u_x'v_n'}}{q^2}$	$\frac{\overline{-u_x'w_\theta'}}{q^2}$	$\frac{n_e}{\delta_r}$	$\frac{\varepsilon}{U_\delta \delta_p{}^*}$	$\frac{\ell_p}{\delta_r}$	$\frac{\ell}{\sqrt{(a+0.6\delta_a)(b+0.6\delta_b)-ab}}$
0.0233	0.767	-0.005	0.053	0.067	0.033	0.041	0.0987	0.0046	0.135	0.006	0.2333	0.0036	0.0280	0.0099
0.0318	0.795	-0.006	0.051	0.063	0.033	0.039	0.0864	0.0103	0.131	0.016	0.3183	0.0084	0.0697	0.0246
0.0415	0.846	-0.004	0.054	0.058	0.031	0.036	0.0720	0.0036	0.126	0.006	0.4150	0.0071	0.0645	0.0228
0.0488	0.870	-0.005	0.055	0.052	0.030	0.035	0.0673	0.0081	0.139	0.017	0.4883	0.0081	0.0761	0.0269
0.0585	0.904	-0.006	0.058	0.050	0.028	0.032	0.0658	0.0136	0.153	0.032	0.5850	0.0078	0.0737	0.0261
0.0666	0.932	-0.007	0.059	0.043	0.026	0.028	0.0456	0.0015	0.139	0.005	0.6658	0.0055	0.0633	0.0224
0.0742	0.957	-0.008	0.058	0.039	0.022	0.023	0.0354	0.0049	0.141	0.019	0.7425	0.0048	0.0629	0.0222
0.0832	0.981	-0.008	0.060	0.029	0.018	0.018	0.0220	-0.0006	0.148	-0.004	0.8317	0.0047	0.0767	0.0271
0.0917	0.991	-0.007	0.060	0.022	0.015	0.013	0.0117	0.0022	0.133	0.025	0.9167	0.0045	0.1008	0.0356
0.1013	1.000	-0.008	0.060	0.011	0.010	0.008	0.0030	0.0014	0.109	0.052	1.0133	0.0024	0.1059	0.0375
0.1118	1.001	-0.008	0.061	0.007	0.007	0.004	0.0010	0.0003	0.090	0.023	1.1183	0.0084	0.6321	0.2235
0.1240	1.001	-0.008	0.060	0.005	0.004	0.003								
0.1765	1.000	-0.008	0.057	0.003	0.002	0.002								
0.2965	1.000	-0.007	0.055	0.002	0.001	0.001								
0.4957	0.998	-0.005	0.051	0.005	0.001	0.001								
0.5892	0.997	-0.005	0.051	0.005	0.001	0.001								

$\delta_p{}^* = 0.0237$ ft $\qquad \delta_r = 0.100$ ft $\qquad \frac{U_\delta}{U_o} = 1.0275$

$a = 0.7598$ ft $\qquad \delta_a = 0.1188$ ft $\qquad b = 0.2533$ ft $\qquad \delta_b = 0.1241$ ft

TABLE 4 (Continued)

TABLE 4B - x/L = 0.810

n_e(ft)	$\frac{u_x}{U_o}$	$\frac{v_n}{U_o}$	$\frac{w_\theta}{U_o}$	$\frac{\sqrt{\overline{u_x'^2}}}{U_o}$	$\frac{\sqrt{\overline{v_n'^2}}}{U_o}$	$\frac{\sqrt{\overline{w_\theta'^2}}}{U_o}$	$100\frac{-\overline{u_x'v_n'}}{U_o^2}$	$100\frac{-\overline{u_x'w_\theta'}}{U_o^2}$	$\frac{-\overline{u_x'v_n'}}{q^2}$	$\frac{-\overline{u_x'w_\theta'}}{q^2}$	$\frac{n_e}{\delta_r}$	$\frac{\varepsilon}{U_\delta \delta_p^*}$	$\frac{\ell_p}{\delta_r}$	$\frac{\ell}{\sqrt{(a+0.6\delta_a)(b+0.6\delta_b)}-ab}$
0.0104	0.668	-0.028	0.037	0.071	0.036	0.041	0.1160	0.0106	0.144	0.013	0.0883	0.0020	0.0098	0.0040
0.0157	0.730	-0.031	0.041	0.068	0.034	0.042	0.1116	0.0164	0.147	0.022	0.1328	0.0058	0.0289	0.0118
0.0286	0.794	-0.033	0.046	0.063	0.033	0.040	0.0962	0.0009	0.143	0.001	0.2422	0.0080	0.0429	0.0176
0.0355	0.841	-0.037	0.046	0.060	0.032	0.039	0.0913	0.0138	0.149	0.022	0.3008	0.0089	0.0488	0.0201
0.0432	0.868	-0.038	0.046	0.055	0.031	0.037	0.0719	0.0100	0.133	0.018	0.3658	0.0104	0.0645	0.0265
0.0512	0.896	-0.040	0.048	0.051	0.030	0.036	0.0738	-0.0037	0.152	-0.008	0.4343	0.0130	0.0792	0.0325
0.0650	0.923	-0.042	0.048	0.048	0.026	0.030	0.0544	0.0045	0.140	0.012	0.5508	0.0089	0.0631	0.0259
0.0723	0.950	-0.044	0.050	0.041	0.025	0.028	0.0471	0.0074	0.150	0.024	0.6123	0.0072	0.0551	0.0226
0.0795	0.972	-0.044	0.050	0.036	0.022	0.026	0.0351	0.0042	0.144	0.017	0.6737	0.0076	0.0669	0.0275
0.0884	0.987	-0.045	0.051	0.030	0.019	0.022	0.0227	0.0028	0.129	0.016	0.7493	0.0076	0.0830	0.0341
0.1033	1.006	-0.046	0.052	0.018	0.013	0.016	0.0075	0.0016	0.100	0.021	0.8757	0.0044	0.0844	0.0346
0.1236	1.012	-0.045	0.052	0.006	0.006	0.006	0.0002	0.0003	0.016	0.026	1.0473	0.0004	0.0450	0.0185
0.2291	1.009	-0.039	0.048	0.003	0.001	0.002								
0.2877	1.005	-0.036	0.047	0.005	0.002	0.002								
0.3596	1.005	-0.033	0.046	0.005	0.001	0.002								

$\delta_p^* = 0.0191$ ft $\qquad \delta_r = 0.118$ ft $\qquad \frac{U_\delta}{U_o} = 1.0214$

$a = 0.6429$ ft $\qquad \delta_a = 0.1549$ ft $\qquad b = 0.2143$ ft $\qquad \delta_b = 0.1423$ ft

TABLE 4 (Continued)

TABLE 4C - x/L = 0.854

n_e(ft)	$\frac{u_x}{U_o}$	$\frac{v_n}{U_o}$	$\frac{w_\theta}{U_o}$	$\frac{\sqrt{\overline{u_x'^2}}}{U_o}$	$\frac{\sqrt{\overline{v_n'^2}}}{U_o}$	$\frac{\sqrt{\overline{w_\theta'^2}}}{U_o}$	$100\frac{\overline{-u_x'v_n'}}{U_o^2}$	$100\frac{\overline{-u_x'w_\theta'}}{U_o^2}$	$\frac{\overline{-u'v'}}{q^2}$	$\frac{\overline{-u'w'}}{q^2}$	$\frac{n_e}{\delta_r}$	$\frac{\varepsilon}{U_\delta \delta_p{}^*}$	$\frac{\ell_p}{\delta_r}$	$\frac{\ell}{\sqrt{(a+0.6\delta_a)(b+0.6\delta_b)-ab}}$
0.0104	0.651	-0.030	0.017	0.073	0.034	0.040	0.1180	0.0087	0.146	0.011	0.0833	0.0020	0.0108	0.0047
0.0157	0.686	-0.033	0.016	0.068	0.035	0.042	0.1113	0.0010	0.148	0.001	0.1253	0.0067	0.0365	0.0160
0.0218	0.734	-0.038	0.016	0.065	0.033	0.041	0.0978	0.0255	0.140	0.036	0.1740	0.0066	0.0386	0.0169
0.0322	0.775	-0.038	0.018	0.060	0.033	0.040	0.0850	0.0019	0.136	-0.003	0.2580	0.0100	0.0629	0.0275
0.0399	0.803	-0.040	0.019	0.060	0.032	0.037	0.0828	0.0034	0.140	0.006	0.3193	0.0097	0.0620	0.0271
0.0476	0.832	-0.042	0.018	0.054	0.031	0.037	0.0710	0.0003	0.135	0.001	0.3807	0.0081	0.0559	0.0244
0.0537	0.855	-0.042	0.019	0.052	0.030	0.035	0.0770	0.0107	0.158	0.022	0.4293	0.0094	0.0623	0.0272
0.0642	0.887	-0.043	0.019	0.048	0.028	0.033	0.0581	0.0012	0.139	0.003	0.5133	0.0098	0.0747	0.0326
0.0723	0.905	-0.043	0.018	0.046	0.027	0.030	0.0596	0.0102	0.161	0.028	0.5780	0.0106	0.0795	0.0347
0.0819	0.932	-0.043	0.018	0.039	0.023	0.027	0.0395	0.0063	0.140	0.022	0.6553	0.0062	0.0573	0.0250
0.0868	0.946	-0.043	0.018	0.036	0.022	0.025	0.0366	0.0062	0.152	0.026	0.6947	0.0062	0.0591	0.0259
0.0941	0.963	-0.045	0.018	0.031	0.019	0.022	0.0238	0.0067	0.131	0.037	0.7527	0.0054	0.0637	0.0278
0.1017	0.974	-0.044	0.018	0.026	0.016	0.018	0.0142	0.0051	0.112	0.040	0.8140	0.0045	0.0698	0.0305
0.1143	0.988	-0.045	0.018	0.017	0.012	0.012	0.0047	0.0019	0.080	0.033	0.9140	0.0024	0.0638	0.0279
0.1389	0.997	-0.042	0.016	0.006	0.006	0.005								
0.1692	0.996	-0.038	0.015	0.004	0.003	0.003								
0.2509	0.997	-0.029	0.011	0.005	0.001	0.001								
0.3782	0.993	-0.019	0.006	0.005	0.001	0.001								
0.4962	0.989	-0.012	0.003	0.004	0.001	0.001								

$\delta_p{}^* = 0.0226$ ft $\delta_r = 0.125$ ft $\frac{U_\delta}{U_o} = 1.0131$

$a = 0.5491$ ft $\delta_a = 0.1902$ ft $b = 0.1830$ ft $\delta_b = 0.1531$ ft

TABLE 4 (Continued)

TABLE 4D - x/L = 0.894

n_e(ft)	$\frac{u_x}{U_o}$	$\frac{v_n}{U_o}$	$\frac{w_\theta}{U_o}$	$\frac{\sqrt{\overline{u_x'^2}}}{U_o}$	$\frac{\sqrt{\overline{v_n'^2}}}{U_o}$	$\frac{\sqrt{\overline{w_\theta'^2}}}{U_o}$	$100\frac{\overline{-u_x'v_n'}}{U_o^2}$	$100\frac{\overline{-u_x'w_\theta'}}{U_o^2}$	$\frac{\overline{-u_x'v_n'}}{q^2}$	$\frac{\overline{-u_x'w_\theta'}}{q^2}$	$\frac{n_e}{\delta_r}$	$\frac{\varepsilon}{U_\delta \delta_p^*}$	$\frac{\ell_p}{\delta_r}$	$\frac{\ell}{\sqrt{(a+0.6\delta_a)(b+0.6\delta_b)-ab}}$
0.0104	0.584	-0.054	-0.004	0.071	0.034	0.042	0.1234	-0.0065	0.156	-0.008	0.0718	0.0020	0.0094	0.0049
0.0153	0.637	-0.058	-0.002	0.066	0.035	0.041	0.1040	-0.0075	0.143	-0.010	0.1052	0.0042	0.0219	0.0112
0.0222	0.698	-0.060	-0.001	0.065	0.034	0.041	0.1068	-0.0099	0.152	-0.014	0.1529	0.0057	0.0294	0.0151
0.0294	0.744	-0.064	-0.001	0.063	0.034	0.040	0.0963	-0.0097	0.145	-0.015	0.2029	0.0076	0.0416	0.0211
0.0371	0.774	-0.066	-0.000	0.058	0.032	0.038	0.0855	0.0064	0.146	0.011	0.2557	0.0094	0.0545	0.0278
0.0456	0.803	-0.068	0.000	0.055	0.033	0.037	0.0864	0.0122	0.156	-0.022	0.3144	0.0110	0.0633	0.0322
0.0553	0.832	-0.068	-0.001	0.053	0.032	0.035	0.0836	-0.0088	0.165	-0.017	0.3810	0.0114	0.0666	0.0339
0.0650	0.861	-0.068	0.000	0.049	0.030	0.033	0.0704	-0.0029	0.160	-0.007	0.4483	0.0101	0.0646	0.0329
0.0775	0.894	-0.070	-0.001	0.044	0.026	0.029	0.0549	-0.0051	0.156	-0.015	0.5345	0.0083	0.0601	0.0306
0.0876	0.922	-0.071	-0.001	0.037	0.023	0.026	0.0413	-0.0017	0.158	-0.006	0.6040	0.0070	0.0583	0.0297
0.0973	0.942	-0.071	-0.002	0.034	0.021	0.022	0.0331	0.0023	0.162	0.011	0.6713	0.0074	0.0688	0.0350
0.1066	0.957	-0.070	-0.003	0.027	0.017	0.018	0.0199	0.0034	0.149	0.025	0.7351	0.0060	0.0713	0.0363
0.1297	0.975	-0.070	-0.002	0.012	0.009	0.009	0.0029	0.0002	0.095	0.005	0.8943	0.0029	0.0900	0.0458
0.1503	0.977	-0.066	-0.004	0.006	0.005	0.005	0.0002	0.0002	0.020	0.024	1.0362	0.0020	0.2575	0.1311
0.1713	0.977	-0.063	-0.005	0.004	0.003	0.003								
0.2129	0.976	-0.058	-0.007	0.004	0.002	0.002								
0.3301	0.976	-0.046	-0.009	0.005	0.001	0.001								
0.4845	0.986	-0.036	-0.009	0.006	0.002	0.001								
0.6174	0.977	-0.029	-0.009	0.002	0.001	0.001								

$\delta_p^* = 0.0246$ ft $\quad \delta_r = 0.145$ ft $\quad \frac{U_\delta}{U_o} = 0.9950$

$a = 0.4369$ ft $\quad \delta_a = 0.2458$ ft $\quad b = 0.1457$ ft $\quad \delta_b = 0.1702$ ft

TABLE 4 (Continued)

TABLE 4E - x/L = 0.914

n_e(ft)	$\frac{u_x}{U_o}$	$\frac{v_n}{U_o}$	$\frac{w_\theta}{U_o}$	$\frac{\sqrt{\overline{u_x'^2}}}{U_o}$	$\frac{\sqrt{\overline{v_n'^2}}}{U_o}$	$\frac{\sqrt{\overline{w_\theta'^2}}}{U_o}$	$100\frac{-\overline{u_x'v_n'}}{U_o^2}$	$100\frac{-\overline{u_x'w_\theta'}}{U_o^2}$	$\frac{-\overline{u_x'v_n'}}{q^2}$	$\frac{-\overline{u_x'w_\theta'}}{q^2}$	$\frac{n_e}{\delta_r}$	$\frac{\varepsilon}{U_\delta \delta_p^*}$	$\frac{\ell_p}{\delta_r}$	$\frac{\ell}{\sqrt{(a+0.6\delta_a)(b+0.6\delta_b)-ab}}$
0.0125	0.596	-0.034	0.037	0.066	0.032	0.043	0.0721	0.0833	0.100	0.115	0.0833	0.0016	0.0098	0.0052
0.0151	0.627	-0.034	0.032	0.067	0.034	0.043	0.0789	0.0653	0.105	0.087	0.1005	0.0032	0.0184	0.0097
0.0203	0.659	-0.035	0.037	0.066	0.034	0.043	0.0741	0.0829	0.100	0.111	0.1354	0.0042	0.0248	0.0131
0.0254	0.702	-0.039	0.057	0.064	0.036	0.044	0.0732	0.0872	0.101	0.120	0.1692	0.0046	0.0276	0.0146
0.0309	0.727	-0.039	0.065	0.061	0.036	0.043	0.0798	0.0607	0.115	0.088	0.2057	0.0072	0.0409	0.0216
0.0360	0.751	-0.040	0.069	0.058	0.033	0.043	0.0591	0.0785	0.094	0.124	0.2401	0.0061	0.0404	0.0213
0.0437	0.774	-0.040	0.076	0.059	0.034	0.043	0.0702	0.0867	0.110	0.136	0.2916	0.0088	0.0534	0.0282
0.0540	0.813	-0.041	0.085	0.054	0.033	0.041	0.0454	0.0716	0.081	0.128	0.3603	0.0051	0.0388	0.0205
0.0666	0.857	-0.042	0.092	0.051	0.031	0.038	0.0491	0.0631	0.099	0.127	0.4441	0.0071	0.0516	0.0272
0.0795	0.886	-0.042	0.101	0.045	0.028	0.035	0.0373	0.0481	0.092	0.119	0.5300	0.0062	0.0515	0.0272
0.0930	0.923	-0.042	0.104	0.038	0.024	0.032	0.0274	0.0404	0.090	0.133	0.6202	0.0048	0.0469	0.0247
0.1059	0.948	-0.039	0.110	0.031	0.021	0.027	0.0142	0.0324	0.066	0.150	0.7061	0.0034	0.0457	0.0241
0.1188	0.968	-0.039	0.114	0.024	0.017	0.022	0.0077	0.0242	0.057	0.179	0.7919	0.0025	0.0464	0.0245
0.1343	0.983	-0.037	0.118	0.014	0.011	0.014	0.0027	0.0099	0.053	0.193	0.8950	0.0015	0.0476	0.0252
0.1549	0.991	-0.034	0.119	0.007	0.006	0.007								
0.1810	0.991	-0.031	0.117	0.004	0.003	0.003								
0.2302	0.989	-0.026	0.114	0.004	0.002	0.002								
0.3104	0.992	-0.019	0.111	0.004	0.002	0.002								
0.3623	0.993	-0.014	0.110	0.004	0.002	0.002								
0.4399	0.994	-0.009	0.108	0.004	0.001	0.002								

$\delta_p^* = 0.0247$ ft $\quad \delta_r = 0.150$ ft $\quad \frac{U_\delta}{U_\infty} = 0.9802$

$a = 0.3690$ ft $\quad \delta_a = 0.2912$ ft $\quad b = 0.1230$ ft $\quad \delta_b = 0.1820$ ft

TABLE 4 (Continued)

TABLE 4F - x/L = 0.934

n_e(ft)	$\frac{u_x}{U_o}$	$\frac{v_n}{U_o}$	$\frac{w_\theta}{U_o}$	$\frac{\sqrt{\overline{u_x'^2}}}{U_o}$	$\frac{\sqrt{\overline{v_n'^2}}}{U_o}$	$\frac{\sqrt{\overline{w_\theta'^2}}}{U_o}$	$100\frac{\overline{-u_x'v_n'}}{U_o^2}$	$100\frac{\overline{-u_x'w_\theta'}}{U_o^2}$	$\frac{\overline{-u_x'v_n'}}{q^2}$	$\frac{\overline{-u_x'w_\theta'}}{q^2}$	$\frac{n_e}{\delta_r}$	$\frac{\varepsilon}{U_\delta \delta_p^*}$	$\frac{\ell_p}{\delta_r}$	$\frac{\ell}{\sqrt{(a+0.6\delta_a)(b+0.6\delta_b)-ab}}$
0.0104	0.538	-0.061	0.008	0.069	0.034	0.041	0.1111	0.0189	0.147	0.025	0.0613	0.0016	0.0072	0.0043
0.0189	0.597	-0.062	0.015	0.067	0.035	0.041	0.1185	0.0340	0.160	0.046	0.1113	0.0064	0.0290	0.0172
0.0282	0.661	-0.068	0.022	0.064	0.035	0.041	0.1048	0.0263	0.149	0.038	0.1657	0.0072	0.0347	0.0206
0.0367	0.697	-0.070	0.024	0.066	0.036	0.040	0.1031	0.0218	0.143	0.030	0.2157	0.0088	0.0428	0.0254
0.0488	0.755	-0.073	0.026	0.058	0.032	0.039	0.0897	0.0133	0.150	0.022	0.2873	0.0092	0.0476	0.0283
0.0589	0.783	-0.071	0.027	0.057	0.033	0.036	0.0874	0.0119	0.156	0.021	0.3466	0.0116	0.0609	0.0362
0.0690	0.812	-0.070	0.028	0.053	0.032	0.035	0.0868	0.0143	0.171	0.028	0.4059	0.0113	0.0596	0.0354
0.0840	0.857	-0.069	0.030	0.048	0.030	0.032	0.0724	0.0172	0.172	0.041	0.4941	0.0099	0.0572	0.0339
0.1042	0.907	-0.069	0.033	0.039	0.024	0.026	0.0452	0.0081	0.165	0.029	0.6127	0.0067	0.0492	0.0292
0.1139	0.932	-0.069	0.034	0.033	0.021	0.022	0.0296	0.0056	0.143	0.027	0.6701	0.0053	0.0478	0.0284
0.1208	0.945	-0.067	0.035	0.030	0.018	0.020	0.0249	0.0034	0.149	0.021	0.7103	0.0058	0.0575	0.0341
0.1349	0.962	-0.068	0.036	0.021	0.014	0.015	0.0105	0.0019	0.120	0.021	0.7936	0.0043	0.0659	0.0391
0.1498	0.971	-0.066	0.035	0.013	0.010	0.010	0.0035	0.0021	0.098	0.059	0.8814	0.0029	0.0778	0.0462
0.1721	0.975	-0.061	0.035	0.006	0.005	0.005	0.0002	0.0006	0.027	0.077	1.0123	0.0007	0.0710	0.0422
0.2036	0.976	-0.057	0.033	0.004	0.003	0.003								
0.2517	0.979	-0.051	0.030	0.003	0.002	0.002								
0.3018	0.987	-0.045	0.029	0.004	0.001	0.002								
0.3527	0.989	-0.040	0.027	0.003	0.002	0.002								
0.4400	0.990	-0.034	0.025	0.003	0.001	0.002								
0.5370	0.997	-0.028	0.022	0.006	0.001	0.001								
0.6061	0.997	-0.024	0.020	0.005	0.001	0.001								

$\delta_p^* = 0.0275$ ft $\delta_r = 0.170$ ft $\frac{U_\delta}{U_o} = 0.9617$

$a = 0.2903$ ft $\delta_a = 0.3625$ ft $b = 0.0968$ ft $\delta_b = 0.2001$ ft

TABLE 4 (Continued)

TABLE 4G - x/L = 0.954

n_e(ft)	$\frac{u_x}{U_o}$	$\frac{v_n}{U_o}$	$\frac{w_\theta}{U_o}$	$\frac{\sqrt{\overline{u_x'^2}}}{U_o}$	$\frac{\sqrt{\overline{v_n'^2}}}{U_o}$	$\frac{\sqrt{\overline{w_\theta'^2}}}{U_o}$	$100\frac{\overline{-u_x'v_n'}}{U_o^2}$	$100\frac{\overline{-u_x'w_\theta'}}{U_o^2}$	$\frac{\overline{-u_x'v_n'}}{q^2}$	$\frac{\overline{-u_x'w_\theta'}}{q^2}$	$\frac{n_e}{\delta_r}$	$\frac{\varepsilon}{U_\delta \delta_p{}^*}$	$\frac{\ell_p}{\delta_r}$	$\frac{\ell}{\sqrt{(a+0.6\delta_a)(b+0.6\delta_b)-ab}}$
0.0104	0.474	-0.066	-0.009	0.068	0.034	0.040	0.1265	0.0011	0.171	0.002	0.0651	0.0016	0.0091	0.0052
0.0177	0.546	-0.069	-0.006	0.069	0.038	0.040	0.1321	-0.0020	0.171	-0.003	0.1104	0.0050	0.0281	0.0162
0.0250	0.592	-0.069	-0.002	0.067	0.036	0.041	0.1252	-0.0037	0.168	-0.005	0.1562	0.0066	0.0381	0.0220
0.0327	0.633	-0.070	-0.000	0.062	0.036	0.040	0.1112	-0.0039	0.165	-0.006	0.2042	0.0065	0.0400	0.0231
0.0423	0.681	-0.069	0.000	0.061	0.035	0.039	0.1007	0.0044	0.156	0.007	0.2646	0.0075	0.0487	0.0282
0.0532	0.714	-0.071	0.002	0.059	0.032	0.039	0.0892	0.0005	0.149	0.001	0.3328	0.0088	0.0606	0.0350
0.0707	0.770	-0.069	0.003	0.053	0.032	0.037	0.0805	-0.0057	0.155	-0.011	0.4417	0.0081	0.0585	0.0338
0.0884	0.820	-0.070	0.005	0.046	0.029	0.033	0.0542	-0.0037	0.134	-0.009	0.5526	0.0064	0.0563	0.0325
0.1054	0.860	-0.068	0.007	0.043	0.026	0.029	0.0525	0.0007	0.154	0.002	0.6589	0.0065	0.0584	0.0338
0.1232	0.906	-0.069	0.008	0.034	0.020	0.023	0.0312	-0.0041	0.148	-0.020	0.7698	0.0049	0.0568	0.0328
0.1413	0.930	-0.066	0.009	0.026	0.017	0.017	0.0184	-0.0011	0.146	-0.009	0.8833	0.0046	0.0695	0.0401
0.1616	0.952	-0.065	0.009	0.013	0.010	0.011	0.0025	0.0003	0.064	0.008	1.0099	0.0011	0.0460	0.0266
0.1785	0.958	-0.062	0.009	0.007	0.006	0.006	0.0007	0.0005	0.061	0.042	1.1156	0.0009	0.0742	0.0428
0.2016	0.959	-0.059	0.008	0.005	0.003	0.004	0.0002	0.0002	0.038	0.043	1.2599	0.0011	0.1725	0.0996
0.2363	0.960	-0.055	0.008	0.003	0.002	0.002								
0.3143	0.961	-0.048	0.006	0.002	0.002	0.002								
0.3947	0.963	-0.043	0.004	0.004	0.002	0.001								
0.4683	0.967	-0.039	0.003	0.003	0.002	0.001								
0.5678	0.970	-0.035	0.002	0.002	0.001	0.002								
0.6126	0.971	-0.034	0.001	0.003	0.002	0.001								

$\delta_p{}^* = 0.0343$ ft $\qquad \delta_r = 0.160$ ft $\qquad \frac{U_\delta}{U_o} = 0.9566$

$a = 0.1995$ ft $\qquad \delta_a = 0.4378$ ft $\qquad b = 0.0665$ ft $\qquad \delta_b = 0.2139$ ft

TABLE 5 - MEASURED MEAN AND TURBULENT VELOCITY CHARACTERISTICS FOR VARYING AXIAL LOCATIONS ALONG 80-DEGREE PLANE

TABLE 5A - x/L = 0.719

n_e (ft)	$\frac{u_x}{U_o}$	$\frac{v_n}{U_o}$	$\frac{w_\theta}{U_o}$	$\frac{\sqrt{\overline{u_x'^2}}}{U_o}$	$\frac{\sqrt{\overline{v_n'^2}}}{U_o}$	$\frac{\sqrt{\overline{w_\theta'^2}}}{U_o}$	$100\frac{-\overline{u_x'v_n'}}{U_o^2}$	$100\frac{-\overline{u_x'w_\theta'}}{U_o^2}$	$\frac{-\overline{u_x'v_n'}}{q^2}$	$\frac{-\overline{u_x'w_\theta'}}{q^2}$	$\frac{n_e}{\delta_r}$	$\frac{\varepsilon}{U_\delta \delta_p^*}$	$\frac{\ell_p}{\delta_r}$	$\frac{\ell}{\sqrt{(a+0.6\delta_a)(b+0.6\delta_b)-ab}}$
0.0182	0.789	0.026	0.088	0.065	0.030	0.040	0.0277	0.0756	0.041	0.113	0.2607	0.0009	0.0128	0.0032
0.0215	0.835	0.029	0.090	0.061	0.031	0.038	0.0361	0.0634	0.060	0.105	0.3071	0.0019	0.0237	0.0059
0.0307	0.870	0.033	0.097	0.056	0.027	0.038	0.0325	0.0607	0.062	0.116	0.4393	0.0036	0.0483	0.0120
0.0352	0.897	0.034	0.098	0.053	0.028	0.037	0.0215	0.0599	0.044	0.122	0.5024	0.0025	0.0421	0.0104
0.0421	0.920	0.037	0.104	0.046	0.025	0.035	0.0181	0.0571	0.045	0.143	0.6012	0.0032	0.0576	0.0143
0.0482	0.940	0.038	0.105	0.045	0.025	0.031	0.0140	0.0440	0.039	0.124	0.6881	0.0022	0.0448	0.0111
0.0538	0.964	0.042	0.107	0.038	0.023	0.028	0.0164	0.0268	0.060	0.097	0.7690	0.0029	0.0557	0.0138
0.0607	0.979	0.042	0.109	0.034	0.021	0.024	0.0061	0.0223	0.028	0.102	0.8667	0.0017	0.0541	0.0134
0.0688	0.994	0.045	0.111	0.029	0.019	0.020	0.0046	0.0163	0.029	0.101	0.9821	0.0016	0.0586	0.0145
0.0841	1.016	0.047	0.111	0.014	0.012	0.011								
0.1068	1.020	0.049	0.111	0.006	0.006	0.005								
0.1402	1.018	0.050	0.107	0.005	0.004	0.004								
0.2106	1.016	0.053	0.103	0.005	0.005	0.004								
0.2931	1.012	0.056	0.099	0.006	0.005	0.003								
0.3727	1.011	0.056	0.098	0.005	0.005	0.003								
0.4612	1.010	0.058	0.095	0.005	0.005	0.004								

$\delta_p^* = 0.0166$ ft $\quad \delta_r = 0.070$ ft $\quad \frac{U_\delta}{U_o} = 1.0267$

$a = 0.7598$ ft $\quad \delta_a = 0.1188$ ft $\quad b = 0.2533$ ft $\quad \delta_b = 0.1241$ ft

TABLE 5 (Continued)

TABLE 5B - x/L = 0.810

n_e(ft)	$\frac{u_x}{U_o}$	$\frac{v_n}{U_o}$	$\frac{w_\theta}{U_o}$	$\frac{\sqrt{\overline{u_x'^2}}}{U_o}$	$\frac{\sqrt{\overline{v_n'^2}}}{U_o}$	$\frac{\sqrt{\overline{w_\theta'^2}}}{U_o}$	$100\,\frac{\overline{-u_x'v_n'}}{U_o^2}$	$100\,\frac{\overline{-u_x'w_\theta'}}{U_o^2}$	$\frac{\overline{-u_x'v_n'}}{q^2}$	$\frac{\overline{-u_x'w_\theta'}}{q^2}$	$\frac{n_e}{\delta_r}$	$\frac{\varepsilon}{U_\delta \delta_p^*}$	$\frac{\ell_p}{\delta_r}$	$\frac{\ell}{\sqrt{(a+0.6\delta_a)(b+0.6\delta_b)-ab}}$
0.0104	0.685	0.005	0.093	0.068	0.029	0.042	0.0345	0.0975	0.048	0.136	0.0801	0.0007	0.0048	0.0022
0.0165	0.738	0.007	0.099	0.068	0.030	0.039	0.0447	0.1016	0.063	0.143	0.1269	0.0033	0.0196	0.0088
0.0218	0.779	0.008	0.106	0.065	0.028	0.039	0.0287	0.0871	0.044	0.133	0.1673	0.0020	0.0153	0.0069
0.0257	0.815	0.011	0.110	0.060	0.029	0.037	0.0378	0.0843	0.065	0.145	0.1981	0.0033	0.0218	0.0098
0.0310	0.837	0.011	0.112	0.057	0.030	0.037	0.0269	0.0741	0.049	0.136	0.2385	0.0040	0.0311	0.0141
0.0419	0.880	0.014	0.118	0.052	0.029	0.036	0.0305	0.0636	0.064	0.133	0.3224	0.0045	0.0332	0.0152
0.0517	0.920	0.017	0.121	0.048	0.026	0.032	0.0276	0.0569	0.068	0.140	0.3974	0.0046	0.0352	0.0159
0.0589	0.944	0.020	0.125	0.044	0.025	0.029	0.0168	0.0478	0.049	0.138	0.4532	0.0035	0.0340	0.0154
0.0702	0.971	0.021	0.127	0.040	0.023	0.026	0.0170	0.0337	0.060	0.120	0.5404	0.0046	0.0449	0.0203
0.0856	1.002	0.024	0.129	0.032	0.020	0.018	0.0061	0.0208	0.036	0.123	0.6583	0.0020	0.0332	0.0150
0.0957	1.019	0.027	0.130	0.023	0.017	0.012	0.0018	0.0099	0.019	0.102	0.7359	0.0008	0.0245	0.0111
0.1159	1.032	0.030	0.130	0.011	0.009	0.007								
0.1785	1.033	0.037	0.124	0.007	0.005	0.004								
0.2671	1.032	0.044	0.118	0.007	0.006	0.004								
0.3668	1.030	0.050	0.116	0.008	0.007	0.004								
0.4420	1.028	0.053	0.114	0.006	0.005	0.004								

$\delta_p^* = 0.0163$ ft　　$\delta_r = 0.130$ ft　　$\frac{U_\delta}{U_o} = 1.0179$

$a = 0.6429$ ft　　$\delta_a = 0.1549$ ft　　$b = 0.2143$ ft　　$\delta_b = 0.1423$ ft

TABLE 5 (Continued)

TABLE 5C - x/L = 0.854

n_e(ft)	$\frac{u_x}{U_o}$	$\frac{v_n}{U_o}$	$\frac{w_\theta}{U_o}$	$\frac{\sqrt{\overline{u_x'^2}}}{U_o}$	$\frac{\sqrt{\overline{v_n'^2}}}{U_o}$	$\frac{\sqrt{\overline{w_\theta'^2}}}{U_o}$	$100\frac{\overline{-u_x'v_n'}}{U_o^2}$	$100\frac{\overline{-u_x'w_\theta'}}{U_o^2}$	$\frac{\overline{-u_x'v_n'}}{q^2}$	$\frac{\overline{-u_x'w_\theta'}}{q^2}$	$\frac{n_e}{\delta_r}$	$\frac{\varepsilon}{U_\delta \delta_p^*}$	$\frac{\ell_p}{\delta_r}$	$\frac{\ell}{\sqrt{(a+0.6\delta_a)(b+0.6\delta_b)-ab}}$
0.0104	0.623	-0.025	0.059	0.066	0.029	0.042	0.0452	0.1065	0.065	0.153	0.0772	0.0007	0.0050	0.0024
0.0181	0.708	-0.020	0.079	0.064	0.030	0.040	0.0449	0.0939	0.068	0.142	0.1340	0.0021	0.0150	0.0071
0.0229	0.757	-0.015	0.086	0.058	0.030	0.040	0.0393	0.1017	0.068	0.175	0.1698	0.0029	0.0216	0.0102
0.0278	0.774	-0.014	0.091	0.060	0.030	0.039	0.0462	0.0971	0.077	0.161	0.2062	0.0058	0.0404	0.0191
0.0331	0.797	-0.011	0.094	0.056	0.030	0.039	0.0322	0.0941	0.058	0.170	0.2451	0.0038	0.0313	0.0147
0.0428	0.835	-0.008	0.101	0.052	0.028	0.037	0.0267	0.0661	0.054	0.134	0.3167	0.0036	0.0331	0.0156
0.0573	0.883	-0.003	0.108	0.048	0.026	0.034	0.0327	0.0568	0.079	0.138	0.4247	0.0051	0.0416	0.0197
0.0674	0.915	0.002	0.109	0.042	0.025	0.033	0.0260	0.0554	0.073	0.156	0.4994	0.0051	0.0465	0.0220
0.0751	0.931	0.004	0.112	0.040	0.024	0.031	0.0246	0.0520	0.080	0.169	0.5562	0.0052	0.0491	0.0231
0.0880	0.968	0.009	0.117	0.032	0.019	0.026	0.0101	0.0322	0.049	0.157	0.6519	0.0023	0.0344	0.0163
0.0981	0.984	0.012	0.120	0.027	0.017	0.021	0.0059	0.0267	0.039	0.179	0.7265	0.0020	0.0388	0.0183
0.1090	0.998	0.014	0.121	0.021	0.014	0.017	0.0007	0.0195	0.007	0.212	0.8074	0.0003	0.0192	0.0090
0.1276	1.008	0.019	0.123	0.010	0.008	0.010								
0.1487	1.009	0.022	0.122	0.006	0.004	0.006								
0.2242	1.010	0.033	0.117	0.004	0.002	0.003								
0.3458	1.009	0.046	0.112	0.004	0.002	0.003								
0.4529	1.010	0.054	0.111	0.003	0.002	0.003								
0.5168	1.009	0.056	0.110	0.003	0.002	0.003								

$\delta_p^* = 0.0200$ ft $\delta_r = 0.135$ ft $\frac{U_\delta}{U_o} = 1.0034$

a = 0.5491 ft $\delta_a = 0.1902$ ft b = 0.1830 ft $\delta_b = 0.1531$ ft

TABLE 5 (Continued)

TABLE 5D - x/L = 0.894

n_e(ft)	$\frac{u_x}{U_o}$	$\frac{v_n}{U_o}$	$\frac{w_\theta}{U_o}$	$\frac{\sqrt{\overline{u_x'^2}}}{U_o}$	$\frac{\sqrt{\overline{v_n'^2}}}{U_o}$	$\frac{\sqrt{\overline{w_\theta'^2}}}{U_o}$	$100\frac{\overline{-u_x'v_n'}}{U_o^2}$	$100\frac{\overline{-u_x'w_\theta'}}{U_o^2}$	$\frac{\overline{-u_x'v_n'}}{q^2}$	$\frac{\overline{-u_x'w_\theta'}}{q^2}$	$\frac{n_e}{\delta_r}$	$\frac{\varepsilon}{U_\delta\delta_p*}$	$\frac{\ell_p}{\delta_r}$	$\frac{\ell}{\sqrt{(a+0.6\delta_a)(b+0.6\delta_b)-ab}}$
0.0104	0.601	-0.041	0.041	0.062	0.031	0.039	0.0466	0.0944	0.074	0.150	0.0694	0.0009	0.0062	0.0033
0.0148	0.638	-0.039	0.048	0.061	0.030	0.039	0.0428	0.0961	0.069	0.155	0.0989	0.0022	0.0163	0.0086
0.0222	0.701	-0.034	0.067	0.061	0.029	0.040	0.0449	0.0931	0.072	0.148	0.1470	0.0028	0.0209	0.0110
0.0330	0.745	-0.028	0.075	0.058	0.032	0.040	0.0379	0.0961	0.064	0.161	0.2200	0.0037	0.0292	0.0154
0.0419	0.787	-0.024	0.081	0.056	0.031	0.037	0.0425	0.0726	0.079	0.135	0.2794	0.0048	0.0359	0.0189
0.0524	0.816	-0.020	0.088	0.049	0.028	0.035	0.0240	0.0589	0.054	0.132	0.3494	0.0035	0.0355	0.0187
0.0626	0.847	-0.019	0.093	0.049	0.026	0.034	0.0307	0.0619	0.072	0.146	0.4172	0.0039	0.0343	0.0181
0.0723	0.883	-0.013	0.097	0.044	0.026	0.033	0.0255	0.0539	0.068	0.143	0.4817	0.0035	0.0342	0.0180
0.0860	0.914	-0.011	0.106	0.039	0.024	0.028	0.0187	0.0409	0.065	0.143	0.5733	0.0036	0.0407	0.0214
0.0989	0.943	-0.008	0.107	0.034	0.020	0.025	0.0104	0.0288	0.047	0.131	0.6594	0.0022	0.0339	0.0178
0.1147	0.969	-0.003	0.111	0.026	0.016	0.019	0.0036	0.0151	0.027	0.115	0.7644	0.0010	0.0273	0.0144
0.1288	0.987	-0.000	0.113	0.018	0.012	0.015	0.0001	0.0097	0.001	0.139	0.8589	0.0000	0.0059	0.0031
0.1542	0.997	0.006	0.113	0.008	0.006	0.009								
0.2056	1.000	0.014	0.112	0.004	0.002	0.003								
0.2731	1.000	0.022	0.109	0.004	0.002	0.003								
0.4081	1.000	0.034	0.106	0.003	0.002	0.003								

$\delta_p* = 0.0236$ ft $\delta_r = 0.150$ ft $\frac{U_\delta}{U_o} = 0.9885$

$a = 0.4369$ ft $\delta_a = 0.2458$ ft $b = 0.1457$ ft $\delta_b = 0.1702$ ft

TABLE 5 (Continued)

TABLE 5E - x/L = 0.914

n_e(ft)	$\frac{u_x}{U_o}$	$\frac{v_n}{U_o}$	$\frac{w_\theta}{U_o}$	$\frac{\sqrt{\overline{u_x'^2}}}{U_o}$	$\frac{\sqrt{\overline{v_n'^2}}}{U_o}$	$\frac{\sqrt{\overline{w_\theta'^2}}}{U_o}$	$100\frac{\overline{-u_x'v_n'}}{U_o^2}$	$100\frac{\overline{-u_x'w_\theta'}}{U_o^2}$	$\frac{\overline{-u_x'v_n'}}{q^2}$	$\frac{\overline{-u_x'w_\theta'}}{q^2}$	$\frac{n_e}{\delta_r}$	$\frac{\varepsilon}{U_\delta \delta_p^*}$	$\frac{\ell_p}{\delta_r}$	$\frac{\ell}{\sqrt{(a+0.6\delta_a)(b+0.6\delta_b)-ab}}$
0.0108	0.566	-0.060	-0.046	0.055	0.031	0.041	0.0753	-0.0503	0.132	-0.088	0.0637	0.0013	0.0078	0.0047
0.0157	0.597	-0.062	-0.048	0.063	0.033	0.042	0.0636	-0.0440	0.093	-0.064	0.0922	0.0036	0.0231	0.0138
0.0211	0.632	-0.060	-0.050	0.065	0.034	0.042	0.0686	-0.0488	0.096	-0.069	0.1244	0.0039	0.0240	0.0144
0.0266	0.667	-0.059	-0.051	0.063	0.033	0.042	0.0615	-0.0402	0.091	-0.060	0.1566	0.0038	0.0250	0.0149
0.0344	0.706	-0.056	-0.051	0.064	0.033	0.041	0.0591	-0.0398	0.085	-0.058	0.2021	0.0051	0.0338	0.0202
0.0446	0.739	-0.051	-0.056	0.058	0.032	0.041	0.0301	-0.0422	0.049	-0.069	0.2626	0.0029	0.0272	0.0163
0.0524	0.771	-0.049	-0.056	0.056	0.032	0.042	0.0453	-0.0391	0.076	-0.066	0.3081	0.0048	0.0363	0.0217
0.0601	0.792	-0.045	-0.057	0.055	0.032	0.038	0.0425	-0.0231	0.077	-0.042	0.3536	0.0058	0.0456	0.0273
0.0730	0.825	-0.042	-0.061	0.051	0.030	0.038	0.0245	-0.0271	0.050	-0.055	0.4294	0.0029	0.0299	0.0178
0.0833	0.861	-0.039	-0.062	0.050	0.027	0.036	0.0246	-0.0364	0.054	-0.080	0.4900	0.0030	0.0304	0.0181
0.0936	0.888	-0.037	-0.065	0.045	0.026	0.035	0.0251	-0.0266	0.064	-0.068	0.5506	0.0040	0.0406	0.0242
0.1065	0.913	-0.036	-0.067	0.043	0.025	0.031	0.0202	-0.0208	0.059	-0.061	0.6265	0.0032	0.0366	0.0219
0.1146	0.933	-0.031	-0.068	0.038	0.022	0.028	0.0181	-0.0198	0.066	-0.072	0.6738	0.0031	0.0373	0.0223
0.1274	0.953	-0.028	-0.070	0.033	0.019	0.023	0.0071	-0.0192	0.035	-0.095	0.7496	0.0017	0.0317	0.0189
0.1429	0.978	-0.025	-0.072	0.028	0.016	0.017	0.0053	-0.0108	0.041	-0.084	0.8405	0.0015	0.0326	0.0195
0.1635	0.997	-0.021	-0.074	0.015	0.010	0.010	0.0012	-0.0024	0.029	-0.057	0.9618	0.0007	0.0300	0.0179
0.2102	1.002	-0.013	-0.073	0.005	0.003	0.003								
0.2804	1.009	-0.004	-0.071	0.003	0.002	0.002								
0.3529	1.011	0.002	-0.068	0.004	0.001	0.002								
0.4096	1.012	0.005	-0.066	0.005	0.001	0.002								

$\delta_p^* = 0.0281$ ft $\quad \delta_r = 0.170$ ft $\quad \frac{U_\delta}{U_o} = 0.9759$

$a = 0.3690$ ft $\quad \delta_a = 0.2912$ ft $\quad b = 0.1230 \quad \delta_b = 0.1820$

TABLE 5 (Continued)

TABLE 5F - x/L = 0.934

n_e(ft)	$\frac{u_x}{U_o}$	$\frac{v_n}{U_o}$	$\frac{w_\theta}{U_o}$	$\frac{\sqrt{\overline{u_x'^2}}}{U_o}$	$\frac{\sqrt{\overline{v_n'^2}}}{U_o}$	$\frac{\sqrt{\overline{w_\theta'^2}}}{U_o}$	$100\,\frac{-\overline{u_x'v_n'}}{U_o^2}$	$100\,\frac{-\overline{u_x'w_\theta'}}{U_o^2}$	$\frac{-\overline{u_x'v_n'}}{q^2}$	$\frac{-\overline{u_x'w_\theta'}}{q^2}$	$\frac{n_e}{\delta_r}$	$\frac{\epsilon}{U_\delta \delta_p^*}$	$\frac{\ell_p}{\delta_m}$	$\frac{\ell}{\sqrt{(a+0.6\delta_a)(b+0.6\delta_b)-ab}}$
0.0104	0.523	-0.070	0.017	0.062	0.031	0.039	0.0633	0.0911	0.101	0.146	0.0579	0.0009	0.0057	0.0036
0.0161	0.584	-0.065	0.032	0.062	0.032	0.038	0.0666	0.0824	0.105	0.130	0.0894	0.0026	0.0164	0.0103
0.0242	0.632	-0.062	0.041	0.058	0.032	0.040	0.0567	0.0836	0.095	0.140	0.1343	0.0039	0.0268	0.0169
0.0318	0.662	-0.056	0.050	0.057	0.032	0.039	0.0468	0.0800	0.081	0.138	0.1769	0.0037	0.0283	0.0178
0.0412	0.706	-0.051	0.057	0.056	0.032	0.039	0.0466	0.0874	0.081	0.153	0.2287	0.0040	0.0302	0.0190
0.0493	0.733	-0.048	0.063	0.056	0.030	0.038	0.0459	0.0754	0.085	0.139	0.2736	0.0044	0.0336	0.0212
0.0585	0.767	-0.044	0.065	0.054	0.029	0.036	0.0344	0.0714	0.068	0.142	0.3250	0.0035	0.0307	0.0193
0.0710	0.803	-0.038	0.072	0.050	0.029	0.033	0.0453	0.0583	0.102	0.131	0.3944	0.0052	0.0399	0.0251
0.0812	0.834	-0.036	0.075	0.046	0.026	0.033	0.0294	0.0484	0.076	0.126	0.4509	0.0034	0.0342	0.0214
0.0913	0.860	-0.032	0.079	0.041	0.026	0.031	0.0292	0.0468	0.090	0.144	0.5069	0.0042	0.0405	0.0254
0.1033	0.885	-0.029	0.083	0.038	0.023	0.028	0.0164	0.0411	0.060	0.151	0.5741	0.0029	0.0365	0.0230
0.1155	0.907	-0.023	0.086	0.035	0.021	0.024	0.0146	0.0328	0.064	0.143	0.6417	0.0028	0.0375	0.0236
0.1280	0.929	-0.022	0.088	0.030	0.017	0.020	0.0082	0.0224	0.052	0.143	0.7111	0.0018	0.0318	0.0199
0.1417	0.948	-0.019	0.091	0.023	0.015	0.016	0.0040	0.0155	0.042	0.159	0.7875	0.0012	0.0308	0.0193
0.1559	0.961	-0.016	0.093	0.014	0.010	0.011	0.0003	0.0076	0.007	0.180	0.8662	0.0002	0.0148	0.0093
0.1749	0.967	-0.011	0.092	0.007	0.007	0.006								
0.2193	0.971	-0.004	0.090	0.005	0.003	0.003								
0.3058	0.974	0.007	0.086	0.004	0.002	0.002								
0.3843	0.985	0.013	0.083	0.004	0.002	0.002								
0.4683	0.988	0.018	0.082	0.004	0.002	0.002								
0.5455	0.989	0.023	0.081	0.003	0.002	0.002								

$\delta_p^* = 0.0305$ ft $\qquad \delta_r = 0.180$ ft $\qquad \frac{U_\delta}{U_o} = 0.9645$

a = 0.2903 ft $\qquad \delta_a = 0.3625$ ft $\qquad$ b = 0.0968 ft $\qquad \delta_b = 0.2001$ ft

TABLE 5 (Continued)

TABLE 5G - x/L = 0.954

n_e(ft)	$\frac{u_x}{U_o}$	$\frac{v_n}{U_o}$	$\frac{w_\theta}{U_o}$	$\frac{\sqrt{\overline{u_x'^2}}}{U_o}$	$\frac{\sqrt{\overline{v_n'^2}}}{U_o}$	$\frac{\sqrt{\overline{w_\theta'^2}}}{U_o}$	$100\frac{\overline{-u_x'v_n'}}{U_o^2}$	$100\frac{\overline{-u_x'w_\theta'}}{U_o^2}$	$\frac{\overline{-u_x'v_n'}}{q^2}$	$\frac{\overline{-u_x'w_\theta'}}{q^2}$	$\frac{n_e}{\delta_r}$	$\frac{\varepsilon}{U_\delta \delta_p^*}$	$\frac{\ell_p}{\delta_r}$	$\frac{\ell}{\sqrt{(a+0.6\delta_a)(b+0.6\delta_b)-ab}}$
0.0104	0.505	-0.067	0.036	0.058	0.030	0.040	0.0571	0.0968	0.097	0.164	0.0548	0.0007	0.0051	0.0035
0.0189	0.552	-0.063	0.053	0.060	0.031	0.041	0.0593	0.1045	0.095	0.167	0.0996	0.0024	0.0180	0.0123
0.0237	0.591	-0.059	0.057	0.061	0.031	0.040	0.0505	0.0923	0.081	0.148	0.1250	0.0021	0.0168	0.0116
0.0362	0.644	-0.050	0.069	0.059	0.032	0.041	0.0522	0.0947	0.085	0.153	0.1908	0.0034	0.0270	0.0185
0.0456	0.687	-0.045	0.075	0.058	0.031	0.038	0.0333	0.0777	0.058	0.134	0.2399	0.0023	0.0224	0.0154
0.0557	0.727	-0.040	0.081	0.055	0.031	0.038	0.0335	0.0861	0.062	0.159	0.2930	0.0033	0.0324	0.0222
0.0633	0.744	-0.038	0.081	0.052	0.029	0.037	0.0319	0.0756	0.064	0.152	0.3333	0.0036	0.0361	0.0248
0.0727	0.772	-0.032	0.083	0.052	0.029	0.036	0.0380	0.0674	0.079	0.140	0.3825	0.0036	0.0329	0.0225
0.0843	0.810	-0.026	0.091	0.047	0.028	0.036	0.0279	0.0760	0.065	0.176	0.4439	0.0031	0.0330	0.0226
0.1002	0.840	-0.022	0.096	0.042	0.025	0.033	0.0280	0.0592	0.080	0.169	0.5272	0.0034	0.0365	0.0250
0.1118	0.873	-0.018	0.100	0.040	0.024	0.030	0.0190	0.0515	0.063	0.171	0.5886	0.0026	0.0335	0.0230
0.1247	0.892	-0.015	0.103	0.037	0.022	0.026	0.0152	0.0406	0.060	0.161	0.6566	0.0028	0.0400	0.0274
0.1406	0.920	-0.012	0.107	0.030	0.018	0.022	0.0077	0.0280	0.045	0.163	0.7399	0.0014	0.0276	0.0189
0.1592	0.948	-0.007	0.109	0.021	0.014	0.015	0.0045	0.0148	0.052	0.173	0.8377	0.0012	0.0313	0.0215
0.1850	0.963	-0.002	0.110	0.010	0.009	0.008								
0.2024	0.965	0.001	0.110	0.007	0.006	0.005								
0.2453	0.968	0.007	0.108	0.005	0.003	0.003								
0.3478	0.974	0.016	0.103	0.005	0.003	0.003								
0.4893	0.987	0.024	0.099	0.004	0.003	0.003								
0.5807	0.989	0.028	0.097	0.004	0.003	0.003								

$\delta_p^* = 0.0354$ ft $\delta_r = 0.190$ ft $\frac{U_\delta}{U_o} = 0.9606$

a = 0.1995 ft $\delta_a = 0.4378$ ft b = 0.0665 ft $\delta_b = 0.2139$ ft

TABLE 6 - MEASURED MEAN AND TURBULENT VELOCITY CHARACTERISTICS FOR VARYING AXIAL LOCATIONS ALONG 83-DEGREE PLANE

TABLE 6A - x/L = 0.854

n_e(ft)	$\frac{u_x}{U_o}$	$\frac{v_n}{U_o}$	$\frac{w_\theta}{U_o}$	$\frac{\sqrt{\overline{u_x'^2}}}{U_o}$	$\frac{\sqrt{\overline{v_n'^2}}}{U_o}$	$\frac{\sqrt{\overline{w_\theta'^2}}}{U_o}$	$100\frac{-\overline{u_x'v_n'}}{U_o^2}$	$100\frac{-\overline{u_x'w_\theta'}}{U_o^2}$	$\frac{-\overline{u_x'v_n'}}{q^2}$	$\frac{-\overline{u_x'w_\theta'}}{q^2}$	$\frac{n_e}{\delta_r}$	$\frac{\varepsilon}{U_\delta \delta_p^*}$	$\frac{\ell_p}{\delta_r}$	$\frac{\ell}{\sqrt{(a+0.6\delta_a)(b+0.6\delta_b)-ab}}$
0.0108	0.578	-0.094	-0.034	0.059	0.035	0.039	0.1215	0.0179	0.195	0.029	0.0722	0.0023	0.0113	0.0059
0.0131	0.609	-0.097	-0.031	0.061	0.035	0.041	0.1193	0.0165	0.181	0.025	0.0873	0.0037	0.0180	0.0094
0.0160	0.643	-0.103	-0.019	0.059	0.036	0.041	0.1172	0.0202	0.182	0.031	0.1066	0.0045	0.0221	0.0116
0.0186	0.666	-0.104	-0.010	0.058	0.035	0.041	0.1081	0.0225	0.172	0.036	0.1238	0.0055	0.0286	0.0150
0.0237	0.691	-0.106	-0.002	0.058	0.035	0.041	0.1055	0.0171	0.167	0.027	0.1581	0.0085	0.0447	0.0234
0.0285	0.715	-0.108	0.007	0.058	0.035	0.039	0.0926	0.0214	0.153	0.035	0.1903	0.0064	0.0358	0.0188
0.0340	0.750	-0.108	0.013	0.055	0.036	0.040	0.0956	0.0266	0.163	0.045	0.2268	0.0069	0.0379	0.0199
0.0418	0.781	-0.109	0.020	0.055	0.035	0.039	0.0935	0.0131	0.162	0.023	0.2784	0.0103	0.0574	0.0301
0.0521	0.811	-0.109	0.028	0.051	0.033	0.037	0.0763	0.0122	0.150	0.024	0.3471	0.0039	0.0237	0.0125
0.0627	0.947	-0.111	0.032	0.049	0.031	0.036	0.0648	0.0169	0.141	0.037	0.4179	0.0000	0.0000	0.0000
0.0704	0.870	-0.110	0.036	0.047	0.031	0.035	0.0670	0.0144	0.154	0.033	0.4695	0.0000	0.0000	0.0000
0.0781	0.889	-0.112	0.039	0.044	0.029	0.035	0.0599	0.0138	0.150	0.034	0.5210	0.0109	0.0759	0.0398
0.0885	0.906	-0.111	0.042	0.041	0.027	0.034	0.0475	0.0203	0.134	0.057	0.5897	0.0096	0.0743	0.0391
0.0988	0.929	-0.109	0.044	0.036	0.024	0.030	0.0381	0.0204	0.135	0.072	0.6584	0.0073	0.0632	0.0331
0.1113	0.952	-0.109	0.044	0.032	0.021	0.027	0.0212	0.0160	0.097	0.073	0.7422	0.0043	0.0496	0.0260
0.1197	0.969	-0.108	0.046	0.026	0.018	0.024	0.0163	0.0136	0.104	0.086	0.7980	0.0037	0.0489	0.0256
0.1348	0.988	-0.107	0.049	0.018	0.013	0.017	0.0050	0.0088	0.062	0.111	0.8989	0.0021	0.0516	0.0271
0.1584	0.998	-0.101	0.051	0.009	0.007	0.009	0.0013	0.0031	0.059	0.148	1.0557	0.0017	0.0830	0.0435
0.1993	1.000	-0.094	0.049	0.004	0.003	0.003								
0.2647	1.000	-0.085	0.046	0.002	0.002	0.002								
0.3558	0.999	-0.078	0.047	0.005	0.004	0.002								

$\delta_p^* = 0.0255$ ft $\quad \delta_r = 0.150$ ft $\quad \frac{U_\delta}{U_o} = 1.0005$

$a = 0.5491$ ft $\quad \delta_a = 0.1902$ ft $\quad b = 0.1830$ ft $\quad \delta_b = 0.1531$ ft

TABLE 6 (Continued)

TABLE 6B - x/L = 0.894

n_e(ft)	$\frac{u_x}{U_o}$	$\frac{v_n}{U_o}$	$\frac{w_\theta}{U_o}$	$\frac{\sqrt{\overline{u_x'^2}}}{U_o}$	$\frac{\sqrt{\overline{v_n'^2}}}{U_o}$	$\frac{\sqrt{\overline{w_\theta'^2}}}{U_o}$	$100\frac{\overline{-u_x'v_n'}}{U_o^2}$	$100\frac{\overline{-u_x'w_\theta'}}{U_o^2}$	$\frac{\overline{-u_x'v_n'}}{q^2}$	$\frac{\overline{-u_x'w_\theta'}}{q^2}$	$\frac{n_e}{\delta_r}$	$\frac{\varepsilon}{U_\delta \delta_p^*}$	$\frac{\ell_p}{\delta_r}$	$\frac{\ell}{\sqrt{(a+0.6\delta_a)(b+0.6\delta_b)-ab}}$
0.0108	0.531	-0.089	-0.039	0.056	0.034	0.037	0.0974	0.0209	0.173	0.037	0.0602	0.0025	0.0135	0.0085
0.0128	0.544	-0.090	-0.033	0.057	0.033	0.038	0.1038	0.0162	0.179	0.028	0.0709	0.0044	0.0234	0.0148
0.0179	0.601	-0.090	-0.020	0.060	0.033	0.038	0.0946	0.0257	0.152	0.041	0.0995	0.0039	0.0216	0.0136
0.0231	0.625	-0.089	-0.009	0.059	0.034	0.039	0.0955	0.0291	0.155	0.047	0.1282	0.0060	0.0336	0.0212
0.0311	0.672	-0.089	0.010	0.058	0.034	0.040	0.0856	0.0327	0.142	0.054	0.1729	0.0055	0.0321	0.0203
0.0389	0.706	-0.087	0.018	0.057	0.032	0.041	0.0785	0.0240	0.133	0.041	0.2159	0.0062	0.0379	0.0239
0.0492	0.744	-0.083	0.028	0.057	0.032	0.040	0.0745	0.0261	0.125	0.044	0.2731	0.0065	0.0408	0.0258
0.0620	0.792	-0.082	0.037	0.055	0.031	0.039	0.0618	0.0338	0.112	0.061	0.3447	0.0057	0.0394	0.0250
0.0749	0.834	-0.080	0.044	0.049	0.030	0.039	0.0595	0.0240	0.124	0.050	0.4163	0.0070	0.0491	0.0310
0.0875	0.863	-0.078	0.050	0.047	0.027	0.037	0.0396	0.0244	0.091	0.056	0.4861	0.0059	0.0511	0.0323
0.1036	0.895	-0.074	0.055	0.044	0.026	0.033	0.0396	0.0255	0.105	0.068	0.5756	0.0065	0.0562	0.0356
0.1371	0.959	-0.069	0.064	0.032	0.020	0.023	0.0179	0.0122	0.091	0.062	0.7616	0.0037	0.0470	0.0297
0.1561	0.985	-0.065	0.066	0.024	0.014	0.017	0.0087	0.0083	0.084	0.080	0.8672	0.0026	0.0482	0.0304
0.1732	0.999	-0.062	0.068	0.013	0.010	0.010	0.0014	0.0029	0.039	0.080	0.9620	0.0009	0.0415	0.0263
0.1967	1.001	-0.058	0.067	0.005	0.005	0.005								
0.2225	1.002	-0.053	0.065	0.004	0.003	0.003								
0.2479	1.002	-0.050	0.064	0.004	0.002	0.002								
0.2798	1.002	-0.045	0.062	0.005	0.002	0.002								
0.3120	1.002	-0.042	0.061	0.005	0.002	0.002								
0.3519	1.003	-0.040	0.060	0.005	0.001	0.001								
0.4141	1.004	-0.034	0.059	0.004	0.002	0.001								
0.4737	1.005	-0.032	0.059	0.004	0.001	0.001								
0.5384	1.004	-0.029	0.059	0.004	0.001	0.001								

$\delta_p^* = 0.0314$ ft $\quad \delta_r = 0.180$ ft $\quad \frac{U_\delta}{U_o} = 0.9859$ ft

$a = 0.4369$ ft $\quad \delta_a = 0{,}2458$ ft $\quad b = 0.1457$ ft $\quad \delta_b = 0.1702$ ft

TABLE 6 (Continued)

TABLE 6C - x/L = 0.914

n_e(ft)	$\frac{u_x}{U_o}$	$\frac{v_n}{U_o}$	$\frac{w_\theta}{U_o}$	$\frac{\sqrt{\overline{u_x'^2}}}{U_o}$	$\frac{\sqrt{\overline{v_n'^2}}}{U_o}$	$\frac{\sqrt{\overline{w_\theta'^2}}}{U_o}$	$100\frac{-\overline{u_x'v_n'}}{U_o^2}$	$100\frac{-\overline{u_x'w_\theta'}}{U_o^2}$	$\frac{-\overline{u_x'v_n'}}{q^2}$	$\frac{-\overline{u_x'w_\theta'}}{q^2}$	$\frac{n_e}{\delta_r}$	$\frac{\varepsilon}{U_\delta \delta_p^*}$	$\frac{\ell_p}{\delta_r}$	$\frac{\ell}{\sqrt{(a+0.6\delta_a)(b+0.6\delta_b)}-ab}$
0.0108	0.486	-0.102	-0.051	0.054	0.031	0.035	0.0850	0.0162	0.165	0.031	0.0586	0.0010	0.0059	0.0038
0.0134	0.544	-0.106	-0.043	0.056	0.033	0.036	0.0839	0.0221	0.151	0.040	0.0725	0.0015	0.0091	0.0059
0.0182	0.579	-0.105	-0.028	0.060	0.033	0.038	0.0866	0.0304	0.141	0.049	0.0986	0.0041	0.0247	0.0160
0.0263	0.620	-0.102	-0.007	0.058	0.033	0.038	0.0815	0.0461	0.136	0.077	0.1421	0.0049	0.0302	0.0196
0.0337	0.658	-0.099	0.007	0.062	0.033	0.041	0.0894	0.0529	0.135	0.080	0.1822	0.0060	0.0351	0.0229
0.0418	0.691	-0.096	0.019	0.061	0.033	0.040	0.0673	0.0382	0.106	0.060	0.2257	0.0054	0.0364	0.0237
0.0521	0.728	-0.096	0.028	0.058	0.033	0.041	0.0730	0.0403	0.120	0.066	0.2814	0.0061	0.0397	0.0259
0.0649	0.776	-0.090	0.040	0.055	0.031	0.039	0.0562	0.0437	0.103	0.080	0.3510	0.0054	0.0400	0.0261
0.0807	0.817	-0.089	0.049	0.053	0.029	0.038	0.0437	0.0279	0.086	0.055	0.4364	0.0049	0.0411	0.0267
0.0965	0.863	-0.085	0.058	0.048	0.027	0.036	0.0424	0.0289	0.099	0.067	0.5217	0.0052	0.0445	0.0289
0.1116	0.895	-0.083	0.063	0.046	0.027	0.033	0.0309	0.0299	0.079	0.076	0.6035	0.0047	0.0471	0.0306
0.1480	0.957	-0.078	0.073	0.034	0.019	0.023	0.0132	0.0147	0.066	0.073	0.8003	0.0028	0.0420	0.0273
0.1658	0.981	-0.075	0.076	0.026	0.015	0.016	0.0099	0.0103	0.087	0.090	0.8960	0.0027	0.0476	0.0310
0.1893	1.000	-0.071	0.077	0.011	0.008	0.009	0.0018	0.0043	0.062	0.151	1.0231	0.0011	0.0458	0.0298
0.2154	1.004	-0.067	0.076	0.006	0.004	0.005								
0.2463	1.004	-0.062	0.073	0.005	0.003	0.002								
0.2721	1.005	-0.059	0.072	0.004	0.002	0.002								
0.3085	1.005	-0.055	0.071	0.005	0.001	0.002								
0.3448	1.007	-0.053	0.070	0.004	0.001	0.002								
0.3886	1.009	-0.048	0.068	0.004	0.002	0.002								
0.4792	1.011	-0.043	0.068	0.005	0.002	0.002								
0.5416	1.012	-0.041	0.068	0.005	0.002	0.002								

$\delta_p^* = 0.0333$ $\quad$ $\delta_r = 0.185$ ft $\quad$ $\frac{U_\delta}{U_o} = 0.9737$

$a = 0.3690$ ft $\quad$ $\delta_a = 0.2912$ ft $\quad$ $b = 0.1230$ ft $\quad$ $\delta_b = 0.1820$ ft

TABLE 6 (Continued)

TABLE 6D - x/L = 0.954

n_e(ft)	$\frac{u_x}{U_o}$	$\frac{v_n}{U_o}$	$\frac{w_\theta}{U_o}$	$\frac{\sqrt{\overline{u_x'^2}}}{U_o}$	$\frac{\sqrt{\overline{v_n'^2}}}{U_o}$	$\frac{\sqrt{\overline{w_\theta'^2}}}{U_o}$	$100\frac{\overline{-u_x'v_n'}}{U_o^2}$	$100\frac{\overline{-u_x'w_\theta'}}{U_o^2}$	$\frac{\overline{-u_x'v_n'}}{q^2}$	$\frac{\overline{-u_x'w_\theta'}}{q^2}$	$\frac{n_e}{\delta_r}$	$\frac{\varepsilon}{U_\delta \delta_p^*}$	$\frac{\ell_p}{\delta_r}$	$\frac{\ell}{\sqrt{(a+0.6\delta_a)(b+0.6\delta_b)-ab}}$
0.0108	0.360	-0.096	-0.049	0.051	0.030	0.028	0.0773	-0.0257	0.180	-0.060	0.0433	0.0010	0.0072	0.0065
0.0163	0.395	-0.093	-0.040	0.055	0.031	0.030	0.0754	0.0038	0.153	0.008	0.0652	0.0016	0.0121	0.0109
0.0208	0.446	-0.091	-0.034	0.060	0.035	0.033	0.0881	0.0180	0.149	0.030	0.0833	0.0019	0.0132	0.0119
0.0289	0.486	-0.088	-0.026	0.062	0.033	0.035	0.0799	0.0343	0.129	0.056	0.1155	0.0033	0.0242	0.0218
0.0361	0.518	-0.083	-0.015	0.063	0.034	0.039	0.0747	0.0539	0.113	0.082	0.1444	0.0028	0.0211	0.0191
0.0443	0.568	-0.079	-0.008	0.063	0.034	0.041	0.0742	0.0580	0.110	0.086	0.1773	0.0029	0.0219	0.0198
0.0550	0.605	-0.075	0.005	0.063	0.035	0.042	0.0723	0.0633	0.104	0.091	0.2198	0.0041	0.0309	0.0279
0.0678	0.649	-0.074	0.014	0.059	0.032	0.043	0.0592	0.0745	0.093	0.117	0.2714	0.0035	0.0297	0.0268
0.0836	0.699	-0.067	0.026	0.060	0.033	0.042	0.0605	0.0566	0.093	0.087	0.3345	0.0036	0.0302	0.0272
0.0991	0.751	-0.064	0.033	0.057	0.032	0.042	0.0587	0.0684	0.098	0.114	0.3964	0.0042	0.0354	0.0319
0.1146	0.783	-0.060	0.040	0.053	0.032	0.040	0.0441	0.0509	0.082	0.094	0.4582	0.0041	0.0400	0.0361
0.1506	0.862	-0.053	0.052	0.045	0.027	0.035	0.0335	0.0374	0.084	0.094	0.6025	0.0034	0.0378	0.0341
0.1687	0.894	-0.051	0.056	0.041	0.025	0.032	0.0305	0.0293	0.091	0.087	0.6746	0.0034	0.0401	0.0361
0.1922	0.933	-0.047	0.061	0.034	0.020	0.027	0.0150	0.0290	0.065	0.126	0.7687	0.0020	0.0341	0.0308
0.2183	0.964	-0.044	0.065	0.021	0.013	0.019	0.0048	0.0137	0.049	0.139	0.8731	0.0010	0.0307	0.0277
0.2492	0.981	-0.041	0.066	0.010	0.007	0.010	0.0001	0.0041	0.003	0.174	0.9967	0.0000	0.0093	0.0084
0.2746	0.986	-0.039	0.066	0.005	0.004	0.004								
0.3114	0.990	-0.035	0.064	0.003	0.002	0.002								
0.3471	0.993	-0.033	0.062	0.004	0.002	0.002								
0.3915	0.994	-0.031	0.060	0.004	0.002	0.002								
0.4798	1.000	-0.025	0.057	0.004	0.002	0.002								
0.5806	1.000	-0.022	0.056	0.002	0.002	0.002								

$\delta_p^* = 0.0534$ ft $\qquad \delta_r = 0.250$ ft $\qquad \frac{U_\delta}{U_o} = 0.9585$

$a = 0.1995$ ft $\qquad \delta_a = 0.4378$ ft $\qquad b = 0.0665$ ft $\qquad \delta_b = 0.2139$ ft

TABLE 7 - MEASURED MEAN AND TURBULENT VELOCITY CHARACTERISTICS FOR VARYING AXIAL LOCATIONS ALONG 86-DEGREE PLANE

TABLE 7A - x/L = 0.854

n_e (ft)	$\frac{u_x}{U_o}$	$\frac{v_n}{U_o}$	$\frac{w_\theta}{U_o}$	$\frac{\sqrt{\overline{u_x'^2}}}{U_o}$	$\frac{\sqrt{\overline{v_n'^2}}}{U_o}$	$\frac{\sqrt{\overline{w_\theta'^2}}}{U_o}$	$100\frac{\overline{-u_x'v_n'}}{U_o^2}$	$100\frac{\overline{-u_x'w_\theta'}}{U_o^2}$	$\frac{\overline{-u_x'v_n'}}{q^2}$	$\frac{\overline{-u_x'w_\theta'}}{q^2}$	$\frac{n_e}{\delta_r}$	$\frac{\varepsilon}{U_\delta \delta_p^*}$	$\frac{\ell_p}{\delta_r}$	$\frac{\ell}{\sqrt{(a+0.6\delta_a)(b+0.6\delta_b)-ab}}$
0.0108	0.529	0.094	-0.028	0.050	0.032	0.039	0.0891	-0.0153	0.179	0.031	0.0637	0.0015	0.0108	0.0064
0.0134	0.551	-0.095	-0.034	0.051	0.033	0.040	0.0853	-0.0293	0.160	-0.055	0.0789	0.0023	0.0164	0.0097
0.0160	0.583	-0.095	-0.038	0.052	0.033	0.040	0.0849	-0.0283	0.156	-0.052	0.0940	0.0024	0.0170	0.0101
0.0211	0.611	-0.098	-0.045	0.050	0.032	0.040	0.0750	0.0236	0.145	-0.045	0.1244	0.0037	0.0280	0.0167
0.0263	0.642	-0.097	-0.051	0.051	0.034	0.040	0.0808	-0.0280	0.152	-0.053	0.1547	0.0040	0.0297	0.0177
0.0340	0.681	-0.098	-0.056	0.050	0.033	0.040	0.0747	-0.0309	0.142	-0.059	0.2001	0.0052	0.0398	0.0237
0.0395	0.699	-0.097	-0.057	0.050	0.032	0.039	0.0655	-0.0304	0.129	-0.060	0.2324	0.0053	0.0430	0.0256
0.0472	0.727	-0.095	-0.058	0.050	0.033	0.040	0.0622	-0.0351	0.119	-0.067	0.2778	0.0051	0.0423	0.0252
0.0566	0.758	-0.093	-0.063	0.050	0.031	0.041	0.0515	-0.0387	0.102	-0.077	0.3328	0.0046	0.0424	0.0252
0.0653	0.784	-0.091	-0.065	0.047	0.031	0.039	0.0563	-0.0426	0.120	-0.091	0.3839	0.0055	0.0481	0.0286
0.0756	0.812	-0.089	-0.066	0.046	0.030	0.038	0.0449	-0.0346	0.101	-0.078	0.4446	0.0045	0.0440	0.0262
0.0859	0.843	-0.086	-0.067	0.042	0.029	0.036	0.0431	-0.0241	0.111	-0.062	0.5052	0.0058	0.0586	0.0348
0.0936	0.854	-0.085	-0.068	0.043	0.028	0.035	0.0368	-0.0187	0.097	-0.049	0.5506	0.0061	0.0666	0.0396
0.1091	0.888	-0.083	-0.070	0.038	0.025	0.031	0.0333	-0.0283	0.109	-0.093	0.6416	0.0043	0.0496	0.0295
0.1197	0.911	-0.081	-0.071	0.036	0.023	0.027	0.0256	-0.0167	0.100	-0.066	0.7041	0.0038	0.0494	0.0294
0.1326	0.932	-0.078	-0.074	0.032	0.021	0.024	0.0213	-0.0173	0.106	-0.086	0.7799	0.0042	0.0599	0.0356
0.1455	0.947	-0.078	-0.073	0.028	0.018	0.019	0.0157	-0.0113	0.109	-0.079	0.8557	0.0037	0.0619	0.0368
0.1648	0.969	-0.074	-0.073	0.017	0.012	0.012	0.0055	-0.0050	0.092	-0.083	0.9694	0.0019	0.0526	0.0313
0.1819	0.979	-0.071	-0.072	0.009	0.008	0.007	0.0005	-0.0020	0.026	-0.106	1.0698	0.0003	0.0330	0.0196
0.2102	0.982	-0.065	-0.071	0.003	0.003	0.004								
0.2466	0.982	-0.059	-0.069	0.002	0.002	0.002								
0.2824	0.987	-0.054	-0.067	0.005	0.002	0.002								

$\delta_p^* = 0.0356$ ft $\qquad \delta_r = 0.170$ ft $\qquad \frac{U_\delta}{U_o} = 0.9970$

$a = 0.5491$ ft $\qquad \delta_a = 0.1902$ ft $\qquad b = 0.1830$ ft $\qquad \delta_b = 0.1531$ ft

TABLE 7 (Continued)

TABLE 7B - x/L = 0.894

n_e(ft)	$\frac{u_x}{U_o}$	$\frac{v_n}{U_o}$	$\frac{w_\theta}{U_o}$	$\frac{\sqrt{\overline{u_x'^2}}}{U_o}$	$\frac{\sqrt{\overline{v_n'^2}}}{U_o}$	$\frac{\sqrt{\overline{w_\theta'^2}}}{U_o}$	$100\frac{-\overline{u_x'v_n'}}{U_o^2}$	$100\frac{-\overline{u_x'w_\theta'}}{U_o^2}$	$\frac{-\overline{u_x'v_n'}}{q^2}$	$\frac{-\overline{u_x'w_\theta'}}{q^2}$	$\frac{n_e}{\delta_r}$	$\frac{\varepsilon}{U_\delta \delta_p^*}$	$\frac{\ell_p}{\delta_r}$	$\frac{\ell}{\sqrt{(a+0.6\delta_a)(b+0.6\delta_b)-ab}}$
0.0108	0.479	-0.122	-0.019	0.044	0.032	0.039	0.0828	-0.0159	0.185	-0.036	0.0516	0.0009	0.0068	0.0050
0.0160	0.523	-0.127	-0.035	0.044	0.032	0.042	0.0725	-0.0372	0.153	-0.079	0.0761	0.0028	0.0218	0.0161
0.0186	0.535	-0.128	-0.040	0.045	0.032	0.042	0.0754	-0.0323	0.158	-0.068	0.0884	0.0033	0.0251	0.0185
0.0237	0.568	-0.131	-0.050	0.045	0.031	0.041	0.0692	-0.0225	0.147	-0.048	0.1129	0.0029	0.0234	0.0172
0.0314	0.596	-0.131	-0.059	0.047	0.031	0.040	0.0690	-0.0375	0.144	-0.078	0.1498	0.0038	0.0309	0.0228
0.0395	0.633	-0.128	-0.064	0.049	0.033	0.041	0.0816	-0.0382	0.158	-0.074	0.1881	0.0048	0.0354	0.0261
0.0472	0.657	-0.128	-0.068	0.049	0.031	0.042	0.0689	-0.0382	0.134	-0.074	0.2249	0.0047	0.0380	0.0280
0.0575	0.693	-0.128	-0.070	0.048	0.033	0.040	0.0664	-0.0445	0.132	-0.089	0.2740	0.0077	0.0628	0.0464
0.0620	0.699	-0.124	-0.070	0.050	0.033	0.040	0.0670	-0.0412	0.130	-0.080	0.2955	0.0075	0.0613	0.0452
0.0730	0.740	-0.123	-0.073	0.049	0.031	0.040	0.0585	-0.0446	0.116	-0.088	0.3476	0.0043	0.0375	0.0277
0.0833	0.765	-0.119	-0.077	0.051	0.033	0.037	0.0691	-0.0509	0.137	-0.101	0.3967	0.0064	0.0513	0.0378
0.0936	0.790	-0.119	-0.077	0.047	0.032	0.036	0.0567	-0.0464	0.126	-0.103	0.4458	0.0055	0.0491	0.0362
0.1065	0.817	-0.115	-0.078	0.046	0.031	0.034	0.0486	-0.0366	0.114	-0.086	0.5071	0.0047	0.0453	0.0334
0.1171	0.844	-0.113	-0.080	0.046	0.030	0.033	0.0530	-0.0312	0.130	-0.077	0.5577	0.0054	0.0495	0.0365
0.1352	0.875	-0.110	-0.084	0.040	0.029	0.029	0.0462	-0.0260	0.140	-0.079	0.6437	0.0062	0.0604	0.0445
0.1558	0.909	-0.107	-0.085	0.036	0.025	0.025	0.0297	-0.0220	0.117	-0.087	0.7418	0.0042	0.0520	0.0383
0.1767	0.941	-0.103	-0.084	0.031	0.021	0.019	0.0202	-0.0144	0.117	-0.084	0.8415	0.0033	0.0486	0.0358
0.1999	0.970	-0.100	-0.083	0.022	0.015	0.011	0.0081	-0.0046	0.097	-0.056	0.9519	0.0017	0.0399	0.0294
0.2237	0.991	-0.095	-0.082	0.010	0.008	0.006	0.0023	-0.0015	0.108	-0.068	1.0654	0.0009	0.0393	0.0289
0.2621	0.996	-0.091	-0.080	0.005	0.003	0.003								
0.3210	0.998	-0.084	-0.077	0.005	0.002	0.002								
0.4460	1.000	-0.071	-0.075	0.004	0.002	0.002								

$\delta_p^* = 0.0451$ ft $\delta_r = 0.210$ ft $\frac{U_\delta}{U_o} = 0.9829$ ft

a = .0.4369 ft $\delta_a = 0.2458$ ft   b = 0.1457 ft $\delta_b = 0.1702$ ft

TABLE 7 (Continued)

TABLE 7C - x/L = 0.914

n_e(ft)	$\frac{u_x}{U_o}$	$\frac{v_n}{U_o}$	$\frac{w_\theta}{U_o}$	$\frac{\sqrt{\overline{u_x'^2}}}{U_o}$	$\frac{\sqrt{\overline{v_n'^2}}}{U_o}$	$\frac{\sqrt{\overline{w_\theta'^2}}}{U_o}$	$100\frac{\overline{-u_x'v_n'}}{U_o^2}$	$100\frac{\overline{-u_x'w_\theta'}}{U_o^2}$	$\frac{\overline{-u_x'v_n'}}{q^2}$	$\frac{\overline{-u_x'w_\theta'}}{q^2}$	$\frac{n_e}{\delta_r}$	$\frac{\varepsilon}{U_\delta \delta_p^*}$	$\frac{\ell_p}{\delta_r}$	$\frac{\ell}{\sqrt{(a+0.6\delta_a)(b+0.6\delta_b)-ab}}$
0.0108	0.457	-0.138	0.006	0.035	0.028	0.034	0.0470	-0.0255	0.149	-0.081	0.0401	0.0007	0.0063	0.0060
0.0134	0.472	-0.142	0.001	0.037	0.029	0.035	0.0555	-0.0259	0.161	-0.075	0.0497	0.0022	0.0174	0.0165
0.0186	0.490	-0.142	-0.008	0.036	0.039	0.036	0.0540	-0.0382	0.131	-0.093	0.0688	0.0029	0.0226	0.0214
0.0289	0.535	-0.146	-0.024	0.042	0.031	0.039	0.0573	-0.0452	0.137	-0.108	0.1069	0.0028	0.0219	0.0207
0.0366	0.564	-0.144	-0.031	0.044	0.030	0.043	0.0606	-0.0422	0.130	-0.091	0.1356	0.0027	0.0201	0.0190
0.0421	0.592	-0.141	-0.036	0.046	0.030	0.041	0.0642	-0.0563	0.136	-0.119	0.1558	0.0028	0.0203	0.0193
0.0550	0.638	-0.138	-0.043	0.050	0.033	0.040	0.0650	-0.0429	0.124	-0.082	0.2035	0.0039	0.0285	0.0271
0.0653	0.670	-0.133	-0.048	0.049	0.032	0.041	0.0704	-0.0475	0.137	-0.092	0.2417	0.0047	0.0328	0.0311
0.0756	0.700	-0.133	-0.051	0.050	0.032	0.039	0.0543	-0.0467	0.107	-0.092	0.2799	0.0040	0.0319	0.0302
0.0833	0.720	-0.129	-0.053	0.050	0.032	0.038	0.0701	-0.0442	0.141	-0.089	0.3085	0.0059	0.0410	0.0389
0.0936	0.742	-0.123	-0.056	0.051	0.034	0.038	0.0614	-0.0453	0.118	-0.087	0.3467	0.0056	0.0419	0.0398
0.1039	0.765	-0.125	-0.058	0.048	0.032	0.038	0.0510	-0.0417	0.107	-0.087	0.3849	0.0048	0.0395	0.0376
0.1197	0.796	-0.121	-0.061	0.048	0.032	0.037	0.0555	-0.0380	0.118	-0.081	0.4433	0.0051	0.0396	0.0377
0.1352	0.834	-0.118	-0.065	0.046	0.030	0.034	0.0562	-0.0354	0.134	-0.084	0.5006	0.0051	0.0396	0.0376
0.1532	0.869	-0.115	-0.066	0.042	0.029	0.030	0.0376	-0.0265	0.109	-0.077	0.5674	0.0045	0.0425	0.0403
0.1687	0.891	-0.113	-0.068	0.040	0.026	0.028	0.0345	-0.0215	0.111	-0.069	0.6247	0.0043	0.0427	0.0405
0.1867	0.924	-0.112	-0.069	0.034	0.023	0.025	0.0217	-0.0195	0.094	-0.085	0.6915	0.0028	0.0355	0.0337
0.2154	0.957	-0.106	-0.072	0.027	0.017	0.015	0.0124	-0.0089	0.097	-0.070	0.7977	0.0023	0.0378	0.0359
0.2415	0.984	-0.102	-0.072	0.017	0.011	0.008	0.0041	-0.0022	0.085	-0.046	0.8943	0.0011	0.0324	0.0307
0.2724	0.995	-0.097	-0.070	0.007	0.005	0.005	0.0001	-0.0007	0.008	-0.072	1.0088	0.0001	0.0114	0.0107
0.3555	1.000	-0.088	-0.067	0.003	0.002	0.002								
0.4537	1.000	-0.079	-0.065	0.002	0.002	0.002								

$\delta_p^* = 0.0514$ ft $\delta_r = 0.270$ ft $\frac{U_\delta}{U_o} = 0.9701$

$a = 0.3690$ ft $\delta_a = 0.2912$ ft $b = 0.1230$ ft $\delta_b = 0.1820$ ft

TABLE 7 (Continued)

TABLE 7D - x/L = 0.954

n_e(ft)	$\frac{u_x}{U_o}$	$\frac{v_n}{U_o}$	$\frac{w_\theta}{U_o}$	$\frac{\sqrt{\overline{u_x'^2}}}{U_o}$	$\frac{\sqrt{\overline{v_n'^2}}}{U_o}$	$\frac{\sqrt{\overline{w_\theta'^2}}}{U_o}$	$100\frac{\overline{-u_x'v_n'}}{U_o^2}$	$100\frac{\overline{-u_x'w_\theta'}}{U_o^2}$	$\frac{\overline{-u_x'v_n'}}{q^2}$	$\frac{\overline{-u_x'w_\theta'}}{q^2}$	$\frac{n_e}{\delta_r}$	$\frac{\varepsilon}{U_\delta \delta_p^*}$	$\frac{\ell_p}{\delta_\pi}$	$\frac{\ell}{\sqrt{(a+0.6\delta_a)(b+0.6\delta_b)-ab}}$
0.0108	0.314	-0.108	0.019	0.033	0.025	0.027	0.0465	-0.0128	0.189	-0.052	0.0328	0.0005	0.0054	0.0064
0.0160	0.335	-0.111	0.010	0.034	0.025	0.032	0.0384	-0.0335	0.136	-0.119	0.0484	0.0012	0.0158	0.0188
0.0211	0.353	-0.109	-0.001	0.039	0.026	0.036	0.0405	-0.0592	0.118	-0.172	0.0641	0.0014	0.0175	0.0208
0.0289	0.381	-0.109	-0.015	0.043	0.028	0.039	0.0445	-0.0751	0.108	-0.182	0.0875	0.0015	0.0179	0.0213
0.0366	0.408	-0.103	-0.023	0.049	0.028	0.041	0.0437	-0.0820	0.089	-0.167	0.1109	0.0014	0.0165	0.0197
0.0469	0.452	-0.098	-0.034	0.057	0.033	0.042	0.0376	-0.0976	0.062	-0.162	0.1421	0.0012	0.0151	0.0180
0.0575	0.489	-0.092	-0.036	0.059	0.032	0.043	0.0304	-0.1009	0.048	-0.159	0.1743	0.0011	0.0162	0.0193
0.0653	0.513	-0.088	-0.040	0.058	0.034	0.042	0.0349	-0.0827	0.056	-0.132	0.1978	0.0013	0.0170	0.0202
0.0730	0.541	-0.083	-0.044	0.060	0.035	0.043	0.0447	-0.0936	0.067	-0.141	0.2212	0.0017	0.0198	0.0236
0.0856	0.574	-0.077	-0.053	0.062	0.036	0.043	0.0373	-0.1004	0.053	-0.144	0.2593	0.0016	0.0203	0.0242
0.1039	0.633	-0.068	-0.057	0.061	0.035	0.042	0.0342	-0.0814	0.051	-0.122	0.3149	0.0016	0.0217	0.0258
0.1178	0.662	-0.063	-0.062	0.059	0.035	0.041	0.0299	-0.0815	0.047	-0.127	0.3569	0.0018	0.0257	0.0306
0.1348	0.696	-0.058	-0.067	0.056	0.034	0.040	0.0331	-0.0757	0.056	-0.129	0.4086	0.0019	0.0261	0.0311
0.1506	0.731	-0.054	-0.069	0.054	0.033	0.038	0.0201	-0.0620	0.037	-0.114	0.4564	0.0012	0.0205	0.0245
0.1712	0.770	-0.050	-0.074	0.052	0.032	0.035	0.0275	-0.0541	0.055	-0.109	0.5189	0.0019	0.0282	0.0335
0.1896	0.801	-0.046	-0.075	0.048	0.028	0.034	0.0165	-0.0480	0.039	-0.113	0.5745	0.0012	0.0234	0.0279
0.2051	0.826	-0.044	-0.077	0.046	0.029	0.033	0.0237	-0.0432	0.059	-0.108	0.6214	0.0018	0.0293	0.0349
0.2283	0.862	-0.040	-0.082	0.041	0.025	0.029	0.0156	-0.0363	0.049	-0.113	0.6917	0.0013	0.0264	0.0315
0.2540	0.896	-0.037	-0.083	0.035	0.023	0.024	0.0122	-0.0221	0.053	-0.096	0.7697	0.0012	0.0274	0.0327
0.2849	0.930	-0.034	-0.085	0.027	0.016	0.017	0.0065	-0.0130	0.052	-0.104	0.8635	0.0009	0.0265	0.0316
0.3217	0.956	-0.031	-0.084	0.013	0.009	0.008								
0.3758	0.961	-0.028	-0.082	0.004	0.003	0.003								
0.4250	0.962	-0.026	-0.079	0.004	0.002	0.002								
0.4869	0.964	-0.023	-0.078	0.005	0.002	0.002								
0.6347	0.969	-0.018	-0.078	0.004	0.002	0.002								

$\delta_p^* = 0.0856$ ft $\qquad \delta_r = 0.330$ ft $\qquad \frac{U_\delta}{U_o} = 0.9570$

$a = 0.1995$ ft $\qquad \delta_a = 0.4378$ ft $\qquad b = 0.0665$ ft $\qquad \delta_b = 0.2139$ ft

TABLE 8 - MEASURED MEAN AND TURBULENT VELOCITY CHARACTERISTICS FOR VARYING AXIAL LOCATIONS ALONG 87-DEGREE PLANE

TABLE 8A - x/L = 0.719

n_e(ft)	$\frac{u_x}{U_o}$	$\frac{v_n}{U_o}$	$\frac{w_\theta}{U_o}$	$\frac{\sqrt{\overline{u_x'^2}}}{U_o}$	$\frac{\sqrt{\overline{v_n'^2}}}{U_o}$	$\frac{\sqrt{\overline{w_\theta'^2}}}{U_o}$	$100\frac{-\overline{u_x'v_n'}}{U_o^2}$	$100\frac{-\overline{u_x'w_\theta'}}{U_o^2}$	$\frac{-\overline{u_x'v_n'}}{q^2}$	$\frac{-\overline{u_x'w_\theta'}}{q^2}$	$\frac{n_e}{\delta_r}$	$\frac{\varepsilon}{U_\delta \delta_p^*}$	$\frac{\ell_p}{\delta_r}$	$\frac{\ell}{\sqrt{(a+0.6\delta_a)(b+0.6\delta_b)-ab}}$
0.0104	0.682	-0.025	0.021	0.073	0.034	0.044	0.0974	-0.0023	0.115	-0.003	0.1211	0.0020	0.0128	0.0039
0.0132	0.734	-0.029	0.025	0.070	0.035	0.042	0.1038	0.0038	0.129	0.005	0.1541	0.0043	0.0260	0.0079
0.0185	0.771	-0.030	0.031	0.067	0.035	0.040	0.1005	0.0100	0.136	0.014	0.2151	0.0091	0.0562	0.0171
0.0266	0.817	-0.028	0.037	0.064	0.032	0.039	0.0854	0.0070	0.128	0.010	0.3091	0.0091	0.0609	0.0185
0.0347	0.862	-0.025	0.039	0.058	0.031	0.039	0.0622	0.0079	0.107	0.014	0.4031	0.0081	0.0636	0.0194
0.0403	0.884	-0.022	0.038	0.053	0.030	0.036	0.0621	0.0078	0.124	0.016	0.4690	0.0092	0.0719	0.0219
0.0480	0.916	-0.022	0.039	0.047	0.026	0.031	0.0439	0.0070	0.115	0.018	0.5581	0.0062	0.0575	0.0175
0.0532	0.938	-0.023	0.040	0.043	0.024	0.027	0.0390	0.0079	0.123	0.025	0.6192	0.0066	0.0658	0.0200
0.0581	0.952	-0.021	0.040	0.038	0.023	0.025	0.0324	0.0065	0.123	0.025	0.6754	0.0072	0.0777	0.0236
0.0662	0.972	-0.021	0.039	0.030	0.018	0.019	0.0128	0.0057	0.081	0.036	0.7694	0.0036	0.0615	0.0187
0.0759	0.989	-0.019	0.036	0.021	0.014	0.013	0.0080	0.0041	0.101	0.051	0.8828	0.0036	0.0794	0.0242
0.0868	0.998	-0.018	0.034	0.009	0.009	0.007								
0.1017	1.000	-0.016	0.032	0.004	0.004	0.004								
0.1313	1.000	-0.014	0.029	0.004	0.002	0.002								
0.2165	0.998	-0.009	0.023	0.005	0.002	0.002								
0.2913	0.994	-0.005	0.020	0.005	0.002	0.002								

$\delta_p^* = 0.0164$ ft $\delta_r = 0.086$ ft $\frac{U_\delta}{U_o} = 1.0251$

a = 0.7598 ft $\delta_a = 0.1188$ ft b = 0.2533 ft $\delta_b = 0.1241$ ft

TABLE 8 (Continued)

TABLE 8B - x/L = 0.810

n_e (ft)	$\frac{u_x}{U_o}$	$\frac{v_n}{U_o}$	$\frac{w_\theta}{U_o}$	$\frac{\sqrt{\overline{u_x'^2}}}{U_o}$	$\frac{\sqrt{\overline{v_n'^2}}}{U_o}$	$\frac{\sqrt{\overline{w_\theta'^2}}}{U_o}$	$100\frac{\overline{-u_x'v_n'}}{U_o^2}$	$100\frac{\overline{-u_x'w_\theta'}}{U_o^2}$	$\frac{\overline{-u_x'v_n'}}{q^2}$	$\frac{\overline{-u_x'w_\theta'}}{q^2}$	$\frac{n_e}{\delta_r}$	$\frac{\varepsilon}{U_\delta \delta_p^*}$	$\frac{\ell_p}{\delta_r}$	$\frac{\ell}{\sqrt{(a+0.6\delta_a)(b+0.6\delta_b)-ab}}$
0.0104	0.626	-0.094	-0.020	0.058	0.035	0.041	0.0974	-0.0051	0.155	-0.008	0.0868	0.0015	0.0087	0.0036
0.0141	0.697	-0.093	-0.015	0.058	0.035	0.039	0.1000	-0.0045	0.161	-0.007	0.1174	0.0035	0.0196	0.0082
0.0169	0.722	-0.097	-0.012	0.059	0.036	0.039	0.0952	0.0003	0.151	0.000	0.1410	0.0058	0.0330	0.0138
0.0250	0.759	-0.098	-0.007	0.057	0.033	0.040	0.0796	0.0107	0.134	0.018	0.2083	0.0063	0.0395	0.0165
0.0298	0.792	-0.095	-0.005	0.057	0.034	0.040	0.0858	0.0070	0.144	0.012	0.2486	0.0074	0.0448	0.0187
0.0383	0.818	-0.096	-0.000	0.053	0.032	0.037	0.0642	-0.0065	0.124	-0.012	0.3194	0.0084	0.0589	0.0246
0.0480	0.858	-0.094	0.004	0.051	0.031	0.037	0.0560	-0.0013	0.114	-0.003	0.4000	0.0079	0.058	0.0245
0.0593	0.885	-0.094	0.007	0.045	0.030	0.034	0.0511	-0.0006	0.127	-0.001	0.4944	0.0084	0.0658	0.0275
0.0670	0.909	-0.093	0.008	0.043	0.027	0.032	0.0478	0.0029	0.132	0.008	0.5583	0.0077	0.0621	0.0259
0.0779	0.938	-0.094	0.011	0.039	0.024	0.031	0.0269	0.0020	0.088	0.007	0.6493	0.0051	0.0546	0.0228
0.0876	0.961	-0.092	0.011	0.033	0.021	0.027	0.0230	0.0024	0.102	0.011	0.7299	0.0054	0.0631	0.0263
0.1013	0.981	-0.090	0.009	0.025	0.017	0.019	0.0128	-0.0032	0.099	-0.025	0.8444	0.0050	0.0786	0.0328
0.1183	0.997	-0.087	0.008	0.013	0.010	0.012	0.0014	0.0004	0.035	0.009	0.9861	0.0010	0.0485	0.0203
0.1482	1.000	-0.081	0.005	0.003	0.004	0.005								
0.2121	1.000	-0.072	0.001	0.002	0.002	0.002								
0.2735	1.000	-0.067	0.002	0.002	0.002	0.002								

$\delta_p^* = 0.0210$ ft $\delta_r = 0.120$ ft $\frac{U_\delta}{U_o} = 1.0119$

$a = 0.6429$ ft $\delta_a = 0.1549$ ft $b = 0.2143$ ft $\delta_b = 0.1423$ ft

TABLE 8 (Continued)

TABLE 8C - x/L = 0.854

n_e(ft)	$\frac{u_x}{U_o}$	$\frac{v_n}{U_o}$	$\frac{w_\theta}{U_o}$	$\frac{\sqrt{\overline{u_x'^2}}}{U_o}$	$\frac{\sqrt{\overline{v_n'^2}}}{U_o}$	$\frac{\sqrt{\overline{w_\theta'^2}}}{U_o}$	$100\frac{-\overline{u_x'v_n'}}{U_o^2}$	$100\frac{-\overline{u_x'w_\theta'}}{U_o^2}$	$\frac{-\overline{u_x'v_n'}}{q^2}$	$\frac{-\overline{u_x'w_\theta'}}{q^2}$	$\frac{n_e}{\delta_r}$	$\frac{\varepsilon}{U_\delta \delta_p^*}$	$\frac{\ell_p}{\delta_r}$	$\frac{\ell}{\sqrt{(a+0.6\delta_a)(b+0.6\delta_b)-ab}}$
0.0104	0.509	-0.066	-0.012	0.043	0.026	0.032	0.0389	0.0426	0.110	0.121	0.0651	0.0005	0.0049	0.0028
0.0141	0.569	-0.062	0.005	0.045	0.027	0.034	0.0305	0.0558	0.077	0.141	0.0880	0.0009	0.0099	0.0055
0.0169	0.588	-0.061	0.014	0.047	0.027	0.034	0.0360	0.0624	0.088	0.153	0.1057	0.0018	0.0195	0.0110
0.0250	0.622	-0.057	0.028	0.047	0.028	0.035	0.0311	0.0733	0.073	0.171	0.1562	0.0019	0.0218	0.0122
0.0327	0.667	-0.050	0.039	0.048	0.028	0.038	0.0247	0.0808	0.054	0.177	0.2042	0.0015	0.0189	0.0106
0.0403	0.701	-0.042	0.046	0.049	0.030	0.036	0.0230	0.0644	0.049	0.138	0.2521	0.0013	0.0169	0.0095
0.0472	0.747	-0.034	0.056	0.049	0.029	0.035	0.0295	0.0592	0.066	0.133	0.2948	0.0018	0.0210	0.0118
0.0577	0.776	-0.028	0.066	0.050	0.028	0.037	0.0240	0.0664	0.052	0.143	0.3604	0.0025	0.0324	0.0181
0.0678	0.808	-0.023	0.073	0.048	0.029	0.037	0.0125	0.0667	0.028	0.148	0.4240	0.0012	0.0220	0.0124
0.0779	0.840	-0.015	0.079	0.046	0.027	0.036	0.0187	0.0605	0.045	0.146	0.4870	0.0021	0.0306	0.0172
0.0957	0.878	-0.009	0.088	0.042	0.027	0.034	0.0224	0.0535	0.062	0.147	0.5979	0.0029	0.0389	0.0217
0.1098	0.915	-0.004	0.094	0.038	0.024	0.030	0.0113	0.0497	0.039	0.171	0.6865	0.0015	0.0287	0.0161
0.1417	0.969	0.007	0.103	0.031	0.019	0.023	0.0059	0.0274	0.032	0.150	0.8859	0.0013	0.0349	0.0196
0.1701	1.000	0.014	0.104	0.014	0.011	0.014								
0.2108	1.005	0.021	0.101	0.005	0.004	0.005								
0.2723	1.004	0.030	0.096	0.006	0.002	0.003								
0.3830	1.007	0.042	0.091	0.005	0.002	0.003								
0.4546	1.009	0.047	0.090	0.003	0.002	0.002								

$\delta_p^* = 0.0327$ ft $\qquad \delta_r = 0.160$ ft $\qquad \frac{U_\delta}{U_o} = 0.9947$

$a = 0.5491$ ft $\qquad \delta_a = 0.1902$ ft $\qquad b = 0.1830$ ft $\qquad \delta_b = 0.1531$ ft

TABLE 8 (Continued)

TABLE 8D - x/L = 0.894

n_e(ft)	$\frac{u_x}{U_o}$	$\frac{v_n}{U_o}$	$\frac{w_\theta}{U_o}$	$\frac{\sqrt{\overline{u_x'^2}}}{U_o}$	$\frac{\sqrt{\overline{v_n'^2}}}{U_o}$	$\frac{\sqrt{\overline{w_\theta'^2}}}{U_o}$	$100\frac{-\overline{u_x'v_n'}}{U_o^2}$	$100\frac{-\overline{u_x'w_\theta'}}{U_o^2}$	$\frac{-\overline{u_x'v_n'}}{q^2}$	$\frac{-\overline{u_x'w_\theta'}}{q^2}$	$\frac{n_e}{\delta_r}$	$\frac{\varepsilon}{U_\delta \delta_p^*}$	$\frac{\ell_p}{\delta_r}$	$\frac{\ell}{\sqrt{(a+0.6\delta_a)(b+0.6\delta_b)-ab}}$
0.0104	0.457	-0.094	-0.001	0.042	0.026	0.032	0.0323	0.0637	0.095	0.186	0.0496	0.0003	0.0037	0.0027
0.0181	0.518	-0.090	0.016	0.045	0.027	0.034	0.0230	0.0785	0.059	0.203	0.0861	0.0008	0.0107	0.0079
0.0286	0.572	-0.082	0.033	0.050	0.029	0.036	0.0231	0.0871	0.050	0.188	0.1361	0.0010	0.0140	0.0103
0.0387	0.624	-0.073	0.048	0.050	0.029	0.038	0.0181	0.1021	0.038	0.213	0.1841	0.0008	0.0129	0.0095
0.0484	0.671	-0.065	0.062	0.052	0.031	0.038	0.0140	0.0984	0.028	0.194	0.2306	0.0008	0.0142	0.0104
0.0654	0.715	-0.055	0.072	0.050	0.029	0.037	0.0105	0.0831	0.022	0.176	0.3115	0.0008	0.0161	0.0119
0.0816	0.771	-0.042	0.083	0.048	0.030	0.036	0.0193	0.0825	0.044	0.186	0.3885	0.0015	0.0232	0.0171
0.0969	0.806	-0.036	0.092	0.045	0.029	0.034	0.0023	0.0754	0.006	0.188	0.4615	0.0003	0.0114	0.0084
0.1090	0.828	-0.031	0.097	0.046	0.029	0.032	0.0063	0.0595	0.016	0.149	0.5190	0.0008	0.0206	0.0151
0.1293	0.867	-0.025	0.101	0.043	0.027	0.030	0.0123	0.0588	0.036	0.170	0.6155	0.0016	0.0294	0.0216
0.1478	0.898	-0.019	0.106	0.038	0.024	0.029	0.0082	0.0439	0.028	0.153	0.7040	0.0011	0.0264	0.0194
0.1680	0.930	-0.013	0.111	0.033	0.021	0.024	0.0077	0.0329	0.036	0.154	0.8000	0.0012	0.0289	0.0213
0.1918	0.960	-0.007	0.113	0.026	0.016	0.017	0.0058	0.0201	0.046	0.161	0.9135	0.0012	0.0326	0.0240
0.2157	0.983	-0.003	0.113	0.015	0.011	0.011	0.0001	0.0073	0.002	0.154	1.0274	0.0000	0.0071	0.0052
0.2509	0.993	0.001	0.110	0.006	0.005	0.006								
0.2925	0.995	0.006	0.107	0.005	0.002	0.003								

$\delta_p^* = 0.0448$ $\qquad \delta_r = 0.210$ ft $\qquad \frac{U_\delta}{U_o} = 0.9811$

$a = 0.4369$ ft $\qquad \delta_a = 0.2458$ ft $\qquad b = 0.1457$ ft $\qquad \delta_b = 0.1702$ ft

TABLE 8 (Continued)

TABLE 8E - x/L = 0.914

n_e(ft)	$\frac{u_x}{U_o}$	$\frac{v_n}{U_o}$	$\frac{w_\theta}{U_o}$	$\frac{\sqrt{\overline{u_x'^2}}}{U_o}$	$\frac{\sqrt{\overline{v_n'^2}}}{U_o}$	$\frac{\sqrt{\overline{w_\theta'^2}}}{U_o}$	$100\frac{-\overline{u_x'v_n'}}{U_o^2}$	$100\frac{-\overline{u_x'w_\theta'}}{U_o^2}$	$\frac{-\overline{u_x'v_n'}}{q^2}$	$\frac{-\overline{u_x'w_\theta'}}{q^2}$	$\frac{n_e}{\delta_r}$	$\frac{\varepsilon}{U_\delta\delta_p^*}$	$\frac{\ell_p}{\delta_r}$	$\frac{\ell}{\sqrt{(a+0.6\delta_a)(b+0.6\delta_b)-ab}}$
0.0083	0.394	-0.085	-0.016	0.038	0.026	0.027	0.0427	0.0179	0.148	0.062	0.0298	0.0003	0.0032	0.0032
0.0135	0.436	-0.088	-0.007	0.039	0.026	0.028	0.0374	0.0207	0.127	0.070	0.0482	0.0008	0.0097	0.0096
0.0186	0.468	-0.088	-0.004	0.041	0.027	0.029	0.0420	0.0288	0.127	0.087	0.0666	0.0012	0.0131	0.0128
0.0238	0.494	-0.086	0.001	0.042	0.027	0.031	0.0316	0.0352	0.091	0.102	0.0850	0.0012	0.0152	0.0150
0.0293	0.511	-0.086	0.005	0.044	0.028	0.032	0.0450	0.0442	0.119	0.117	0.1045	0.0018	0.0189	0.0186
0.0341	0.534	-0.082	0.008	0.044	0.029	0.032	0.0348	0.0539	0.091	0.142	0.1218	0.0013	0.0160	0.0158
0.0447	0.565	-0.077	0.014	0.047	0.029	0.034	0.0286	0.0492	0.069	0.118	0.1598	0.0014	0.0189	0.0185
0.0547	0.600	-0.072	0.017	0.047	0.030	0.034	0.0353	0.0544	0.083	0.128	0.1954	0.0018	0.0212	0.0209
0.0653	0.630	-0.064	0.020	0.048	0.030	0.035	0.0319	0.0687	0.071	0.153	0.2334	0.0018	0.0231	0.0227
0.0756	0.658	-0.060	0.023	0.047	0.030	0.035	0.0344	0.0729	0.080	0.171	0.2702	0.0023	0.0275	0.0271
0.0914	0.688	-0.053	0.026	0.046	0.031	0.034	0.0255	0.0694	0.060	0.164	0.3265	0.0020	0.0278	0.0274
0.1069	0.722	-0.047	0.028	0.047	0.029	0.033	0.0276	0.0637	0.067	0.154	0.3818	0.0021	0.0280	0.0276
0.1249	0.759	-0.041	0.031	0.044	0.029	0.034	0.0216	0.0572	0.054	0.144	0.4462	0.0018	0.0274	0.0270
0.1446	0.793	-0.033	0.033	0.042	0.028	0.033	0.0224	0.0513	0.061	0.140	0.5164	0.0021	0.0315	0.0311
0.1713	0.837	-0.024	0.034	0.039	0.026	0.031	0.0157	0.0478	0.050	0.152	0.6118	0.0016	0.0292	0.0287
0.1974	0.874	-0.019	0.035	0.035	0.025	0.027	0.0198	0.0388	0.077	0.151	0.7050	0.0024	0.0375	0.0370
0.2283	0.913	-0.011	0.035	0.030	0.020	0.021	0.0084	0.0238	0.049	0.138	0.8154	0.0012	0.0301	0.0297
0.2776	0.955	-0.002	0.035	0.016	0.010	0.011	0.0011	0.0055	0.024	0.122	0.9915	0.0003	0.0222	0.0218
0.3424	0.963	0.008	0.030	0.004	0.002	0.002								
0.4744	0.970	0.020	0.026	0.002	0.001	0.001								
0.6351	0.972	0.031	0.024	0.004	0.001	0.001								

$\delta_p^* = 0.0644$ ft $\delta_r = 0.280$ ft $\frac{U_\delta}{U_o} = 0.9688$

$a = 0.3690$ ft $\delta_a = 0.2912$ ft $b = 0.1230$ ft $\delta_b = 0.1820$ ft

TABLE 8 (Continued)

TABLE 8F - x/L = 0.934

n_e(ft)	$\frac{u_x}{U_o}$	$\frac{v_n}{U_o}$	$\frac{w_\theta}{U_o}$	$\frac{\sqrt{\overline{u_x'^2}}}{U_o}$	$\frac{\sqrt{\overline{v_n'^2}}}{U_o}$	$\frac{\sqrt{\overline{w_\theta'^2}}}{U_o}$	$100\frac{\overline{-u_x'v_n'}}{U_o^2}$	$100\frac{\overline{-u_x'w_\theta'}}{U_o^2}$	$\frac{\overline{-u_x'v_n'}}{q^2}$	$\frac{\overline{-u_x'w_\theta'}}{q^2}$	$\frac{n_e}{\delta_r}$	$\frac{\varepsilon}{U_\delta\delta_p^*}$	$\frac{\ell_p}{\delta_r}$	$\frac{\ell}{\sqrt{(a+0.6\delta_a)(b+0.6\delta_b)}-ab}$
0.0104	0.339	-0.132	-0.039	0.042	0.028	0.030	0.0531	0.0257	0.156	0.075	0.0353	0.0004	0.0041	0.0042
0.0222	0.390	-0.135	-0.026	0.047	0.030	0.034	0.0556	0.0520	0.131	0.123	0.0751	0.0016	0.0163	0.0168
0.0314	0.440	-0.128	-0.019	0.052	0.031	0.037	0.0512	0.0824	0.102	0.164	0.1065	0.0015	0.0161	0.0165
0.0472	0.498	-0.120	-0.013	0.059	0.033	0.039	0.0528	0.0901	0.088	0.150	0.1599	0.0021	0.0216	0.0223
0.0637	0.556	-0.109	-0.006	0.060	0.033	0.040	0.0363	0.0945	0.057	0.149	0.2161	0.0015	0.0187	0.0193
0.0832	0.622	-0.097	0.002	0.061	0.036	0.041	0.0377	0.0998	0.057	0.150	0.2819	0.0018	0.0218	0.0225
0.1005	0.668	-0.090	0.010	0.063	0.036	0.040	0.0493	0.0966	0.072	0.141	0.3407	0.0026	0.0283	0.0292
0.1183	0.715	-0.081	0.012	0.059	0.035	0.037	0.0505	0.0818	0.083	0.135	0.4011	0.0031	0.0326	0.0336
0.1337	0.747	-0.076	0.014	0.054	0.034	0.036	0.0325	0.0711	0.060	0.131	0.4531	0.0025	0.0331	0.0341
0.1523	0.776	-0.069	0.016	0.054	0.033	0.035	0.0384	0.0603	0.073	0.114	0.5161	0.0029	0.0356	0.0366
0.1701	0.815	-0.066	0.020	0.050	0.032	0.033	0.0295	0.0533	0.064	0.116	0.5766	0.0024	0.0335	0.0344
0.1883	0.838	-0.062	0.022	0.045	0.030	0.031	0.0298	0.0466	0.078	0.121	0.6381	0.0031	0.0428	0.0440
0.2270	0.898	-0.055	0.024	0.038	0.025	0.026	0.0148	0.0313	0.055	0.117	0.7695	0.0015	0.0300	0.0308
0.2614	0.940	-0.053	0.024	0.029	0.019	0.019	0.0129	0.0165	0.083	0.106	0.8862	0.0019	0.0392	0.0404
0.2929	0.964	-0.052	0.023	0.017	0.013	0.011	0.0025	0.0065	0.042	0.111	0.9929	0.0006	0.0293	0.0302
0.3426	0.977	-0.048	0.019	0.004	0.005	0.005								
0.3984	0.981	-0.045	0.015	0.003	0.003	0.003								
0.4497	0.986	-0.040	0.012	0.005	0.003	0.003								

$\delta_p^* = 0.0735$ ft $\quad \delta_r = 0.295$ ft $\quad \frac{U_\delta}{U_o} = 0.9606$

$a = 0.2903$ ft $\quad \delta_a = 0.3625$ ft $\quad b = 0.0968$ ft $\quad \delta_b = 0.2001$ ft

TABLE 9 - MEASURED MEAN AND TURBULENT VELOCITY CHARACTERISTICS FOR VARYING AXIAL LOCATIONS ALONG 90-DEGREE PLANE

TABLE 9A - x/L = 0.719

n_e(ft)	$\frac{u_x}{U_o}$	$\frac{v_n}{U_o}$	$\sqrt{\frac{\overline{u_x'^2}}{U_o}}$	$\sqrt{\frac{\overline{v_n'^2}}{U_o}}$	$100\,\frac{\overline{-u_x'v_n'}}{U_o^2}$	$\frac{\overline{-u_x'v_n'}}{q^2}$	$\frac{n_e}{\delta_r}$	$\frac{\varepsilon}{U_\delta \delta_p^*}$	$\frac{\ell_p}{\delta_r}$	$\frac{\ell}{\sqrt{(a+0.6\delta_a)(b+0.6\delta_b)-ab}}$
0.0104	0.683	-0.054	0.070	0.037	0.1226	0.183	0.1132	0.0025	0.0137	0.0044
0.0165	0.719	-0.051	0.066	0.035	0.1068	0.164	0.1793	0.0077	0.0456	0.0148
0.0218	0.769	-0.055	0.066	0.034	0.1000	0.144	0.2364	0.0065	0.0398	0.0129
0.0318	0.839	-0.053	0.057	0.032	0.0785	0.137	0.3460	0.0082	0.0567	0.0184
0.0399	0.872	-0.055	0.053	0.030	0.0639	0.127	0.4339	0.0083	0.0632	0.0206
0.0476	0.907	-0.053	0.048	0.028	0.0530	0.123	0.5172	0.0072	0.0603	0.0196
0.0524	0.926	-0.055	0.045	0.026	0.0519	0.134	0.5697	0.0079	0.0664	0.0216
0.0581	0.946	-0.054	0.040	0.024	0.0408	0.129	0.6313	0.0070	0.0672	0.0218
0.0657	0.968	-0.054	0.031	0.020	0.0168	0.076	0.7147	0.0040	0.0594	0.0193
0.0735	0.983	-0.053	0.024	0.016	0.0111	0.079	0.7989	0.0041	0.0753	0.0245
0.0840	0.994	-0.052	0.017	0.013	0.0065	0.086	0.9130	0.0047	0.1112	0.0362
0.1026	1.000	-0.050	0.006	0.005						
0.1280	0.999	-0.048	0.003	0.002						
0.1579	0.998	-0.045	0.003	0.002						
0.1862	0.997	-0.043	0.004	0.002						
0.2376	0.997	-0.041	0.004	0.002						

$\delta_p^* = 0.0173$ ft $\delta_r = 0.092$ ft $\frac{U_\delta}{U_o} = 1.0246$

$a = 0.7598$ ft $\delta_a = 0.1188$ ft $b = 0.2533$ ft $\delta_b = 0.1241$ ft

TABLE 9 (Continued)

TABLE 9B - x/L = 0.810

n_e(ft)	$\frac{u_x}{U_o}$	$\frac{v_n}{U_o}$	$\frac{\sqrt{\overline{u_x'^2}}}{U_o}$	$\frac{\sqrt{\overline{v_n'^2}}}{U_o}$	$100\,\frac{-\overline{u_x'v_n'}}{U_o^2}$	$\frac{-\overline{u_x'v_n'}}{q^2}$	$\frac{n_e}{\delta_r}$	$\frac{\varepsilon}{U_\delta \delta_p^*}$	$\frac{\ell_p}{\delta_r}$	$\frac{\ell}{\sqrt{(a+0.6\delta_a)(b+0.6\delta_b)}-ab}$
0.0104	0.599	-0.115	0.054	0.034	0.0965	0.221	0.0755	0.0019	0.0114	0.0055
0.0128	0.625	-0.118	0.051	0.032	0.0873	0.210	0.0930	0.0033	0.0213	0.0102
0.0157	0.651	-0.122	0.050	0.032	0.0759	0.179	0.1135	0.0033	0.0226	0.0108
0.0205	0.692	-0.124	0.049	0.032	0.0780	0.165	0.1486	0.0044	0.0300	0.0144
0.0262	0.718	-0.124	0.048	0.032	0.0729	0.149	0.1896	0.0061	0.0432	0.0207
0.0334	0.751	-0.125	0.047	0.030	0.0579	0.126	0.2421	0.0046	0.0367	0.0176
0.0412	0.790	-0.126	0.046	0.031	0.0608	0.138	0.2983	0.0055	0.0426	0.0204
0.0521	0.823	-0.124	0.043	0.030	0.0543	0.139	0.3774	0.0074	0.0607	0.0291
0.0626	0.849	-0.121	0.044	0.029	0.0552	0.149	0.4535	0.0064	0.0518	0.0248
0.0723	0.888	-0.122	0.038	0.027	0.0369	0.135	0.5236	0.0048	0.0473	0.0227
0.0828	0.907	-0.121	0.038	0.025	0.0370	0.157	0.5996	0.0072	0.0714	0.0343
0.0941	0.931	-0.119	0.034	0.023	0.0284	0.153	0.6818	0.0057	0.0645	0.0310
0.1042	0.948	-0.118	0.031	0.020	0.0214	0.155	0.7548	0.0051	0.0662	0.0317
0.1252	0.978	-0.116	0.016	0.012	0.0050	0.123	0.9070	0.0020	0.0529	0.0254
0.1494	0.989	-0.112	0.006	0.006	0.0002	0.031	1.0827	0.0003	0.0408	0.0196
0.1834	0.989	-0.105	0.004	0.002						
0.2234	0.989	-0.100	0.003	0.002						
0.2715	0.988	-0.096	0.004	0.001						

$\delta_p^* = 0.0260$ ft $\quad \delta_r = 0.138$ ft $\quad \frac{U_\delta}{U_o} = 1.0095$

$a = 0.6429$ ft $\quad \delta_a = 0.1549$ ft $\quad b = 0.2143$ ft $\quad \delta_b = 0.1423$ ft

TABLE 9 (Continued)

TABLE 9C - x/L = 0.854

n_e(ft)	$\frac{u_x}{U_o}$	$\frac{v_n}{U_o}$	$\frac{\sqrt{\overline{u_x'^2}}}{U_o}$	$\frac{\sqrt{\overline{v_n'^2}}}{U_o}$	$100\,\frac{\overline{-u_x'v_n'}}{U_o^2}$	$\frac{\overline{-u_x'v_n'}}{q^2}$	$\frac{n_e}{\delta_r}$	$\frac{\varepsilon}{U_\delta \delta_p^*}$	$\frac{\ell_p}{\delta_r}$	$\frac{\ell}{\sqrt{(a+0.6\delta_a)(b+0.6\delta_b)}-ab}$
0.0104	0.491	-0.087	0.046	0.027	0.0643	0.200	0.0521	0.0007	0.0057	0.0040
0.0161	0.539	-0.093	0.042	0.027	0.0582	0.177	0.0804	0.0017	0.0148	0.0104
0.0205	0.574	-0.099	0.040	0.026	0.0454	0.128	0.1025	0.0015	0.0149	0.0104
0.0278	0.618	-0.099	0.040	0.028	0.0521	0.134	0.1392	0.0027	0.0246	0.0172
0.0359	0.643	-0.099	0.039	0.027	0.0451	0.124	0.1796	0.0031	0.0301	0.0211
0.0440	0.675	-0.097	0.040	0.026	0.0464	0.130	0.2200	0.0032	0.0311	0.0217
0.0517	0.698	-0.095	0.040	0.026	0.0458	0.131	0.2583	0.0038	0.0371	0.0259
0.0622	0.726	-0.092	0.042	0.027	0.0495	0.143	0.3108	0.0041	0.0389	0.0272
0.0718	0.755	-0.087	0.043	0.026	0.0508	0.163	0.3592	0.0037	0.0345	0.0242
0.0812	0.788	-0.083	0.042	0.027	0.0479	0.170	0.4058	0.0043	0.0410	0.0286
0.0928	0.807	-0.081	0.042	0.028	0.0476	0.179	0.4642	0.0061	0.0588	0.0411
0.1070	0.837	-0.076	0.041	0.026	0.0416	0.171	0.5350	0.0048	0.0487	0.0340
0.1247	0.874	-0.072	0.041	0.025	0.0458	0.200	0.6237	0.0054	0.0529	0.0370
0.1434	0.911	-0.069	0.037	0.024	0.0399	0.205	0.7171	0.0055	0.0572	0.0400
0.1616	0.938	-0.066	0.033	0.021	0.0278	0.184	0.8079	0.0043	0.0536	0.0375
0.1813	0.970	-0.062	0.026	0.016	0.0159	0.172	0.9067	0.0029	0.0486	0.0340
0.2133	0.996	-0.058	0.011	0.008	0.0021	0.111	1.0667	0.0009	0.0425	0.0297
0.2727	1.000	-0.046	0.002	0.002						
0.3802	1.000	-0.032	0.001	0.001						
0.4881	1.000	-0.024	0.002	0.002						

$\delta_p^* = 0.0421$ ft $\delta_r = 0.200$ ft $\frac{U_\delta}{U_o} = 0.9917$

$a = 0.5491$ ft $\delta_a = 0.1902$ ft $b = 0.1830$ ft $\delta_b = 0.1531$ ft

TABLE 9 (Continued)

TABLE 9D - x/L = 0.894

n_e(ft)	$\frac{u_x}{U_o}$	$\frac{v_n}{U_o}$	$\frac{\sqrt{\overline{u_x'^2}}}{U_o}$	$\frac{\sqrt{\overline{v_n'^2}}}{U_o}$	$100\frac{\overline{-u_x'v_n'}}{U_o^2}$	$\frac{\overline{-u_x'v_n'}}{q^2}$	$\frac{n_e}{\delta_r}$	$\frac{\varepsilon}{U_\delta \delta_p^*}$	$\frac{\ell_p}{\delta_r}$	$\frac{\ell}{\sqrt{(a+0.6\delta_a)(b+0.6\delta_b)}-ab}$
0.0104	0.443	-0.118	0.040	0.028	0.0638	0.236	0.0372	0.0005	0.0042	0.0042
0.0169	0.498	-0.128	0.035	0.024	0.0380	0.142	0.0604	0.0009	0.0099	0.0098
0.0213	0.525	-0.133	0.034	0.024	0.0372	0.118	0.0762	0.0012	0.0130	0.0128
0.0290	0.556	-0.135	0.032	0.024	0.0344	0.109	0.1036	0.0015	0.0177	0.0174
0.0367	0.582	-0.134	0.033	0.023	0.0310	0.103	0.1310	0.0018	0.0221	0.0218
0.0467	0.603	-0.128	0.032	0.023	0.0248	0.089	0.1670	0.0016	0.0220	0.0217
0.0541	0.624	-0.124	0.034	0.023	0.0280	0.101	0.1932	0.0019	0.0250	0.0246
0.0657	0.643	-0.114	0.034	0.023	0.0281	0.111	0.2348	0.0025	0.0321	0.0315
0.0840	0.685	-0.104	0.037	0.025	0.0292	0.126	0.3000	0.0024	0.0300	0.0295
0.1066	0.723	-0.092	0.039	0.025	0.0304	0.142	0.3807	0.0027	0.0339	0.0333
0.1293	0.768	-0.081	0.038	0.027	0.0347	0.158	0.4616	0.0029	0.0339	0.0333
0.1571	0.822	-0.072	0.040	0.027	0.0377	0.164	0.5610	0.0033	0.0372	0.0366
0.1874	0.876	-0.065	0.037	0.024	0.0284	0.147	0.6693	0.0030	0.0387	0.0380
0.2056	0.902	-0.061	0.032	0.023	0.0252	0.161	0.7342	0.0032	0.0443	0.0435
0.2234	0.923	-0.059	0.032	0.020	0.0229	0.160	0.7979	0.0031	0.0442	0.0435
0.2512	0.959	-0.057	0.023	0.014	0.0111	0.150	0.8973	0.0018	0.0360	0.0354
0.2804	0.981	-0.054	0.011	0.009	0.0018	0.091	1.0015	0.0006	0.0297	0.0292
0.3180	0.988	-0.049	0.003	0.002						
0.3976	0.990	-0.039	0.003	0.001						
0.5007	0.996	-0.028	0.006	0.001						

$\delta_p^* = 0.0620$ ft $\delta_r = 0.280$ ft $\frac{U_\delta}{U_o} = 0.9784$

$a = 0.4369$ ft $\delta_a = 0.2458$ ft $b = 0.1457$ ft $\delta_b = 0.1702$ ft

TABLE 9 (Continued)

TABLE 9E - $x/L = 0.934$

n_e(ft)	$\frac{u_x}{U_o}$	$\frac{v_n}{U_o}$	$\frac{\sqrt{\overline{u_x'^2}}}{U_o}$	$\frac{\sqrt{\overline{v_n'^2}}}{U_o}$	$100\frac{\overline{-u_x'v_n'}}{U_o^2}$	$\frac{\overline{-u_x'v_n'}}{q^2}$	$\frac{n_e}{\delta_r}$	$\frac{\varepsilon}{U_\delta \delta_p^*}$	$\frac{\ell_p}{\delta_r}$	$\frac{\ell}{\sqrt{(a+0.6\delta_a)(b+0.6\delta_b)-ab}}$
0.0104	0.367	-0.133	0.037	0.026	0.0564	0.236	0.0274	0.0003	0.0034	0.0045
0.0165	0.418	-0.148	0.033	0.024	0.0406	0.163	0.0434	0.0006	0.0071	0.0093
0.0222	0.456	-0.154	0.031	0.023	0.0221	0.074	0.0583	0.0004	0.0072	0.0096
0.0294	0.483	-0.154	0.032	0.023	0.0235	0.077	0.0774	0.0008	0.0122	0.0162
0.0338	0.497	-0.155	0.031	0.022	0.0197	0.068	0.0890	0.0008	0.0137	0.0181
0.0448	0.517	-0.153	0.032	0.022	0.0236	0.083	0.1178	0.0014	0.0215	0.0285
0.0629	0.552	-0.143	0.033	0.023	0.0229	0.092	0.1656	0.0014	0.0228	0.0303
0.0775	0.575	-0.133	0.032	0.022	0.0202	0.104	0.2039	0.0015	0.0253	0.0335
0.1022	0.605	-0.115	0.033	0.023	0.0222	0.134	0.2689	0.0017	0.0280	0.0373
0.1264	0.644	-0.099	0.035	0.024	0.0252	0.138	0.3327	0.0019	0.0292	0.0387
0.1677	0.692	-0.081	0.036	0.024	0.0281	0.150	0.4412	0.0021	0.0309	0.0410
0.1968	0.739	-0.072	0.038	0.024	0.0326	0.159	0.5178	0.0023	0.0312	0.0414
0.2403	0.801	-0.060	0.039	0.026	0.0352	0.162	0.6325	0.0027	0.0344	0.0457
0.2763	0.853	-0.055	0.036	0.024	0.0323	0.170	0.7272	0.0026	0.0347	0.0460
0.3200	0.908	-0.051	0.030	0.020	0.0251	0.190	0.8421	0.0023	0.0355	0.0471
0.3552	0.947	-0.050	0.023	0.015	0.0117	0.159	0.9346	0.0015	0.0333	0.0441
0.4020	0.971	-0.046	0.008	0.006	0.0007	0.068	1.0579	0.0003	0.0236	0.0313
0.4518	0.974	-0.040	0.004	0.001						
0.5200	0.983	-0.034	0.003	0.002						
0.6453	0.987	-0.027	0.006	0.001						

$\delta_p^* = 0.0958$ ft $\quad \delta_r = 0.380$ ft $\quad \frac{U_\delta}{U_o} = 0.9572$

$a = 0.2903$ ft $\quad \delta_a = 0.3625$ ft $\quad b = 0.0968$ ft $\quad \delta_b = 0.2001$ ft

TABLE 9 (Continued)

TABLE 9F - x/L = 0.954

n_e(ft)	$\frac{u_x}{U_o}$	$\frac{v_n}{U_o}$	$\frac{\sqrt{\overline{u_x'^2}}}{U_o}$	$\frac{\sqrt{\overline{v_n'^2}}}{U_o}$	$100\frac{\overline{-u_x'v_n'}}{U_o^2}$	$\frac{\overline{-u_x'v_n'}}{q^2}$	$\frac{n_e}{\delta_r}$	$\frac{\varepsilon}{U_\delta \delta_p^*}$	$\frac{\ell_p}{\delta_r}$	$\frac{\ell}{\sqrt{(a+0.6\delta_a)(b+0.6\delta_b)}-ab}$
0.0104	0.326	-0.126	0.035	0.025	0.0512	0.232	0.0237	0.0003	0.0031	0.0050
0.0177	0.370	-0.140	0.033	0.024	0.0365	0.140	0.0402	0.0006	0.0083	0.0132
0.0274	0.410	-0.145	0.031	0.024	0.0333	0.107	0.0623	0.0008	0.0110	0.0174
0.0367	0.442	-0.144	0.030	0.023	0.0261	0.093	0.0833	0.0008	0.0131	0.0208
0.0472	0.463	-0.142	0.032	0.023	0.0267	0.096	0.1072	0.0011	0.0177	0.0281
0.0637	0.499	-0.136	0.031	0.023	0.0245	0.102	0.1449	0.0010	0.0170	0.0270
0.0864	0.544	-0.122	0.032	0.023	0.0173	0.094	0.1964	0.0009	0.0178	0.0282
0.1114	0.578	-0.109	0.035	0.024	0.0186	0.101	0.2532	0.0013	0.0250	0.0397
0.1389	0.609	-0.093	0.033	0.023	0.0139	0.084	0.3157	0.0011	0.0244	0.0387
0.1741	0.646	-0.074	0.035	0.025	0.0159	0.087	0.3956	0.0012	0.0255	0.0405
0.2149	0.695	-0.054	0.036	0.025	0.0237	0.121	0.4884	0.0018	0.0302	0.0479
0.2537	0.739	-0.041	0.040	0.024	0.0281	0.127	0.5765	0.0020	0.0308	0.0488
0.2973	0.798	-0.032	0.038	0.025	0.0261	0.127	0.6758	0.0017	0.0268	0.0425
0.3325	0.846	-0.029	0.038	0.023	0.0220	0.113	0.7557	0.0015	0.0263	0.0417
0.3628	0.883	-0.026	0.034	0.022	0.0225	0.137	0.8246	0.0016	0.0279	0.0443
0.3947	0.922	-0.024	0.030	0.020	0.0183	0.140	0.8972	0.0014	0.0275	0.0437
0.4251	0.953	-0.023	0.024	0.015	0.0131	0.166	0.9661	0.0013	0.0298	0.0474
0.4638	0.980	-0.021	0.012	0.009	0.0028	0.126	1.0542	0.0005	0.0252	0.0401
0.5091	0.990	-0.018	0.004	0.002						
0.6065	0.991	-0.024	0.004	0.002						
0.6687	0.991	-0.023	0.005	0.002						

$\delta_p^* = 0.1201$ ft $\quad \delta_r = 0.440$ ft $\quad \frac{U_\delta}{U_o} = 0.9517$

$a = 0.1995$ ft $\quad \delta_a = 0.4378$ ft $\quad b = 0.0665$ ft $\quad \delta_b = 0.2139$ ft

REFERENCES

1. Huang, T.T. et al., "Stern Boundary-Layer Flow on Axisymmetric Bodies," 12th Symposium on Naval Hydrodynamics, Washington, D.C. (5-9 Jun 1978). Available from National Academy of Sciences, Wash., D.C., pp. 127-147 (1979).

2. Huang, T.T. et al., "Boundary-Layer Flow on an Axisymmetric Body with an Inflected Stern," DTNSRDC Report 80/064 (1980).

3. Preston, J.H., "The Effect of the Boundary Layer and Wake on the Flow Past a Symmetrical Aerofoil at Zero Incidence; Part I, The Velocity Distribution at the Edge of and Outside the Boundary Layer and Wake," ARC R&M 2107 (1945).

4. Lighthill, M.J., "On Displacement Thickness," Journal of Fluid Mechanics, Vol. 4, pp. 383-392 (1958).

5. Dawson, C. and J. Dean, "The XYZ Potential Flow Program," NSRDC Report 3892 (1972).

6. Cebeci, T. et al., "A General Method for Calculating Three-Dimensional Laminar and Turbulent Boundary Layers on Ship Hulls," McDonnell Douglas Corporation Report J7998 (1978). Also Ocean Engineering, Vol. 7, pp. 229-289, Pergamon Press, Great Britain (1980).

7. Cebeci, T. and A.M.O. Smith, "Analysis of Turbulent Boundary Layers," Academic Press, New York (1974).

8. McCarthy, J.H. et al., "The Roles of Transition, Laminar Separation, and Turbulence Stimulation in the Analysis of Axisymmetric Body Drag," 11th Office of Naval Research Symposium on Naval Hydrodynamics, London (1976).

9. Huang, T.T. and C.H. von Kerczek, "Shear Stress and Pressure Distribution on a Surface Ship Model: Theory and Experiment," 9th Office of Naval Research Symposium on Naval Hydrodynamics, Paris (1972). Proceedings are available in U.S. Government Printing Office as ACR-203, Vol. 2.

10. Wang, H.T. and T.T. Huang, "Calculation of Potential Flow/Boundary Layer Interaction on Axisymmetric Bodies," The American Society of Mechanical Engineers Symposium on Turbulent Boundary Layers, Niagara Falls, N.Y., pp. 47-57 (18-20 Jun 1979).

11. Keller, H.B., "A New Difference Scheme for Parabolic Problems," Numerical Solution of Partial Differential Equations, II, J. Bramble (ed.), Academic Press, New York (1970).

12. Shiloh, K. et al., "The Structure of a Separating Turbulent Boundary Layer. Part 3: Transverse Velocity Measurements," Journal of Fluid Mechanics, Vol. 113 (1981).

13. Bradshaw, P. et al., "Calculation of Boundary Layer Development Using the Turbulent Energy Equation," Journal of Fluid Mechanics, Vol. 28 (1967).

INITIAL DISTRIBUTION

Copies	
1	WES
1	U.S. ARMY TRAS R&D Marine Trans Div
1	CHONR/438 Lee
2	NRL 1 Code 2027 1 Code 2629
1	ONR/Boston
1	ONR/Chicago
1	ONR/New York
1	ONR/Pasadena
1	ONR/San Francisco
1	NORDA
3	USNA 1 Tech Lib 1 Nav Sys Eng Dept 1 B. Johnson
3	NAVPGSCOL 1 Lib 1 T. Sarpkaya 1 J. Miller
1	NOSC/Lib
1	NCSC/712
1	NCEL/131
1	NSWC, White Oak/Lib
1	NSWC, Dahlgren/Lib
1	NUSC/Lib

Copies	
16	NAVSEA 1 SEA 033 1 SEA 03D 1 SEA 03R22 1 SEA 05T 1 SEA 05H 1 SEA 312 1 SEA 32 1 SEA 321 1 SEA 3213 1 SEA 32R 1 SEA 521 1 SEA 524 1 SEA 62P 3 SEA 996
1	NAVFAC/032C
1	NADC
1	NAVSHIPYD PTSMH/Lib
1	NAVSHIPYD PHILA/Lib
1	NAVSHIPYD NORVA/Lib
1	NAVSHIPYD CHASN/Lib
1	NAVSHIPYD LBEACH/Lib
2	NAVSHIPYD MARE 1 Lib 1 Code 250
1	NAVSHIPYD PUGET/Lib
1	NAVSHIPYD PEARL/Code 202.32
1	NAVSEC, NORVA/6660.03, Blount
12	DTIC
1	AFOSR/NAM
1	AFFOL/FYS, J. Olsen

Copies	
2	MARAD 1 Div of Ship R&D 1 Lib
1	NASA/HQ/Lib
1	NASA/Ames Res Ctr, Lib
2	NASA/Langley Res Ctr 1 Lib 1 D. Bushnell
1	NBS/Lib
1	NSF/Eng Lib
1	LC/Sci & Tech
1	DOT/Lib TAD-491.1
2	MMA 1 National Maritime Res Ctr 1 Lib
1	U of Bridgeport/E. Uram
2	U of Cal/Dept Naval Arch, Berkeley 1 Lib 1 W. Webster
2	U of Cal., San Diego 1 A.T. Ellis 1 Scripps Inst Lib
5	CIT 1 Aero Lib 1 T.Y. Wu 1 A.J. Acosta 1 I. Sabersky 1 D. Coles
1	City College, Wave Hill/Pierson
1	Catholic U of Amer/Civil & Mech Eng
1	Colorado State U/Eng Res Ctr

Copies	
1	U of Connecticut/Scottron
1	Cornell U/Shen
1	Florida Atlantic U/Tech Lib
2	Harvard U 1 G. Carrier 1 Gordon McKay Lib
1	U of Hawaii/Bretschneider
1	U of Illinois/J. Robertson
4	U of Iowa 1 Lib 1 L. Landweber 1 J. Kennedy 1 V.C. Patel
1	Johns Hopkins U/Lib
1	Kansas State U/Nesmith
1	U of Kansas/Civil Eng Lib
1	Lehigh U/Fritz Eng Lab Lib
4	MIT 1 Lib 1 J.R. Kerwin 1 P. Leehey 1 J.N. Newman
2	U of Minn/St. Anthony Falls 1 Lib 1 R. Arndt
1	U of Mich/NAME/Lib
1	U of Notre Dame/Eng Lib
1	New York U/Courant Inst/Lib
3	Penn State 1 B.R. Parkin 1 R.E. Henderson 1 ARL Lib

Copies	
1	Princeton U/Mellor
1	U of Rhode Island/F.M. White
1	Science Application, Inc. Annapolis, MD C. von Kerczek
1	SIT/Lib
1	U of Texas/Arl Lib
1	Utah State U/Jeppson
2	Southwest Res Inst 1 Applied Mech Rev 1 Abramson
3	Stanford U 1 Eng Lib 1 R. Street, Dept Civil Eng 1 S.J. Kline, Dept Mech Eng
1	Stanford Res Inst/Lib
1	U of Virginia/Aero Eng Dept
1	U of Washington/Arl Tech Lib
2	VPI 1 Dept Mech Eng 1 J. Schetz, Dept Aero & Ocean Eng
2	Webb Inst 1 Lib 1 Ward
1	Woods Hole/Ocean Eng
1	Worchester PI/Tech Lib
1	SNAME/Tech Lib
1	Bell Aerospace
1	Bethlehem Steel/Sparrows Point

Copies	
1	Bethlehem Steel/New York/Lib
2	Boeing Company/Seattle 1 Marine System 1 P. Rubbert
1	Bolt, Beranek & Newman/Lib
1	Exxon, NY/Design Div/Tank Dept
1	Exxon Math & System, Inc.
1	General Dynamics, EB/Boatwright
1	Flow Research
1	Gibbs & Cox/Tech Info
1	Grumman Aerospace Corp/Lib
5	Hydronautics 1 Lib 1 E. Miller 1 V. Johnson 1 C.C. Hsu 1 M. Tulin
1	Lockheed, Sunnyvale/Waid
1	Lockheed, California/Lib
1	Lockheed, Georgia/Lib
1	McDonnell Douglas, Long Beach 1 T. Cebeci
1	Newport News Shipbuilding/Lib
1	Nielsen Eng & Res
1	Northrop Corp/Aircraft Div
1	Rand Corp
1	Rockwell International 1 B. Ujihara
1	Sperry Rand/Tech Lib

Copies	
1	Sun Shipbuilding/Chief Naval Arch
1	Robert Taggart
1	TRW Systems Group/Lib
1	TRACOR
1	United Technology/East Hartford, Conn
2	Westinghouse Electric 1 M.S. Macovsky 1 Gulino

CENTER DISTRIBUTION

Copies	Code	Name
1	1500	W.B. Morgan
1	1504	V.J. Monacella
1	1507	D.S. Cieslowski
1	1508	R.S. Rothblum
1	152	W.C. Lin
1	1521	P. Pien
1	1521	W. Day
1	1522	G. Dobay
1	1522	M. Wilson
1	154	J. McCarthy
1	154	P. Granville
1	1540.1	B. Yim
1	1540.2	R. Cumming
30	1542	T.T. Huang
3	1542	N.C. Groves
1	1542	G.S. Belt
1	1542	Y.T. Lee
1	1542	M.S. Chang
1	1544	T. Brockett
1	1544	R. Boswell
1	1544	E. Caster
1	1544	S. Jessup
1	1544	K.F. Lin
1	1560	M. Martin

Copies	Code	Name
1	1561	G. Cox
1	1563	W.E. Smith
1	1564	J. Feldman
1	1572	E. Zarnick
1	1606	T.C. Tai
1	1615	R.J. Furey
1	1802.1	H. Lugt
1	1802.2	F. Frenkiel
1	1840	J. Schot
1	1843	H. Haussling
1	19	M.M. Sevik
1	1940	J.T. Shen
1	1942	B.E. Bowers
1	1942	T.M. Farabee
1	1942	F.E. Geib
1	1942	T.C. Mathews
10	5211.1	Reports Distribution
1	522.1	Unclassified Lib (C)
1	522.2	Unclassified Lib (A)

DTNSRDC ISSUES THREE TYPES OF REPORTS

1. DTNSRDC REPORTS, A FORMAL SERIES, CONTAIN INFORMATION OF PERMANENT TECHNICAL VALUE. THEY CARRY A CONSECUTIVE NUMERICAL IDENTIFICATION REGARDLESS OF THEIR CLASSIFICATION OR THE ORIGINATING DEPARTMENT.

2. DEPARTMENTAL REPORTS, A SEMIFORMAL SERIES, CONTAIN INFORMATION OF A PRELIMINARY, TEMPORARY, OR PROPRIETARY NATURE OR OF LIMITED INTEREST OR SIGNIFICANCE. THEY CARRY A DEPARTMENTAL ALPHANUMERICAL IDENTIFICATION.

3. TECHNICAL MEMORANDA, AN INFORMAL SERIES, CONTAIN TECHNICAL DOCUMENTATION OF LIMITED USE AND INTEREST. THEY ARE PRIMARILY WORKING PAPERS INTENDED FOR INTERNAL USE. THEY CARRY AN IDENTIFYING NUMBER WHICH INDICATES THEIR TYPE AND THE NUMERICAL CODE OF THE ORIGINATING DEPARTMENT. ANY DISTRIBUTION OUTSIDE DTNSRDC MUST BE APPROVED BY THE HEAD OF THE ORIGINATING DEPARTMENT ON A CASE-BY-CASE BASIS.